神経発達の退縮におけるグアニンヌクレオチド交換因子ＫＩＡＡ０３８０の機能

参考画像

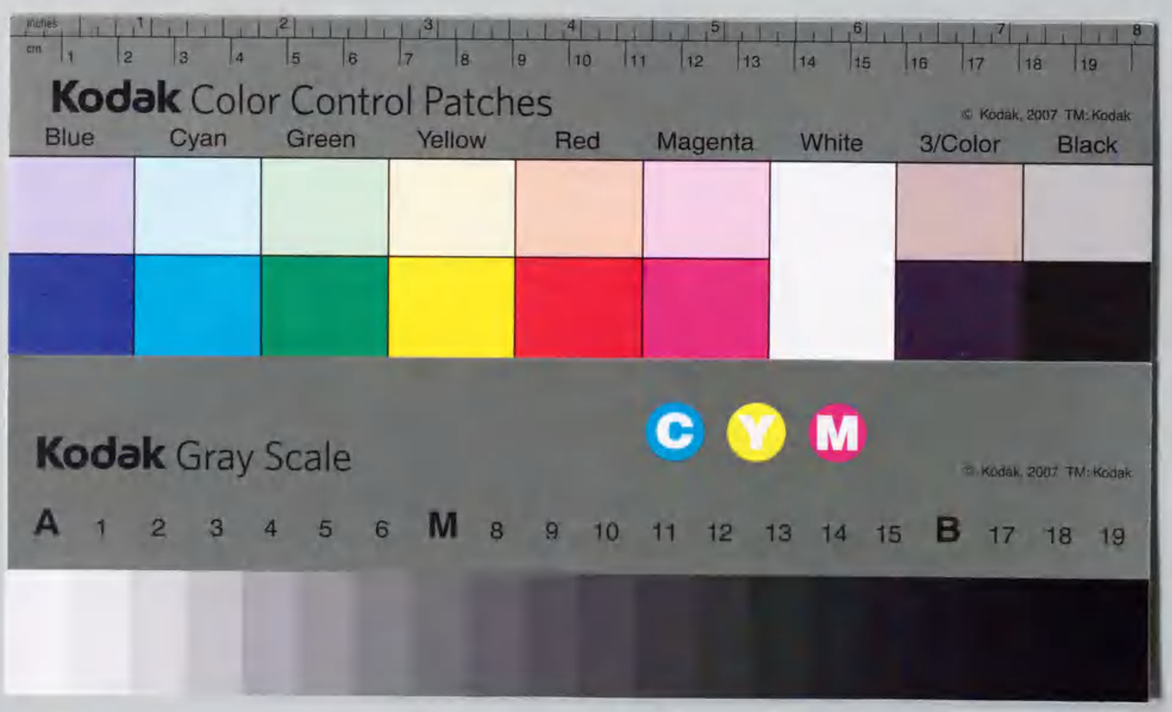

学位論文

神経突起の退縮におけるグアニンヌクレオチド交換因子 KIAA0380 の機能

名古屋大学大学院理学研究科生命理学専攻

冨樫秀彰

本論文で用いた略号

GEF: guanine nucleotide exchange factor
DH: Dbl homology
PH: pleckstrin homology
RGS: regulator of G protein
GTP: guanosine 5'-triphosphate
GDP: guanosine 5'-diphosphate
GST: glutathione S-transferase
Tris: tris (hydroxymethyl) aminomethane
DTT: dithiothreitol
PMSF: phenylmethylsulfonyl fluoride
PBS: phosphate buffered saline
TCA: trichloroacetic acid
EDTA: ethylenediaminetetraacetic acid
SDS: sodium dodecyl sulfate
PAGE: polyacrylamide gel electrophoresis
PCR: polymerase chain reaction
FITC:fluorescein isothiocyanate
LPA: lysophosphatidic acid

目次

要旨

アクチンを主体とする細胞骨格系は、細胞形態の維持に必要なだけではなく、細胞の運動や細胞質分裂時の推進力を生み出すという非常にダイナミックな性質を有している。アクチン細胞骨格の重要な制御因子として、低分子量Gタンパク質である Rho ファミリーが近年注目を集めており、細胞外の刺激に対する分子スイッチとして機能し、アクチン細胞骨格の再構築を制御していることが明らかになってきた。Rho ファミリータンパク質の機能を理解するためには、細胞内における Rho シグナル伝達系の活性化状態を厳密に、そして簡易に検出するシステムが必要となる。

まず、細胞内での Rho の活性化状態を検出するために、中間径フィラメント・ビメンチンのヘッドドメイン(VH)を Rho の下流分子の一つである Rho キナーゼの N 末端に付加したキメラタンパク質(VH-RhoK)と、ビメンチンのヘッドドメイン中の 71 番目のセリン残基(Rho キナーゼによって特異的にリン酸化される)のリン酸化を特異的に認識する抗リン酸化ペプチド抗体(TM71)を用いて、新たな Rho シグナル伝達系の活性化検出システムを考案した。そのシステムを評価した結果、VH-RhoK を強制発現させた細胞において、Rho シグナル伝達系が活性化されると、VH-RhoK は分子内リン酸化の様式でリン酸化され、そのリン酸化を TM71 で検出できることがわかった。また、TM71 で検出されるリン酸化は、Rho シグナル伝達系を活性化したときにのみ検出され、同じ Rho ファミリーである Rac や Cdc42 では検出されないことから、Rho シグナル伝達系の活性化を特異的に検出できることが解った。

次に、そのシステムを用いて、Rho シグナル伝達系を活性化する因子の同定を試みた。Rho の活性化因子としては Rho グアニンヌクレオチド交換因子(RhoGEF)がある。RhoGEF は、一般的に、DH (Dbl homology)ドメインと、PH (pleckstrin homology)ドメインを持つことが知られている。EST データーベース上で、DH ドメインと PH ドメインに相同性を持つ配

列を含み、現在まで機能解析がなされていないタンパク質を検索したところ、KIAA0380 と呼ばれるタンパク質が候補となる分子としてあげられた。そこで、先に述べた Rho 活性化検出システムに適用し、解析した結果、この分子が Rho シグナル伝達系を活性化する RhoGEF であることが解った。

このようにして Rho 特異的な RhoGEF であることを見いだした KIAA0380 について、さらなる解析をすすめた。まず、この RhoGEF をマウス繊維芽細胞 Swiss3T3 において強制発現したときに、細胞がどのような形態をとるのかを観察したところ、強力な cortical アクチンの再構築と、細胞の球状化が観察された。次に、cortical アクチンの再構築を誘導するために必要なドメインを明らかにするために、各種欠失変異体を作製し、それらを細胞内で発現させた際の形態変化を観察した。その結果、この GEF が細胞膜直下に局在し、cortical アクチンの再構築を誘導することによって細胞を球状化させるためには、活性ドメインである DH ドメインと PH ドメインに加え、そのカルボキシル末端側近傍に位置するプロリンリッチモチーフが必須であることがわかった。つまり、プロリンリッチモチーフが、細胞膜直下において選択的に Rho シグナル伝達系を活性化し、cortical アクチンの再構築を誘導するために重要なモチーフであることが明らかとなった。

神経細胞において、リゾホスファチジン酸(LPA)刺激により引き起こされる突起の退縮、細胞の球状化には、三量体 G タンパク質G_{12}やG_{13}から Rho を介するシグナル伝達系が重要な役割を演じていることが知られている。そのため、G_{12}やG_{13}のαサブユニット($G\alpha_{12}$及び$G\alpha_{13}$)と相互作用し、Rho を活性化する分子の存在が推察されていた。KIAA0380 が持つ RGS (regulator of G-protein signal)ドメインは、$G\alpha_{12}$や$G\alpha_{13}$と相互作用するドメイン構造であることが知られている。そこで、この RhoGEF が、突起の退縮を制御するシグナル伝達系に関わっているかどうか検討した。まず、この RhoGEF に対する抗体を作製し、免疫沈降を行った結果、マウス神経芽

細胞 Neuro2a において、この RhoGEF が内在性に発現していることがわかった。そして、細胞内局在を免疫染色により観察すると、cortical アクチンの再構築が活発に誘導されている神経突起の先端に限局して存在している様子が観察された。また、この RhoGEF のドミナントネガティブ変異体を強制発現させた Neuro2a 細胞では、LPA による神経突起の退縮が有意に阻害された。これらの結果は、この RhoGEF が、神経細胞における突起の退縮を制御する Rho 依存的なシグナル伝達系の一員であることを強く示唆している。

序論

1) 低分子量 G タンパク質 Rho

低分子量 G タンパク質(あるいは GTPase とも呼称される)である Rho ファミリーと呼ばれる一群のタンパクの中で、特に Rho、Rac、Cdc42 は、近年急速に研究が進み、アクチン細胞骨格の構築や、遺伝子の転写を誘導するシグナル伝達経路を制御していることが明らかにされてきた。繊維芽細胞において、Rho がアクチンストレスファイバーや、それに付随する接着斑を、Rac と Cdc42 が波うち膜(ラメリポディア)と糸状仮足(フィロポディア)の形成を、それぞれ制御している[1-4](図 1)。このような働きに加え、これら 3 つの GTPase は、細胞の多種多様な機能発現の引き金になっていることが報告されている。例えば、Rho は細胞周期の G1 期の進行や SRF 転写因子の活性化に必要であり、細胞質分裂に際しても重要な役割を演じている。

Rho によって制御される細胞骨格の変化は、細胞の種類によっても大きく異なっている。神経細胞において、Rho は、アクチン繊維の cortical shell を形成する[5]。その収縮は、LPA の刺激に応答し、神経突起の退縮や、成長円錐の崩壊に関係していると考えられている[5-10]。しかしながら、それらの多彩な応答と、生化学的な機構との関係は、まだ明らかではない。

2) Rho グアニンヌクレオチド交換因子(RhoGEF)

Rho ファミリータンパク質は細胞内のシグナル伝達系を制御する分子スイッチとして機能すると考えられている。つまり、GTP が結合した活性型と、GDP が結合した不活性型が存在する。Rho 及びそのファミリータンパク質を制御する因子として、25 種類以上のグアニンヌクレオチド交換因子(guanine nucleotide exchange factor: GEF)と、10 種類以上の GTPase 活性化因子(GTPase activating protein: GAP)、少なくとも 3 種類以上のグアニンヌクレオチド解離阻害因子(GDP-dissociation inhibitor: GDI)が存在して

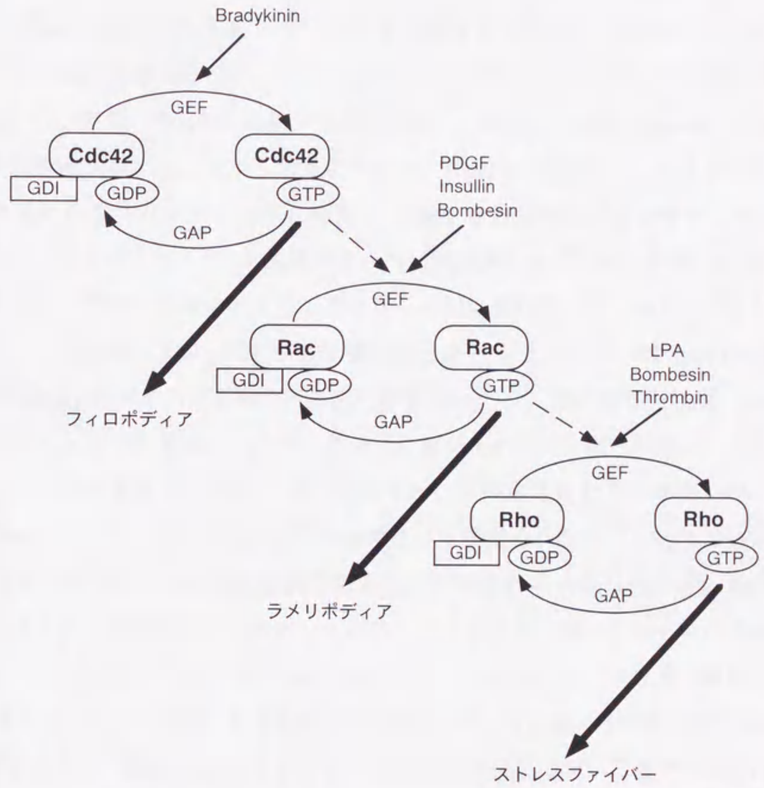

図 1　細胞骨格制御における Rho-GTPase カスケード

Cdc42、Rac、Rho は、細胞外からの様々な刺激を受けて、GTP が結合した活性型になる。繊維芽細胞において、活性化した Cdc42、Rac、Rho は、それぞれ、フィロポディア、ラメリポディア、ストレスファイバーを形成する。GDI: グアニンヌクレオチド解離阻害因子. GAP: GTPase 活性化因子. GEF: グアニンヌクレオチド交換因子.

いる[11-13]。

Rho の様な低分子量 G タンパク質に対する GEF は、がん遺伝子 Dbl に含まれる領域 DH (Dbl-homology)ドメインを持っている[11]。がん遺伝子 Dbl は、当初、NIH3T3 細胞で発現させると、細胞の focus formation や形質転換を誘導することから発見された[14]。生化学的解析から、Dbl が、低分子量 G タンパク質 Cdc42 に結合した GDP を解離する活性を持つことが明らかにされ、さらに、欠失変異体を用いた実験により、その活性には DH ドメインが最も重要なドメインであることが示された[15-17]。また、DH ドメインに加え、Dbl が適正な細胞内局在をとるためには PH (pleckstrin homology)ドメインが必要であることが示された[18]。Dbl の発見以降、DH ドメインと PH ドメインをもつタンパク質が次々と見いだされた。それらは、形質転換能を指標に、がん遺伝子として同定されたものが多いが、Tiam1 のように細胞の浸潤活性を指標にして同定されたり[19]、Fgd1 や Vav のように、正常な発生に必須であることが示されているものや[20]、Ect2 のように、細胞質分裂に関係していることが明らかになっているものもある[21]。一般的に、DH ドメインと PH ドメインを直列にもつタンパク質は、Rho ファミリーに対する GEF として活性を持っているようであるが、DH ドメインと PH ドメインをもつすべてのタンパク質について当てはまるわけではない。さらに、DH ドメインと PH ドメインを持つタンパク質の中には、Rho のような低分子量 G タンパク質に対する GEF 活性が、あまり特異的ではないものが存在する(表 1)。

そのため、GEF の Rho ファミリーに対する活性の特異性を同定し、その機能を解析するために、さらなる研究が必要とされている。近年、細胞内で強制発現させ、その形態を観察することで、*in vitro* だけでなく、*in vivo* における Rho ファミリーの GEF の機能解析も報告されている。例えば、マイクロインジェクション法により、Lbc がストレスファイバーを誘導することや Fgd1 がフィロポディアを形成することが明らかになり、それらは、それぞれ Rho と Rac を活性化していることを示している[22]。さらに

DH-PH ドメインを含むタンパク質	Rho GTPase に対する GEF の特異性	生理的特性	組織特異性
Dbl	Cdc42, Rho	発ガン	脳、副腎、生殖腺
Lbc	Rho	発ガン	心臓、肺、骨格筋
Lfc	Rho	発ガン	造血性細胞、腎臓、肺
Lsc/p115RhoGEF	Rho	発ガン	造血性細胞、腎臓、肺
Dbs	?	発ガン	腎臓、肺、特に脳に多い
Tiam1	Rac	転移、発ガン	脳、精巣
Vav	Rac, Cdc42, Rho	発ガン、リンパ性細胞増殖	造血性細胞
FGD1	Cdc42	顔面生殖器形成異常に関連	脳、心臓、肺、腎臓
Trio	Rac, Rho	細胞の遊走に関連	遍在性
Ost	Rho, Cdc42 (GTP 結合型 Rac に結合)	発ガン	脳、心臓、肺、肝臓
Bcr	Rac, Cdc42, Rho (Rac に対する GAP 活性)	白血病に関連	特に脳に多い
Abr	Rac,Cdc42,Rho(Rac,Cdc42 に対する GAP 活性	?	特に脳に多い
Ect2	Rho, Rac, Cdc42[21]	発ガン	精巣、腎臓、肝臓、脾臓
RhoGEF (190kD)[80]	Rho	?	?
p116 (Rip)[80]	Rho	?	?
CDEP[81]	?	?	遍在性
Brx[82]	Cdc42	?	estrogen 応答性組織
mNET1[83]	Rho	?	?
GEF-H1[84]	Rac, Rho	?	?
STEF[85]	Rac	?	胎生期軟骨、神経
KIAA0380	Rho	?	脳、心臓
hPEM-2[86]	Cdc42	?	脳
Kalirin-7[87]	Rac	?	脳

Van Aelst and D'Suza-Schorey Genes & Dev. 11:2295-2322 (1997)より、一部改変

表 1　哺乳動物において Rho ファミリーに関与する GEF

Fgd1 は、MAP キナーゼの一種である stress-activated kinase/c-Jun amino-termial kinase (SAPK/JNK)のシグナル伝達系を活性化し、その活性化は Cdc42 や Rac を介していることが見いだされている。Dbl と Vav は、Cdc42、Rac、Rho を介して、それぞれフィロポディア、ラメリポディア、ストレスファイバーの形成を誘導し、また、SAPK/JNK を活性化することも知られている [23]。多くの GEF は、DH ドメインと PH ドメインのほかにも、Src-homology ドメインのような、シグナル伝達系に関与する分子が持つドメイン構造も持っており、純粋な GEF 活性以外の機能も持っていることが推測される [11]。しかしながら、Rho ファミリーの GEF がどのような分子を介して上流のシグナル伝達系と繋がっているのかについては、RGS ドメインをもつ RhoGEF が G_{13} を上流因子として持つ例の他は、ほとんど知られていない。

3) Rho キナーゼ

Rho が関わるシグナル伝達系において、Rho の下流に位置する標的分子としていくつかの分子がここ数年間に見いだされており(図 2)、その一つが Rho キナーゼ/ROCK である。このキナーゼは、ミオシン軽鎖の直接的なリン酸化並びに、ミオシンホスファターゼのミオシン結合サブユニットのリン酸化を介したそのホスファターゼ活性の不活性化により、ミオシン軽鎖のリン酸化を制御している [24-26]。また、ERM ファミリー(ezrin, radixin, moesin)や adducin なども、*in vivo*、*in vitro* の両方で、Rho キナーゼによりリン酸化されることが提唱されている [27-29]。Rho キナーゼは、アクチンストレスファイバーや接着斑の形成 [30-32]、平滑筋の収縮 [33]、ミオシン繊維の構築、転写因子 c-fos の発現 [26]、中間径フィラメントの細胞質分裂時における等分配 [34-35]、神経突起の退縮 [36-37]などを制御していると考えられている。このように機能的に重要なキナーゼであるにもかかわらず、Rho キナーゼの活性化状態を *in vivo* において統括的に検出する方法は、これまで存在しなかった。

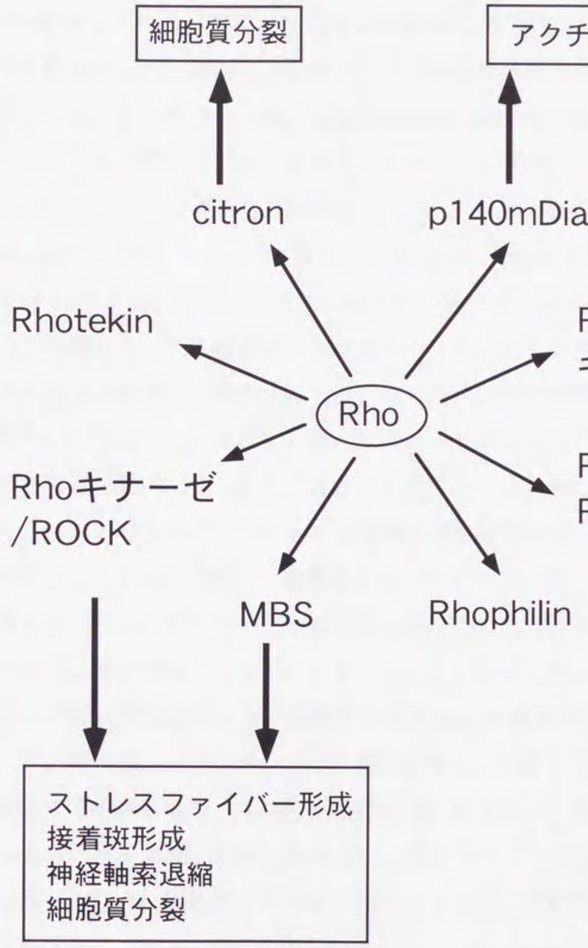

図 2　Rho の標的タンパク質と、その細胞骨格系の制御

4) 中間径フィラメント

中間径フィラメントは、細胞骨格の構成成分の一つである。フィラメントの構成タンパク質は、分子量とアミノ酸配列の違いにより、6 つのタイプに分類され、発生や分化の過程で組織特異的な発現様式を示すことが知られている [38-40]。中間径フィラメントタンパク質は、アミノ末端側よりヘッド、ロッド、テイルと呼ばれる 3 つのドメイン構造を持っており、homophilic (ケラチンタンパク質については heterophilic であるが)に重合して直径 10 nm のフィラメントを形成する。我々は、*in vitro* の再構成系を用いた実験から、その構成タンパク質のヘッドドメインが、各種プロテインキナーゼによりリン酸化されると、フィラメントの脱重合がおきることを明らかにした [41-54]。さらに、様々なキナーゼがヘッドドメインのセリン残基を部位特異的にリン酸化することを明らかにしてきた [41, 44, 46-48](図 3)。また、*in vivo* においても *in vitro* と同様な部位特異的リン酸化によって、中間径フィラメントの重合、脱重合が制御されているのかどうか、*in vivo* 中間径フィラメントキナーゼを明らかにするために、種々のプロテインキナーゼによる中間径フィラメントタンパク質の各リン酸化部位について、そのリン酸化状態を特異的に認識する抗体(抗リン酸化抗体)を作製してきた [55-61]。例えば、ビメンチンの 71 番目のセリン残基のリン酸化を特異的に認識する抗体の場合、リン酸化された 71 番目のセリン残基を中心に前後 5 残基のアミノ酸とアミノ末端あるいはカルボキシル末端側にシステイン残基を含む 11 残基のアミノ酸からなるペプチドを合成する。これを末端のシステイン残基を介して Keyhole Limpet Homocyanin に結合させ抗原とし、免疫して抗体を得る。このようにして作製された抗体は、リン酸化された 71 番目のセリンを含む配列を非常に特異的に認識することを確認している [62]。このような抗リン酸化抗体を用いることによって、細胞内での中間径フィラメントタンパク質の部位特異的なリン酸化を可視化できるようになり、その時間的、空間的変動の解析が可能となったのである。さらにはこれらの知見は *in vivo* 中間径フィラメントキナーゼの同定に大い

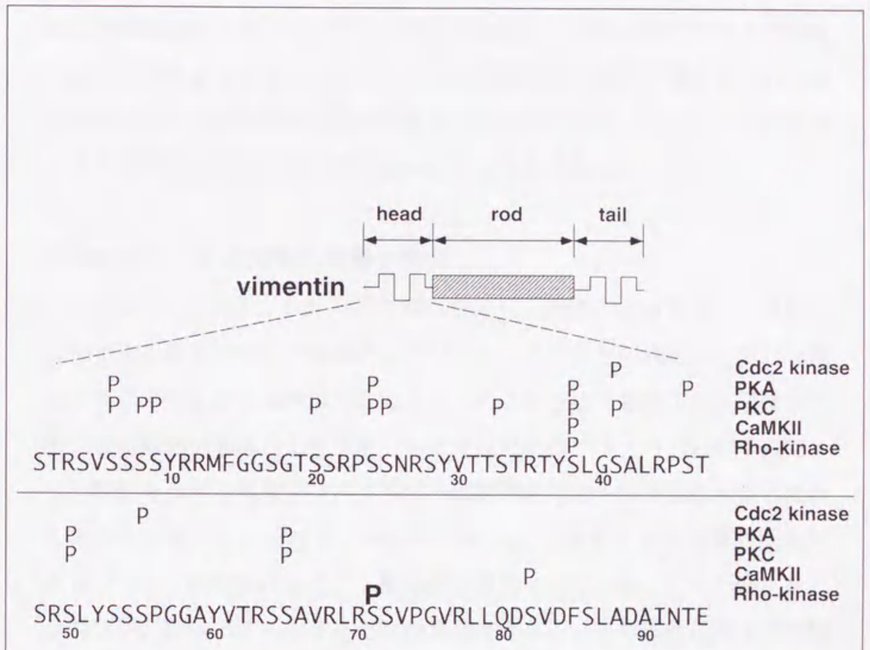

図 3　各種プロテインキナーゼによるリン酸化部位

各種プロテインキナーゼは、中間径フィラメントのヘッドドメインををリン酸化する。マウスのビメンチンにおいて、各キナーゼがリン酸化する部位を、P で示した。71 番目のセリン残基は、Rho キナーゼによって特異的にリン酸化される部位である(P: 太字)。PKA: cAMP 依存性キナーゼ. PKC: プロテインキナーゼ C. CaMKII: カルシウム/カルモジュリン依存性キナーゼ II

なる貢献を果たした。現在では、我々が開発した抗リン酸化ペプチド抗体の作成法と概念の確立により、この特殊抗体は多彩なリン酸化タンパク質の細胞内局在・動態や細胞機能の解析に広く利用され、それらリン酸化タンパク質の細胞機能に果たす役割の解明の一翼を担っている。

5) Rho キナーゼの活性化状態の検出

中間径フィラメントタンパク質、つまり、基質となるタンパク質のリン酸化体の細胞内分布・動態及びそれを担うキナーゼの同定に、抗リン酸化抗体は非常に有効な手段である。さらにこの方法を発展させ、活性型キナーゼの細胞内動態の全貌を明らかにするために、キナーゼの分子内に、リン酸化をうける基質タンパク質の一部配列を付加する方法を考案した。この方法を用いるためには、少なくとも 1)リン酸化される基質が既知である、2)リン酸化されるアミノ酸部位が特定されている、3)リン酸化される部位が、標的とするキナーゼに特異的である、4)その部位に対する部位特異的リン酸化抗体の作製がなされている(もしくは作製を行う)などの条件が必要である。我々は、中間径フィラメントのヘッドドメインのリン酸化について詳細な解析を進めてきた経緯があるため、各種キナーゼによるヘッドドメインの部位特異的リン酸化に関して多くのデータの蓄積がある。そこで、本論では、ビメンチンのヘッドドメインと Rho キナーゼ、及び、Rho キナーゼによるビメンチンヘッドドメイン中の特異的なリン酸化部位を認識する抗体を用いて、Rho キナーゼの活性化状態を、*in vivo* において直接的に検出する新たなシステムについて報告した。

6) グアニンヌクレオチド交換因子 KIAA0380 の機能

上記のシステムを評価した結果、Rho シグナル伝達系の活性化を検出できることがわかったので、実際の応用として、KIAA0380 と呼ばれるタンパク質に適用を試みた。KIAA0380 は、かずさ DNA 研究所において進められているヒト cDNA プロジェクトにおいて塩基配列が決定された遺

伝子である[63]。そのアミノ酸配列中にDHドメインとPHドメインに相同性を持つ領域を持つことからRhoGEFであることが予想されたが、その生化学・生理学的な解析はなされていなかった。そこで、新たに考案したシステムを用いて、KIAA0380がRhoを特異的に活性化することを示した。そして、KIAA0380の生体内での機能について、特に、神経系の細胞における役割について検討を加えた。

材料と方法

1) 遺伝子並びに抗体

pEF-BOS-RhoK、pEF-BOS-RhoK (KDTT)は、貝淵弘三博士(名古屋大学医学部)から供与して頂いた。pRK5-Myc-Rho、pRK5-Myc-Rac、pRK5-Myc-Cdc42、pRK5-Myc-L63Rho、pRK5-Myc-L61Rac、pRK5-Myc-L61Cdc42、pRK5-Myc-N19Rho は、A. Hall 博士(University College London, UK)から、pcDNA3.1-KIAA0380 は、長瀬隆弘博士(かずさ DNA 研究所)および T. Kozasa 博士(University of Texas)から、pEXV-Myc-p115RhoGEF は、G. Bollag 博士(Onyx Pharmaceuticals, CA)から、それぞれ供与していただいた。また、p115RhoGEF に対するポリクローナル抗体は G. Bollag 博士から供与していただいた。

2) 抗リン酸化モノクローナル抗体の作製

中間径フィラメントの 71 番目のセリン残基のリン酸化を認識するモノクローナル抗体(以下、TM71 と呼称)の作製法は、過去に報告した[61]ので、その詳細については省略し、概略を簡単に述べる。アミノ末端のアミノ酸をシステインとし、目的とするセリン残基の前後 5 残基のアミノ酸を含み、かつ、これらのセリン残基がリン酸化されているペプチド(CAVRLR[phosphoS71]SVPGV)を合成した。このペプチドを、Keyhole Limpet Homocyanin に結合させ、抗原として用いた。これをフロイントアジュバントとともにラットに免疫し、脾細胞をミエローマ細胞と融合させ、ハイブリドーマを作製した。

3) Rho キナーゼのキメラタンパク質と活性型 Rho キナーゼの作製

3-1) pRK5-Myc-VH-RhoK-WT

Rho キナーゼの野生型をコードしたプラスミド(pEF-BOS-Myc-RhoK-WT)を、制限酵素 BamHI で切断後、アガロースゲル電気泳動し、Rho キ

ナーゼをコードする配列(5.0 kbp)を切り出した。その断片を、哺乳動物細胞発現用プラスミドベクター pRK5 の BamHI サイトに挿入した(pRK5-RhoK-WT)。次に、マウスビメンチンの cDNA をテンプレートとして、5'プライマー(5'-cgggaattcgccatggaacaaaaactcctctcagaagaggatctgtctaccaggtctgtgtcctcg-3')と、3'プライマー(5'-gggggaactcagtgttgatgccgtcgg-3')で、PCR を行って、Myc タグとビメンチンのヘッドドメインをコードする DNA 断片を得た。その産物を制限酵素 EcoRI で処理し、pRK5-RhoK-WT の EcoRI-SmaI サイトに挿入した(pRK5-Myc-VH-RhoK-WT)。DNA シークエンスにより変異がないことを確認した。

3-2) pRK5-Myc-VH-RhoK-KDTT

Rho キナーゼのキナーゼドメインを不活化し、Rho 結合領域を削った変異体(pEF-BOS-RhoK-KDTT)をコードしたプラスミドを、制限酵素 BamHI で切断後、アガロースゲル電気泳動し、Rho キナーゼの不活性型変異体をコードする配列(2.0 kbp)を切り出した。その断片を、哺乳動物細胞発現用プラスミドベクター pRK5 の BamHI サイトに挿入した(pRK5-RhoK-KDTT)。次に、ビメンチンの cDNA をテンプレートとして、5'プライマー(5'-cgggaattcgccatggaacaaaaactcctctcagaagaggatctgtctaccaggtctgtgtcctcg-3')と、3'プライマー(5'-gggggaactcagtgttgatgccgtcgg-3')で、PCR を行って、Myc タグとビメンチンのヘッドドメインをコードする DNA 断片を得た。その産物を制限酵素 EcoRI で処理し、pRK5-RhoK-KDTT の EcoRI-SmaI サイトに挿入した(pRK5-Myc-VH-RhoK-KDTT)。DNA シークエンスにより変異がないことを確認した。

3-3) pRK5-Myc-RhoK-CAT

Rho キナーゼの制御ドメインを削り、構成的活性型にした Rho キナーゼをコードしたプラスミド(pEF-BOS-Myc-RhoK-CAT)を、制限酵素 BamHI で切断後、Rho キナーゼの構成的活性型をコードする配列(2.0 kbp)を切り

出した。その断片を、Myc タグ付加型哺乳動物細胞発現用プラスミドベクター pRK5-Myc の BamHI サイトに挿入した(pRK5-Myc-RhoK-CAT)。

4) FLAG タグを付加した Rho、Rac、Cdc42 の作製

pRK5-Myc-Rho、pRK5-Myc-Rac、pRK5-Myc-Cdc42 を制限酵素 BamHI-EcoRI で処理して、Rho、Rac、Cdc42 をコードする配列を切り出し、それぞれ FLAG タグ付加型 pRK5 ベクターの BamHI-EcoRI サイトに挿入した。

5) KIAA0380 の各種欠失変異体の作製

5-1) pRK5-Myc-KIAA0380FL

pcDNA3.1-HisC-KIAA0380 を制限酵素 NotI で切断後、その末端を Klenow 処理により平滑化し、さらに制限酵素 EcoRI-SalI で処理して、KIAA0380 の全長(aa 1-1522)をコードする配列(5.6 kbp)を Myc タグが付加した状態で切り出した。その断片を pRK5 ベクターの EcoRI-SmaI サイトに挿入した。

5-2) pRK5-Myc-KIAA0380ΔDH

まず、DH ドメインを欠いた KIAA0380 の RGS ドメインが、三量体 G タンパク質のαサブユニットを吸収することで、ドミナントネガティブ効果を持つことのないように、RGS ドメインに、変異(I364L, W365G, F368L, L369P)を導入した。変異の導入には、site-directed mutagenesis キット(Stratagene 社)を用いた。sense オリゴマー(5'-gcttggggaaagacctcgggaatattctcccggagaaaaatgcg-3')と anti-sense オリゴマー(5'-cgcatttttctccgggagaatattcccgaggtctttccccaagc-3')と、テンプレート(pRK5-Myc-KIAA0380)を用いて、PCR をかけ、反応液を制限酵素 DpnI で処理した後、大腸菌(DH5α)に形質転換した。大腸菌からプラスミドを回収し、正しく変異が導入されていることを DNA シークエンサーで確認した。次に、RGS ドメインに変異を導入した変異体(pRK5-Myc-KIAA0380RGSm)を

テンプレートとして DH ドメインを除いた上流(aa 1-735)と下流の配列(aa 958-1522)を PCR によってそれぞれ増幅し、結合することによって、DH ドメインの欠失変異体を作製した。まず、pRK5-Myc-KIAA0380RGSm をテンプレートとして、5'プライマー(5'-cggaattcgccatggaacaaaaactcatctcag-3')と3'プライマー(5'-ggggtaccctcattgatgacctcttgccg-3')で PCR をかけ、その産物を制限酵素 EcoRI-KpnI で処理して、上流の配列(2.4 kbp)を切り出し、クローニングベクター pUC19 の EcoRI-KpnI サイトに挿入した(pUC19-KIAA0380-DN-N)。次に、pRK5-Myc-KIAA0380RGSm をテンプレートとして、5'プライマー(5'-ggggtaccctggagagggccagcaac-3')と 3'プライマー(5'-gctctagattatggtcctggtgacgc-3')を用いて PCR をかけ、その産物を制限酵素 KpnI-XbaI で処理して、下流の配列(1.7 kbp)を切り出し、pUC19-KIAA0380-DN-N の KpnI-XbaI サイトに挿入した(pUC19-KIAA0380ΔDH)。最後に pUC19-KIAA0380ΔDH を制限酵素 EcoRI-XbaI で処理して、DH ドメインを削った KIAA0380 をコードする配列(4.1 kbp)を切り出し、pRK5 ベクターの EcoRI-XbaI サイトに挿入した。DNA シークエンスにより変異がないことを確認した。

5-3) pRK5-Myc-KIAA0380DH-PH-C

pcDNA3.1-HisC-KIAA0380 を、制限酵素 BamHI で処理し、KIAA0380 の DH ドメイン以降(aa 485-1522)をコードする配列(3.0 kbp)を切り出した。その断片を、pRK5-Myc ベクターの BamHI サイトに挿入した。

5-4) pRK5-Myc-KIAA0380DH-PH-Pro

pcDNA3.1-HisC-KIAA0380 をテンプレートとして、5'プライマー(5'-cgggatcccggcaagaggtcatcaatgag-3')と 3'プライマー(5'-cgggaattcttagaacacgtctgagtcatccagttc-3')で PCR を行って、KIAA0380 の DH-PH-Pro (aa 735-1119)をコードする配列(1.2 kbp)を得た。その産物を制限酵素 BamHI-EcoRI で処理し、pRK5-Myc ベクターの BamHI-EcoRI サイトに

挿入した。DNA シークエンスにより変異がないことを確認した。

5-5)　pRK5-Myc-KIAA0380RGS-DH-PH

pcDNA3.1-HisC-KIAA0380 をテンプレートとして、5'プライマー(5'-tcatattccaggatctggagaaactg-3')と 3'プライマー(5'-cgggaattcttagaacacgtctgagtcatccagttc-3')で PCR を行って、KIAA0380 の RGS-DH-PH (aa 301-1080)をコードする配列(2.3 kbp)を得た。その産物を制限酵素 BamHI-EcoRI で処理し、pRK5-Myc ベクターの BamHI-EcoRI サイトに挿入した。DNA シークエンスにより変異がないことを確認した。

5-6)　pRK5-Myc-KIAA0380DH-PH

pcDNA3.1-HisC-KIAA0380 をテンプレートとして、5'プライマー(5'-cggggatcccggcaagaggtcatcaatgag-3')と 3'プライマー(5'-cgggaattcttagtgcctggtggcattccgcacgg-3')で PCR を行って、KIAA0380 の DH-PH (aa 735-1080)をコードする配列(1.0 kbp)を得た。その産物を制限酵素 BamHI-EcoRI で処理し、pRK5-Myc ベクターの BamHI-EcoRI サイトに挿入した。DNA シークエンスにより変異がないことを確認した。

5-7)　pRK5-Myc-KIAA0380DH

pcDNA3.1-HisC-KIAA0380 をテンプレートとして、5'プライマー(5'-cggggatcccggcaagaggtcatcaatgag-3')と 3'プライマー(5'-cgggaattcttagctcttgaactctgctgccagg-3')で PCR を行って、KIAA0380 の DH (aa 735-958)をコードする配列(0.6 kbp)を得た。その産物を制限酵素 BamHI-EcoRI で処理し、pRK5-Myc ベクターの BamHI-EcoRI サイトに挿入した。DNA シークエンスにより変異がないことを確認した。

5-8)　pRK5-Myc-KIAA0380N

pRK5-Myc-KIAA0380FL を、制限酵素 EcoRI-BamHI で処理し、KIAA0380

の N 末端(aa 1-300, 301-592)をコードする配列(0.5, 0.9 kbp)を切り出した。その断片を、pRK5-Myc ベクターの EcoRI-BamHI サイトに挿入した。

5-9)　pRK5-Myc-KIAA0380C

pcDNA3.1-HisC-KIAA0380 を、制限酵素 BglII-XhoI で処理し、KIAA0380 の C 末端(aa 1056-1522)をコードする配列(1.9 kbp)を切り出した。その断片を、pRK5-Myc ベクターの BamHI-SalI サイトに挿入した。

6) KIAA0380 に対するポリクローナル抗体の作製

6-1) GST 融合型タンパク質発現用プラスミド DNA の作製

KIAA0380 を認識する抗体を作製するための抗原として、KIAA0380 のカルボキシル末端タンパク質断片(KIAA0380-ProC; aa 1080-1522)を用いた。pcDNA3.1-KIAA0380 をテンプレートとして、5'プライマー(5'-ccggaattccgaagaggccgtgcggaatgc-3')と 3'プライマー(5'-ataagaatgcggccgcttatggtcctggtgacgcgg-3')で PCR を行い、得られた産物を制限酵素 EcoRI-NotI で処理して、KIAA0380-ProC をコードする配列を得た。その断片を、GST 融合タンパク質発現用ベクター pGEX-4T3 の、EcoRI-NotI サイトに挿入した。プラスミドは、大腸菌 DH5αに導入した後、大量調整し、組みかえタンパク質として発現させるためのホストとなる大腸菌 BL21 (DE3)に形質転換した。

6-2) 抗原の大量調整

ホストとなる大腸菌を 100 ml のアンピシリン(最終濃度 100 μg/ml)を含む LB 培地(LB/Amp)で一昼夜、37 °C で振とう培養(230 rpm)し、翌日、900 ml の LB/Amp を加え、さらに 1 時間培養した。その後、培地に最終濃度 1 mM になるように isoproryl-β-D-thiogalactoside (IPTG)を添加し、30 °C で振とう培養(230 rpm)し、GST 融合タンパク質の発現を誘導した。4 時間後、培養液を遠心(5000 x g, 10 min.)により集菌し、その菌体は-20 °C で保存した。

以上の操作を繰り返し、大量の菌体を得た後、GST 融合タンパク質を精製した。保存しておいた菌体 25 ml を、冷却した 175 ml の溶解 buffer (50 mM Tris-HCl (pH 7.5), 50 mM NaCl, 5 mM $MgCl_2$, 1 mM DTT, 1 mM PMSF)に懸濁し、氷上で超音波破砕(SONIFIER model S125, BRANSON 社, LV 4, 10 sec. x 6)した。破砕液を遠心(12000 x g, 15 min., 4 °C)し、その上清を新しいチューブに移した。溶解 buffer を用いて 50 %の懸濁液にした 5 ml のグルタチオンセファロースビーズ(Amersham 社)を、チューブに添加して、穏やかに混和(4 °C, 30 min.)した。混和後、遠心(2000 x g, 5 min., 4 °C)してビーズを落とし、上清を除いた。ビーズを冷却した洗浄 buffer (50 mM Tris-HCl (pH 7.5), 150 mM NaCl, 5 mM $MgCl_2$, 1 mM DTT)に懸濁後、遠心(2000 x g, 5 min., 4 °C)し、洗浄した。洗浄を 3 回繰り返した後、カラムに詰め、溶出 buffer (5 mM のグルタチオンを含む洗浄 buffer)で溶出(1 ml x 8)し、各フラクションのタンパク質濃度をブラッドフォード法で測定した。タンパク質濃度の高いフラクションを集め、1 mg のタンパク質に対して、10 U のトロンビンを添加し、4 °C で 3 時間、穏やかに混和して、融合した GST と KIAA0380 を切断した。そのタンパク質溶液を、透析(50 mM Tris-HCl (pH 7.5), 50 mM NaCl, 5 mM $MgCl_2$, 1 mM DTT)し、グルタチオンを除いた後、洗浄 buffer を用いて 75 %の懸濁液にした 1 ml のグルタチオンセファロースビーズと、洗浄 buffer を用いて 75 %の懸濁液にした 50 μl の p-aminobenzamidine アガロースビーズ(Sigma 社)を加え、4 °C で一昼夜、穏やかに混和した。GST とトロンビンを各ビーズに吸着させた後、遠心(2000 x g, 5 min, 4 °C)してビーズを除き、溶液をセントリコン(Amicon 社)で 1 mg/ml 程度にまで濃縮した。濃縮したタンパク質溶液は液体窒素を用いて急速に凍結し、-80 °C で保存した。

6-3) 免疫

免疫する動物として、ニュージーランドホワイト(ウサギ、メス、体重 2 kg)を用いた。初回免疫は 1 mg の KIAA0380-ProC を完全フロイントアジ

ュバントで免疫し、その後 2 週間ごとに 0.5 mg の KIAA0380-ProC を不完全フロイントアジュバントで免疫した。3 回目の免疫から 2 週間後に全採血して、血液を 37 °C で 1 時間インキュベートした後、遠心(3000 rpm, 15 min.)した上清を抗 KIAA0380 血清とした。

6-4) 抗体の精製

抗原カラムを作製するために、2 ml の KIAA0380-ProC 溶液(1 mg/ml)を、0.1 M リン酸 buffer (pH 7.8)で透析した。そのタンパク質溶液に 0.2 g の AF-tresyl toyoparl ビーズ(TOHSO 社)を添加し、4 °C で一昼夜、穏やかに混和した。翌日、その懸濁液を 30 分間静置して、上清を除いた後、2.5 ml の固定化 buffer (0.1 M Tris-HCl (pH 8.0), 0.5 M NaCl)を添加し、4 °C で 1 時間、穏やかに混和した。その後、懸濁液を 30 分間静置し、上清を除いた。ビーズを 2 ml の 10 mM Tris-HCl (pH 7.5)に懸濁し、カラム(5 x 50 mm; 室町化学工業)に詰めた。カラムを、5 ml の buffer (50 mM Tris-HCl (pH 7.5))、5 ml の buffer (50 mM Tris-HCl (pH 7.5), 0.5 M NaCl)、10 ml の buffer (0.1 M glycine-HCl (pH 2.5))、10 ml の buffer (50 mM Tris-HCl (pH 7.5))で順番に洗浄した。56 °C で 30 分間インキュベートして非動化した 5 ml の抗 KIAA0380 血清を、カラムに通して、抗 KIAA0380 抗体をカラムに吸着させた。カラムを、15 ml の buffer (50 mM Tris-HCl (pH 7.5), 0.5M NaCl)、5 ml の buffer (50 mM Tris-HCl (pH 7.5))で順番に洗浄した後、溶出 buffer (0.1 M glycine-HCl (pH 2.5))で、カラムに吸着した抗体を溶出した(500 μl/tube)。溶出に際して、予め、1.5 ml 容のチューブに 150 μl の 1 M Tris-HCl (pH 8.0)を入れておき、一滴溶出される度に混和して、速やかに中和した。各フラクションのタンパク質濃度を測定し、タンパク濃度の高いものを透析(10 mM Tris-HCl (pH 7.5), 10 mM NaCl, 1 mM DTT)した。透析した抗体溶液は、分注(50 μl/tube)して液体窒素中で急速冷凍した後、-80°C で保存した。

7) 細胞培養

Swiss3T3、COS7、Neuro2a 細胞は、10 %ウシ胎児血清(FCS)を添加した Dulbecco's modified Eagle's medium (DMEM)中で、37 °C、5 % CO_2で培養した。MDCKII 細胞は、10 %のウシ血清を添加した DMEM 中で培養した。

8) マイクロインジェクション

マイクロインジェクションする DNA は DNA 精製キット(QIAGEN 社)で精製し、0.1 μg/μl となるように PBS で希釈した後、遠心(15000 x g, 30 min.)した上清を用いた。血清非存在下で 24 時間培養した Swiss3T3 細胞の核に、調製した DNA 溶液をインジェクター(Transjector 5246, Micro-manipulator 5171; Eppendorf 社)により注入した。3 時間後に細胞を固定、染色し、細胞を観察した。

9) トランスフェクション

COS7、Neuro2a 細胞へのトランスフェクションは、Lipofectamine (Gibco-BRL 社)を用いた。Lipofectamin の使用量は試薬に添付された説明書によったが、使用するプラスミド DNA 量は、各プラスミド DNA に応じて、細胞毒性を示さない程度に調節した。トランスフェクション後、24 時間経過したものを各実験に用いた。

10) 免疫細胞染色

24 穴または 6 穴プレートに、コラーゲンまたはポリ-D-リジンコートを施したカバースリップを入れ、その上に細胞をまいたものを免疫細胞染色に使用した。細胞は、冷却した PBS で軽く洗浄した後、冷却した 3.7 % ホルマリン(in PBS)中に 15 分間浸して固定した。例外的に、RhoA に対する抗体を使用するときには、10 % トリクロロ酢酸(in PBS)を用いて固定した。細胞を固定後、冷却した PBS 中に 5 分間浸して洗浄してから、0.2 % Triton X-100 (in PBS)中に 5 分間浸して細胞膜の透過性を上げた。再び、PBS で洗浄(5 min., x 2)し、免疫細胞染色用カバースリップとした。使用する一

次抗体を、10 %ヤギ血清を含む PBS で適度に希釈し、カバースリップ上に静かにのせ、37 °C で 2 時間インキュベートしたのち、PBS で洗浄(5 min., x 3)した。続いて、二次抗体を PBS で適度に希釈し、カバースリップ上に静かにのせた。アクチン繊維を共染色する必要があるときには、二次抗体希釈液に、0.4 unit/ml となるようにローダミン-ファロイジン溶液(Molecular Probes 社)を添加した。37 °C で 1 時間インキュベートした後、PBS で洗浄(5 min., x3)した。カバースリップが乾かないように注意しながら、蛍光保護剤(mowiol 4-88; CALBIOCHEM 社)を滴下したカバーグラス上に静かにのせて、マニキュアで封入した。強制発現させたタンパク質を観察するための一次抗体として抗 Myc タグモノクローナル抗体(9E10)を、その二次抗体として、FITC-labeled anti-mouse IgG (BIOSOURCE 社)を使用した。KIAA0380 を染色するために、一次抗体としてアフィニティ精製した抗 KIAA0380 抗体を、二次抗体として Alexa 488 anti-rabbit IgG (Molecular probes 社)を使用した。RhoA、チューブリン、ビメンチンを染めるために、抗 RhoA 抗体(Santa Cruz 社)、抗チューブリン抗体(Sigma 社)、抗ビメンチンマウスモノクローナル抗体(4H4)を、それぞれ使用した。細胞は共焦点レーザー顕微鏡(LSM-GB200, Olympus 社)を使用して観察した。

11) グアニンヌクレオチド交換活性

GST 融合タンパク質として発現するように設計された Rho、Rac、Cdc42、及び KIAA0380 の DH-PH ドメインを含む組みかえタンパク質(KIAA0380-RGS-DH-PH)は、大腸菌体内で組みかえタンパク質として発現させ、グルタチオンセファロースビーズを用いて精製した。GST-Rho、GST-Rac、GST-Cdc42、各 50 nmol を、100 μl の反応 buffer (50 mM Tris-HCl (pH 7.5), 1 mM DTT, 5 mM EDTA)に入れ、[^{35}S]でラベルした GTPγS (100 pmol, 4 kcpm/pmol)と共に、KIAA0380 の DH-PH ドメインを含む組みかえタンパク質(20 pmol)を添加した。室温で 10 分間反応させた後、洗浄 buffer (50 mM Tris-HCl (pH 7.5), 5 mM $MgCl_2$, 50 mM NaCl)で 1 ml になるように希釈し、

その希釈液を、洗浄 buffer でしめらせておいたニトロセルロースフィルター(45 mm, Schleicher and Schuell 社)にしみこませた。フィルターを、真空吸引できるようにトラップに取り付け、10 ml の洗浄 buffer をフィルターに透過させて、フィルターを洗浄した。フィルターを乾燥させた後、シンチレーションカウンターにより、フィルターに残存する GTPγS 結合型低分子量 G タンパク質の放射活性を測定した。

12) グアニンヌクレオチド結合状態解析

35 mm ディッシュに 75 %コンフルエントになるようにまいた COS7 細胞に、FLAG-Rho、FLAG-Rac、FLAG-Cdc42 を発現させ、同時に KIAA0380 を発現させたものとさせないものを用意した。リン酸を含まない DMEM に 0.1 mCi/ml の放射性リン酸を添加した培地中で 4 時間培養し、細胞をラベルした。ラベル後、溶解 buffer (20 mM Tris-HCl (pH 7.5), 150 mM NaCl, 20 mM $MgCl_2$, 1 mM Na_3VO_4, 0.5 % Triton X-100, 1 mM PMSF, 10 μg/ml aprotinin)で溶解し、溶解液をかき取り、チューブに移した。チューブを遠心(15000 x g, 15 min.)し、上清を新たなチューブに移した。チューブに 6 μg 相当の抗 FLAG モノクローナル抗体 M2 (Kodak 社)と、溶解 buffer を用いて 50 %の懸濁液にした 20 μl のプロテイン G セファロース 4B ビーズ (Amersham 社)を添加し、4 °C で穏やかに混和した。45 分後、チューブを遠心(15000 x g, 20 sec.)し、上清を除いた後、洗浄 buffer (20 mM Tris-HCl (pH 7.5), 150 mM NaCl, 20 mM $MgCl_2$, 1 mM Na_3VO_4, 0.5 % Triton X-100, 1 mM PMSF, 10 μg/ml aprotinin)で、ビーズを 2 度洗浄した後、12 μl のサンプル buffer (20 mM Tris-HCl (pH 7.5), 20 mM EDTA, 2 % SDS, 1 mM GTP, 1 mM GDP)を添加して、65 °C で 5 分間インキュベートした。チューブを遠心(15000 rpm, 20 sec.)してビーズを沈め、その上清から、0.5 μl の溶液を取ってバイアルにいれ、放射活性を測定した。検出された放射活性をもとに、各サンプルの総放射活性が等しくなるような、サンプル量を算出した。次に、ポリエチレンイミンシートの薄層(20 cm x 20 cm)を用意し、各 1 cm

の幅のレーンになるように、スパーテルの尾を使って薄層に溝を刻んだ。薄層をメタノールで軽く洗浄した後、薄層の下端から 2.5 cm のところに、印を付け、調製したサンプルをスポットした。スポットした薄層を展開槽にいれ、展開 buffer (0.6M H_2KPO_4-H_3PO_4 (pH 3.4))で展開した。展開後、薄層を乾かし、BAS 2500 (Fuji Film 社)により、放射活性を測定した。

13) ウエスタンブロッティング

各実験においてタンパク質を強制発現させた細胞は、冷却した PBS で洗浄した後、SDS サンプル buffer (50 mM Tris-HCl (pH 6.8), 2.5 % SDS, 4 % glycerol, 1.5 % 2-mercaptoethanol, 0.003 % bromo-phenol-blue)で溶解してかき取り、チューブに移した。チューブを熱し(98 °C, 3 min.)、タンパク質を熱変性した後、SDS ポリアクリルアミドゲル電気泳動にかけた。ゲルからタンパク質をニトロセルロース膜に転写し、5 % スキムミルクを TBS (20 mM Tris-HCl (pH 7.5), 150 mM NaCl)に溶かしたブロッキング溶液中で、膜をブロッキングした(室温, 30 min.)。ブロッキングした膜を、一次抗体溶液(一次抗体 in ブロッキング溶液)に浸し、室温で 2 時間振とうした。膜を、TBST (0.1 % Tween20 in TBS)で軽く洗った後、二次抗体溶液(二次抗体 in TBST)に浸し、室温で 1 時間振とうした。二次抗体として、horseradish-peroxidase を付加した IgG (Biorad 社)を用いた。二次抗体を反応させた後、TBST に浸し、20 分間振とうして洗浄した。3 回洗浄した後、TBST をふき取り、膜を乾かさないようにしながら、RENEISSANCE キット(NEM 社)で化学発光させた。膜をラップで包み、X 線フィルム(X-OMAT, Kodak 社)に感光させ、現像した。

14) 免疫沈降

10 cm ディッシュに 50 %コンフルエントになるように Neuro2a 細胞をまき、血清非存在下で 24 時間培養した後、400 μl の RIPA buffer (50 mM Tris-HCl (pH 7.5), 0.1 % SDS, 0.5 % deoxycholic acid, 1.0 % NP-40, 150 mM

NaCl, 3 mM PMSF, 20 μg/ml aprotinin, 20 μg/ml leupeptin)で溶解した。細胞溶解液を遠心(15000 x g, 4 °C, 10 min.)し、その上清を別のチューブに移した後、4 μg の精製抗体を添加した。4 °C で 1 時間穏やかに混和した後、RIPA buffer で 50 % の懸濁液にした 40 μl のプロテイン G セファロースビーズを添加した。続けて 4 °C で 1 時間穏やかに混和した後、上清を遠心(15000 rpm, 20 sec.)で除き、残ったプロテイン G ビーズを、1 ml の RIPA buffer で 3 回洗浄した。RIPA buffer を除いた後、プロテイン G ビーズを 40 μl の SDS-PAGE 用サンプル buffer に懸濁し、熱変性(98 °C, 3 min.)させたものをサンプルとして、SDS-PAGE 並びにウエスタンブロットで解析した。

結果

1) Rho シグナル伝達系の活性化状態の検出

我々は、ビメンチンのヘッドドメイン(VH)の 71 番目のセリン残基(以下 Ser71)が Rho キナーゼにより特異的にリン酸化されること、また、ラットモノクローナル抗体 TM71 は、その部位特異的なリン酸化を認識することを過去に報告した[62]。この特徴から、TM71 は、*in vivo* における Rho キナーゼのビメンチンリン酸化活性を検出するために有用なツールとなっている。そこで、Rho キナーゼのアミノ末端に直接 VH (2 番目から 87 番目のアミノ酸)を付加したキメラタンパク質(VH-RhoK)を作製し、この VH-RhoK が、Rho が活性化された際に、自己リン酸化キナーゼとしての特性を有するかどうかについて、TM71 を利用することで検討を加えた(図 4)。このように、VH を含むタンパク質断片と Rho キナーゼを融合した VH-RhoK は、Rho キナーゼ本来の細胞内局在を模倣することが期待され、細胞内での活性型 Rho キナーゼの分布・動態を解析できる可能性があると考えられた。

Rho キナーゼは、*in vivo*、*in vitro* のいずれにおいても、低分子量 GTPase である Rho によって活性化されることが示されている。そこで、細胞内において Rho が VH-RhoK を活性化したときに、付加した VH の Ser71 がリン酸化されるかどうかを検討した。COS7 細胞に、VH-RhoK と共に、低分子量 GTPase の各種変異型を強制発現させた後、その細胞を溶解し、TM71 及び抗 Myc モノクローナル抗体(9E10)を用いたウエスタンブロットで解析した。共発現させる低分子量 GTPase として、活性型 Rho (L63Rho)、不活性型 Rho (N19Rho)、活性型 Rac (L61Rac)、活性型 Cdc42 (L61Cdc42)を用いた。図 5 に示したように、活性型の Rho は Ser71 のリン酸化を強力に誘導したが、不活性型の Rho、活性型 Rac、活性型 Cdc42 は、リン酸化を誘導しなかった。この結果は、VH-RhoK の Ser71 が、活性型の Rho 依存的に特異的にリン酸化されることを示している。

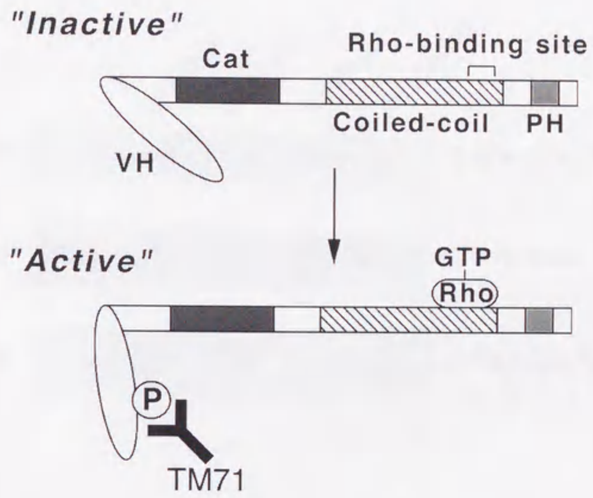

図 4　Rho シグナル伝達系の活性化検出法

Rho キナーゼのアミノ末端にビメンチンのヘッドドメイン(VH)を付加したキメラタンパク質を作製した。Rho 結合領域に活性型 Rho が結合し、VH を付加した Rho キナーゼが活性化されると、Rho キナーゼの活性ドメイン(Cat)近傍にある VH の 71 番目のセリン残基がリン酸化される。そのリン酸化を、抗リン酸化モノクローナル抗体(TM71)で検出する。

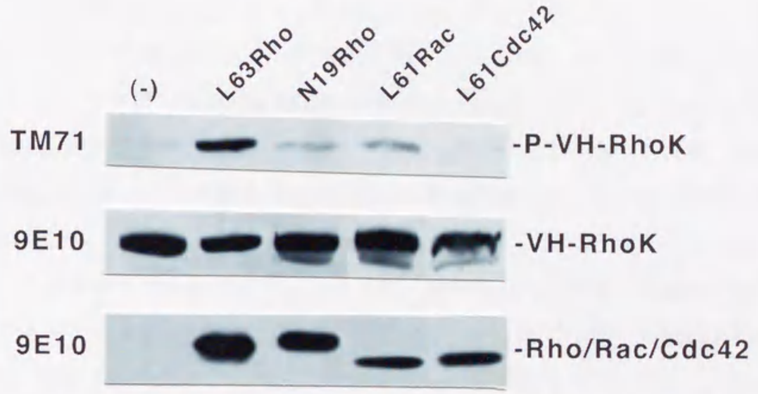

図 5　活性型 Rho による VH-RhoK のリン酸化

VH-RhoK と共に Myc タグを付加した活性型 Rho (L63Rho)、不活性型 Rho (N19Rho)、活性型 Rac (L61Rac)、活性型 Cdc42 (L61Cdc42) を COS7 細胞に発現させ、24 時間後に細胞を溶解してウエスタンブロットを行った。Myc タグ、Ser71 のリン酸化を、それぞれ抗 Myc モノクローナル抗体(9E10)、抗リン酸化モノクローナル抗体(TM71)で検出した。

図 6 に示したように、Ser71 のリン酸化には 2 種類のメカニズムが考えられる。一つは、活性化した VH-RhoK の分子内で自己リン酸化的におきるリン酸化(intramolecular)で、もう一方は、他の VH-RhoK、または内在性の RhoK によっておきるリン酸化(intermolecular)である。実際に検出されるリン酸化がどちらのメカニズムによるのか明らかにするために、次のような実験を行った。まず、野生型の Rho キナーゼに VH を付加したキメラタンパク質の他に、不活性型の Rho キナーゼに VH を付加したキメラタンパク質(VH-RhoK-KDTT)を作製した。そして、VH-RhoK、VH-RhoK-KDTT の遺伝子を COS7 細胞にトランスフェクションした後、血清存在下、あるいは非存在下において 24 時間培養した。その後、細胞を溶解し、ウエスタンブロットによって、Ser71 のリン酸化を検出できるかどうかを検討した。図 7 に示したように、血清存在下で培養した細胞では、Rho が活性化しているため、VH-RhoK の Ser71 のリン酸化が検出されるが、VH-RhoK-KDTT の Ser71 のリン酸化は検出されなかった。これは、キメラタンパク質の Ser71 が、同一分子内でリン酸化されていることを示している。また、COS7 細胞内で、VH-RhoK-KDTT と共に、活性型 Rho キナーゼ(CAT: 制御ドメインを欠き、常に活性型のキナーゼとして機能する)を共発現させると、内在性のビメンチンの Ser71 のリン酸化が検出されるにもかかわらず、VH-RhoK-KDTT の Ser71 のリン酸化は検出されない。すなわち、キメラタンパク質の VH は同一分子以外のキナーゼによってリン酸化されないことを示す。これらの結果より、VH-RhoK は Rho の活性依存的に、自己リン酸化(intramolecular)され、そのリン酸化を TM71 によって検出できることがわかった。

ところで、活性型 Rho キナーゼを発現させた場合は、内在性のビメンチンの Ser71 のリン酸化が検出されるが、血清による Rho の活性化では内在性のビメンチンの活性化は観察されなかった。これは、制御ドメインを欠いた活性型 Rho キナーゼが、上流の分子の制御を受けていないため、本来あるべき細胞内局在からはずれ、内在性のビメンチンをリン酸化する

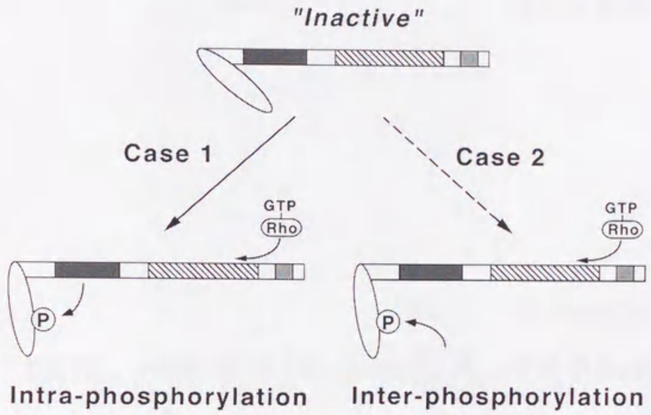

図 6　VH-RhoK のリン酸化機構に関するモデル

VH-RhoK の Ser71 のリン酸化は、「同一分子内でリン酸化される(intramolecular)」、または、「別の Rho キナーゼ分子によってリン酸化される(intermolecular)」、の 2 通り考えられる。

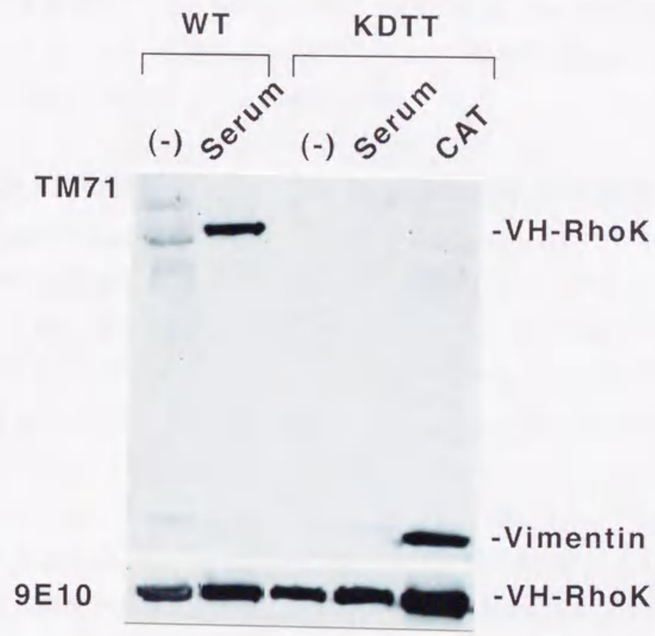

図 7　活性化された VH-RhoK の分子内リン酸化

野生型の Rho キナーゼにビメンチンのヘッドドメイン(VH)を付加したキメラタンパク質(WT)と、不活性型の Rho キナーゼに VH を付加したキメラタンパク質(KDTT)を、それぞれ COS7 細胞に発現させ、血清存在下または非存在下で 24 時間培養した後、細胞を溶解してウエスタンブロットした。Myc タグ、Ser71 のリン酸化を、それぞれ抗 Myc モノクローナル抗体(9E10)、抗リン酸化モノクローナル抗体(TM71)で検出した。血清存在下では Rho が活性化されるので、WT においては Ser71 がリン酸化されるが、KDTT では同一分子内のキナーゼ活性がないために Ser71 はリン酸化されない。また、KDTT と共に、制御ドメインを欠いた構成的活性型 Rho キナーゼを発現させると、内在性のビメンチンの Ser71 がリン酸化されるにもかかわらず、KDTT の Ser71 はリン酸化されない。

ためであると思われる。言い換えれば、VH-RhoK は、Rho から Rho キナーゼに至るシグナル伝達系の上流にある分子の制御下での活性化状態を反映して自己リン酸化していると考えられる。

2) KIAA0380 が有する Rho に対する特異的な GEF 活性

前段で検証した通り、新たに構築したシステムは、Rho シグナル伝達系の活性化状態を検出できることが示されたので、次に、このシステムを用いて、Rho の活性化因子の同定を試みた。対象とした分子は、KIAA0380 と呼ばれるタンパク質で、かずさ DNA 研究所で進められているヒト cDNA ランダムクローニングプロジェクトにおいて見いだされた分子である[63]。KIAA0380 は、PDZ ドメイン、RGS ドメイン、DH ドメイン、PH ドメイン、プロリンリッチモチーフなどの多くのドメイン構造をもっているが、なかでも DH-PH ドメインは Rho の活性化因子である Rho グアニンヌクレオチド交換因子(RhoGEF; Rho guanine nucleotide exchange factor)が持つ活性ドメインとして知られている。そこで、KIAA0380 が RhoGEF として機能し、Rho シグナル伝達系を活性化するのかどうかについて、新たに構築したシステムを用いて検討を試みた。

まず、トランスフェクションによって、COS7 細胞に VH-RhoK と KIAA0380、または活性ドメインである DH ドメインを欠いた KIAA0380ΔDH を共発現させた。24 時間培養後、細胞を溶解して、SDS-PAGE にて展開し、TM71 を用いたウエスタンブロットにより VH-RhoK の Ser71 のリン酸化を検出した。図 8 に示したように、既知の RhoGEF である p115RhoGEF を発現させたときと同様に、KIAA0380 を共発現させた場合にも、VH-RhoK の Ser71 のリン酸化が検出された。また、RhoGEF の活性ドメインである DH ドメインを欠いた変異型の KIAA0380ΔDH を発現させた際には、Ser71 のリン酸化は観察されなかった。したがって、KIAA0380 は、その DH ドメインの活性依存的に、Rho キナーゼシグナル伝達系を活性化する、すなわち、KIAA0380 が RhoGEF として機能してい

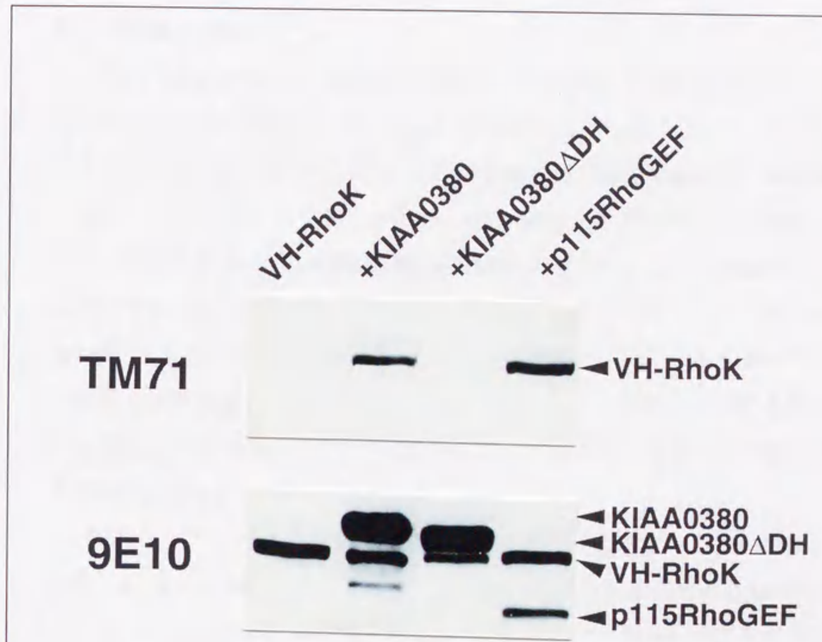

図 8　KIAA0380 による Rho の活性化

COS7 細胞に VH-RhoK と共に、KIAA0380、または GEF 活性ドメインである DH ドメインを欠いた KIAA0380ΔDH を共発現させ、24 時間培養後、細胞を溶解して、ウエスタンブロットした。Myc タグ、Ser71 のリン酸化を、それぞれ抗 Myc モノクローナル抗体(9E10)、抗リン酸化モノクローナル抗体(TM71)で検出した。ポジティブコントロールとしては、既知の RhoGEF である p115RhoGEF を用いた。VH-RhoK と共に KIAA0380 を発現させた場合には、VH-RhoK の Ser71 のリン酸化が検出されたが、活性ドメインである DH ドメインを欠いた変異型の KIAA0380ΔDH を共発現させても、Ser71 のリン酸化は観察されなかった。

ることが強く示唆された。

次に、KIAA0380 が、直接的に Rho の GTP/GDP 交換を促進しているのかどうかについて検討した。*in vitro* の実験として、あらかじめ GDP を結合させておいたレコンビナントタンパク質 Rho、Rac、Cdc42 に、GTPγS を添加してインキュベートしたとき、GTP 融合タンパク質として発現させた KIAA0380 断片(KIAA0380-RGS-DH-PH)の有無により、その交換活性が変化するかどうか比較した。図 9 に示したように、活性ドメインである DH-PH ドメインを含む KIAA0380 の断片は、Rho の GDP/GTP 交換活性を 3 倍近く上昇させるが、Rac、Cdc42 ではそのような活性化は認められなかった。この *in vitro* のデータについては、他のグループからも同様な結果が報告されている [64]。

Dbl ファミリー(Rho ファミリーの GEF)に属するタンパク質のいくつかは、*in vitro* と *in vivo* の間で異なった基質特異性を示すことがある [22,65]。そこで、*in vivo* の系における基質特異性も検討した。FLAG タグを付加した Rho、Rac、Cdc42 を発現させた COS7 細胞を放射性無機リン酸 ^{32}Pi を含む培地中で培養し、細胞内のリン酸をラベルした後、細胞を溶解し、FLAG タグに対する抗体で Rho、Rac、Cdc42 を免疫沈降した。沈降物を薄層上に展開し GTP と GDP を分離した後、そのオートラジオグラフを行うことで、Rho、Rac、Cdc42 に結合している GDP と GTP を定量した。図 10 に示したように活性型である GTP 結合型の Rho、Rac、Cdc42 の比率は、それぞれ 16.4%, 5.8%、5.9%であった。次に、同様の条件下で、KIAA0380 を共発現すると、活性型の Rho 比率は、34.4%まで上昇したが、Rac、Cdc42 については有意な上昇は認められなかった。この結果は、KIAA0380 が Rho 特異的な RhoGEF として *in vitro* のみならず *in vivo* でも機能していることを示しており、また、今回構築した Rho シグナル伝達系の活性化を検出するシステムが、そのシグナル伝達系を解析していく上で有効な方法であることを検証した。

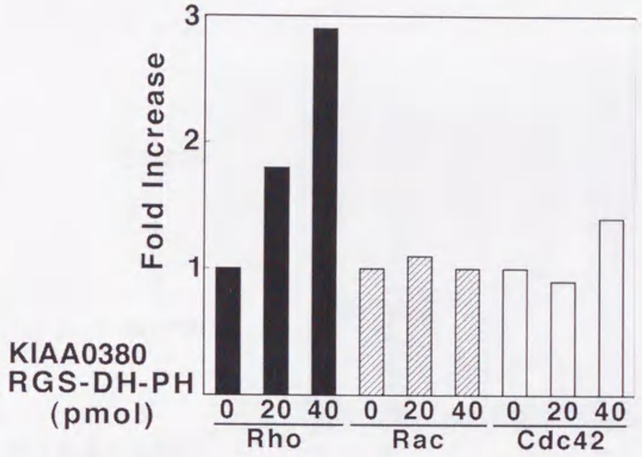

図 9　KIAA0380 が持つ Rho に特異的な GEF 活性

精製レコンビナントタンパク質 Rho、Rac、Cdc42（GDP 結合型）を含む反応液中に、[^{35}S]GTPγS を添加して GDP/GTP 交換反応を進めた。縦軸は反応後に Rho、Rac、Cdc42 に結合している[^{35}S]GTPγS 量の比を示す。GEF 活性ドメインである DH-PH ドメインを含む KIAA0380 断片(KIAA0380-RGS-DH-PH)により、Rho に結合する[^{35}S]GTPγS 量は 3 倍近く上昇したが、Rac、Cdc42 では、そのような上昇はみられなかった。

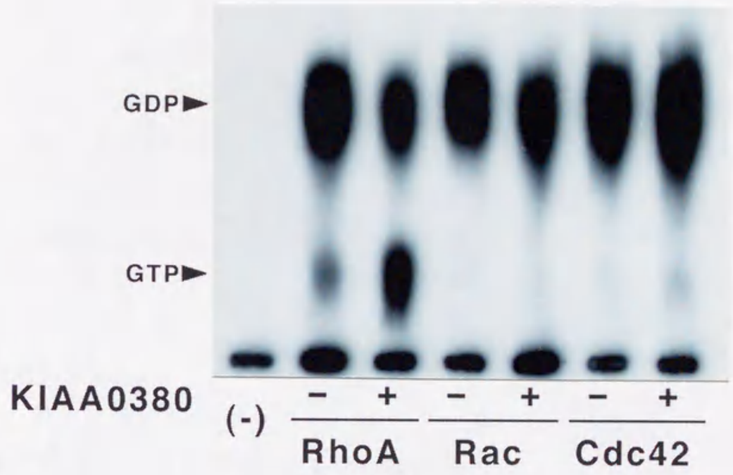

図 10　KIAA0380 が持つ Rho に特異的な GEF 活性

FLAG タグを付加した Rho、Rac、Cdc42 を発現させた COS7 細胞を、放射性無機リン酸 ^{32}Pi を含む培地中で培養し、細胞内のリン酸をラベルした後、細胞を溶解し、FLAG タグに対する抗体で Rho、Rac、Cdc42 を免疫沈降した。沈降物を薄層(ポリエチレンエミンシート)上に展開し GTP と GDP を分離した後、そのオートラジオグラフを行った。KIAA0380 を共発現させると、Rho に結合する GTP 量は特異的に増大した。

3) KIAA0380 が誘導する細胞の球状化

RhoGEF はアクチン細胞骨格系の制御に関与するシグナル伝達系に関与する分子であると考えられている。KIAA0380 が、どのようなアクチン細胞骨格の制御に関わっているのかを明らかにするために、さらなる解析を行った。まず、Myc タグを付加した KIAA0380 を発現するようなプラスミドを、Swiss3T3 細胞にマイクロインジェクションし、細胞の形態がどのように変化するのかを観察した(図 11)。KIAA0380 を発現した細胞は、9 割以上が顕著な球状化を引き起こし、強力な cortical アクチンの再構築を引き起こした。また、強制発現させた KIAA0380 は細胞膜の直下に局在し、再構築を起こしているアクチン繊維と同じ局在を示した。一方、ポジティブコントロールとして発現させた p115RhoGEF は、6 割以上の細胞においてアクチンストレスファイバーを誘導したが、細胞の球状化は引き起こさなかった。

4) プロリンリッチモチーフの重要性

KIAA0380 及び p115RhoGEF は、いずれも Rho シグナル伝達系を活性化するにもかかわらず、細胞内で強制発現させると異なった形態を誘導した。そのような差異をもたらすために重要な機能ドメインを明らかにするために、KIAA0380 の各種欠失変異体を作成し、それぞれの変異体が誘導する細胞の形態を比較した。図 12A に示したような各種欠失変異体を Swiss3T3 細胞で発現させ、細胞の形態をアクチン繊維の性状に着目して分類すると、3 種類に分けられることがわかった。すなわち、1)発現したタンパク質が細胞膜直下に限局して存在し、cortical アクチンの再構築が誘導され、細胞が球状化する。2)ストレスファイバーが形成されるが、細胞の球状化は引き起こさない。3)変化しない。の 3 つである(図 12B)。それらの結果を整理したものを図 13A にまとめた。つまり、cortical アクチンの再構築を誘導し、細胞の球状化を引き起こすためには、活性ドメインである DH-PH ドメインに加えて、その直後のカルボキシル末端側に存

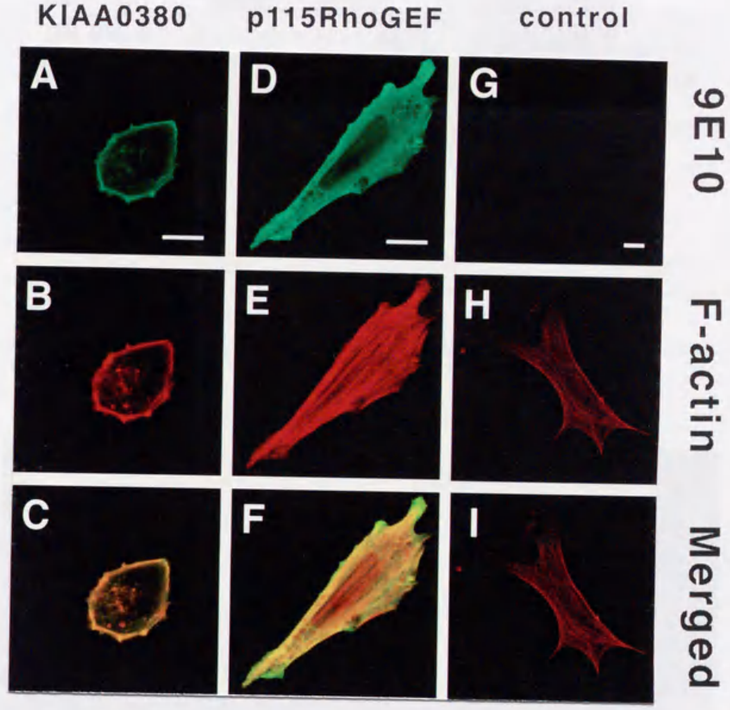

図 11　KIAA0380 を発現させた Swiss3T3 細胞の形態

血清非存在下で培養した Swiss3T3 細胞に、KIAA0380 または p115RhoGEF を発現するプラスミドをマイクロインジェクションした。3 時間後に細胞を固定し、間接蛍光抗体染色法により染色した。発現しているタンパク質(緑)は、1 次抗体として抗 Myc モノクローナル抗体(9E10)を、2 次抗体として抗マウス IgG-FITC を使用して染色した。アクチン繊維(赤)はローダミン-ファロイジンにより染色した。スケールバーは 10 μm。

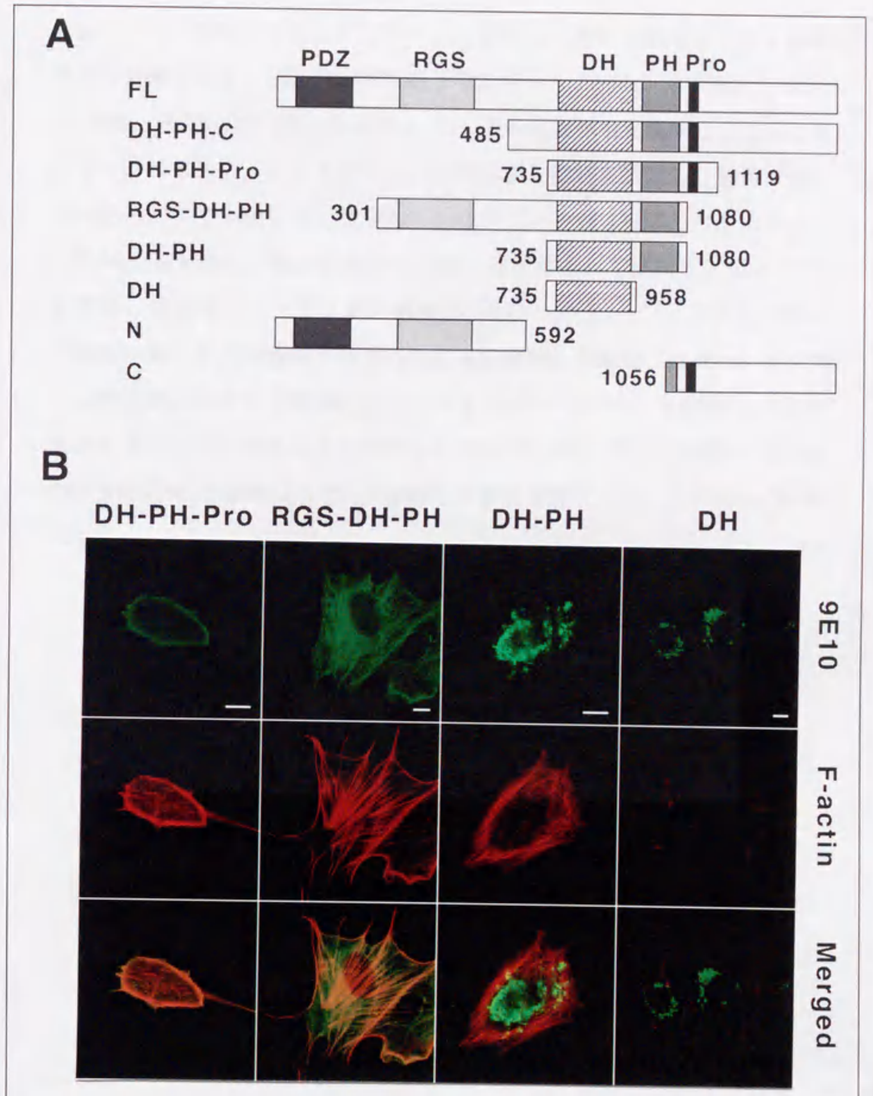

図 12　KIAA0380 の欠失変異体が誘導する細胞の形態

(A) KIAA0380 の各種欠失変異体。PDZ: PDZ ドメイン．RGS: RGS モチーフ．DH: Dbl homology ドメイン．PH: pleckstrin homology ドメ

イン．Pro: プロリンリッチモチーフ．図中に示された数字はアミノ酸配列上の位置を示す。(B) 血清非存在下で培養した Swiss3T3 細胞に、DH-PH-Pro、RGS-DH-PH、DH-PH、DH の各変異体を発現するプラスミドをマイクロインジェクションした。3 時間後に細胞を固定し、間接蛍光抗体染色法により染色した。発現しているタンパク質(緑)は、1 次抗体として抗 Myc モノクローナル抗体(9E10)を、2 次抗体として抗マウス IgG-FITC を使用して染色した。アクチン繊維(赤)はローダミン-ファロイジンにより染色した。欠失変異体を発現したときの細胞の形態は、cortical アクチンの再構築と球状化が誘導されているもの(DH-PH-Pro を参照)、ストレスファイバーが形成されるもの(RGS-DH-PH、DH-PH を参照)、変化しないもの(DH を参照)という 3 種類の形態に分類できた。スケールバーは 10 μm。

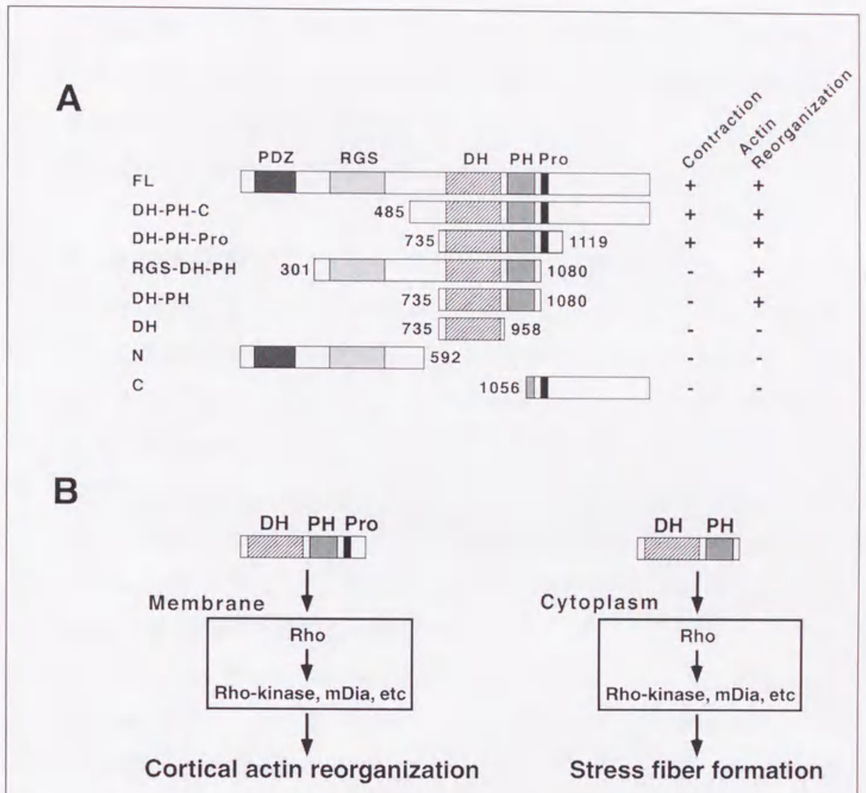

図 13　プロリンリッチモチーフの働きに関するモデル

A: 各欠失変異体を発現させたときの Swiss3T3 細胞の形態を示した。cortical アクチンの再構築が誘導され、球状化したものを「Contraction」、アクチンの再構築(ストレスファイバー形成を含む)が誘導されたものを「Actin Reorganization」とした。B: プロリンリッチモチーフの働きにより、細胞膜に局在する GEF が、その周囲に存在する Rho を活性化し、cortical アクチンの再構築を誘導する。

在するプロリンリッチモチーフが必須であり、DH-PH ドメインのみでは、アクチンストレスファイバーの形成を誘導するものの、細胞の球状化は引き起こさない。そして、DH-PH ドメインを欠くものではアクチン繊維に何ら変化を引き起こさないのである(図 13B)。

5) 他の細胞系においても誘導される細胞の球状化

KIAA0380 が引き起こす細胞の球状化という現象が、様々な細胞系において普遍的にみられる現象なのかどうか検証するため、Swiss3T3 細胞以外のいくつかの細胞系を用いて、KIAA0380 がもたらす形態変化を観察した。イヌ腎臓上皮系細胞である MDCKII 細胞は、足場依存的に一層の細胞集団を形成し、細胞同士が強固に接着する性質を持っている。この細胞に、KIAA0380 を発現させると、Swiss3T3 細胞を用いたときと同様の強力な cortical アクチンの再構築が誘導され、強固な細胞間接着に抗して球状化している様子が観察された(図 14)。

KIAA0380 の遺伝子転写産物量の組織特異性を、ノーザンブロットにより解析すると、脳に多く発現しているとの報告がある[63, 66]。そこで、マウス神経芽細胞種由来の Neuro2a 細胞において、KIAA0380 を強制発現させたときの形態変化を観察した(図 15)。通常、Neuro2a 細胞を血清非存在下で培養すると、細胞は扁平(flat)になり、神経突起の伸展が観察される。ところが、この細胞に KIAA0380 を発現させると、神経突起は伸展せず、細胞は球状化する。また、Swiss3T3 細胞や MDCKII 細胞と同様、KIAA0380 は細胞膜直下に限局して存在し、cortical アクチンの再構築が誘導された。これらの結果は、MDCKII 細胞や Neuro2a 細胞においても、KIAA0380 による Rho シグナル伝達系の活性化が、cortical アクチンの再構築を引き起こすことを示している。

6) 神経芽細胞 Neuro2a における KIAA0380 の発現

先に述べたように、KIAA0380 遺伝子の転写産物の組織特異性をノー

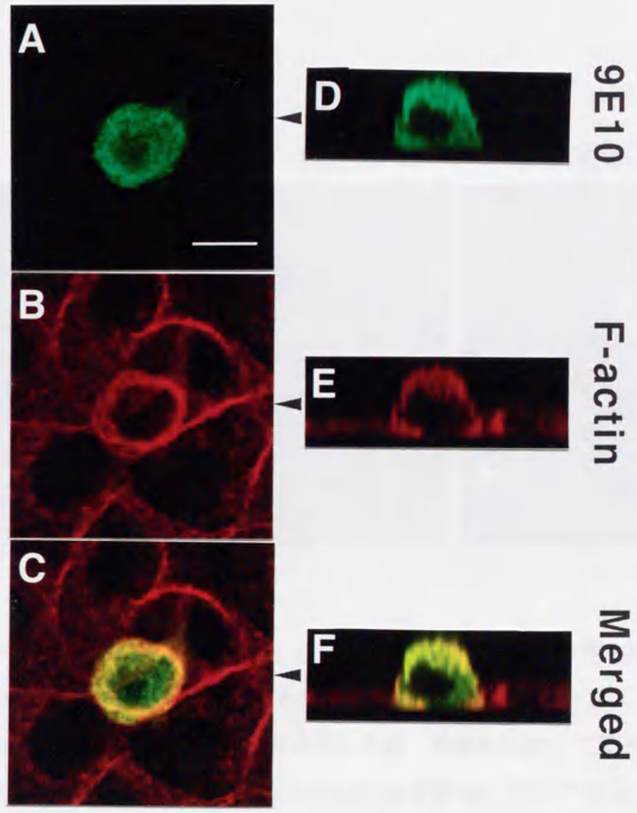

図 14　KIAA0380 を発現させた MDCKII 細胞の形態

血清非存在下で培養した MDCKII 細胞に、KIAA0380 を発現するプラスミドをマイクロインジェクションし、3 時間後に細胞を固定して染色した。発現しているタンパク質(緑)は、1 次抗体として抗 Myc モノクローナル抗体(9E10)を使用し、2 次抗体として抗マウス IgG-FITC を使用して染色した。アクチン繊維(赤)はローダミン-ファロイジンにより染色した。左側(A, B, C)は X-Y 平面の観察像で、右側(D, E, F)は、それぞれの矢頭の位置での X-Z 断面像である。スケールバーは 10 μm。

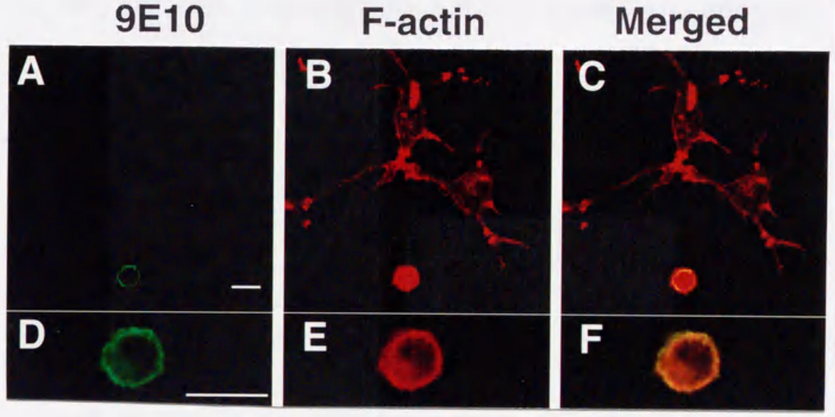

図 15　KIAA0380 を発現させた Neuro2a 細胞の形態

Neuro2a 細胞に、KIAA0380 を発現するプラスミドをトランスフェクションし、血清非存在下で 24 時間培養した後、細胞を固定して染色した。発現しているタンパク質(緑)は、1 次抗体として抗 Myc モノクローナル抗体(9E10)を、2 次抗体として抗マウス IgG-FITC を使用して染色した。アクチン繊維(赤)はローダミン-ファロイジンにより染色した。下段(D, E, F)は、上段(A, B, C)の視野中で、KIAA0380 を発現している細胞をさらに拡大し、共焦点レーザー顕微鏡で観察したものである。スケールバーは、10μm。

ザンブロットで解析すると、脳に多く発現しているという報告があるが、タンパク質レベルでも KIAA0380 が脳に多く発現しているのかどうかは明らかではない。そこで、神経系の細胞における KIAA0380 の発現並びに局在を解析するために、KIAA0380 の抗体を作製した。まず、組みかえタンパク質として発現した KIAA0380 のカルボキシル末端側断片(aa 1056-1522)を抗原として、ウサギに免疫して得た血清から、同じ抗原を固定化したアフィニティクロマトグラフィーを用いて抗体を精製した。そして、その抗体を用いて、マウス神経芽細胞種由来の Neuro2a 細胞に KIAA0380 が発現しているかどうかを免疫沈降によって検討した。図 16 に示したとおり、Neuro2a 細胞は KIAA0380 をタンパク質レベルで十分量発現していることがわかった。一方、RGS ドメイン構造を持つ RhoGEF であるという点で KIAA0380 と近縁の p115RhoGEF の発現を、同様の免疫沈降により検討したが、Neuro2a においてはタンパク質レベルの発現が認められなかった。

神経系由来の株化された培養細胞において、Rho が大きく関わっている現象として、受容体にカップリングした三量体 G タンパク質に依存的な神経突起の退縮がある。特に、リゾフォスファチジン酸(LPA)の刺激によって活性化される Rho シグナル伝達系は、G_{12} あるいは G_{13} タンパク質を介しているとが考えられており、G_{12} や G_{13} タンパク質のαサブユニットが結合する RGS ドメインをもつ RhoGEF は、そのシグナル伝達系の一員である可能性が高い。RGS ドメインを持つ RhoGEF である KIAA0380 と p115RhoGEF のうち、KIAA0380 のみを発現し、かつ、神経突起を形成するという Neuro2a の特性は、神経系の細胞での Rho シグナル伝達系における RhoGEF の役割を解析するうえで、有効な細胞系であると考えた。

7) Neuro2a 細胞における KIAA0380 の細胞内局在

Neuro2a に発現している内在性の KIAA0380 の細胞内局在を明らかにするために、アフィニティー精製した抗 KIAA0380 ポリクローナル抗体を用いて免疫染色を行った。図 17 に示したように、血清非存在下で培養し

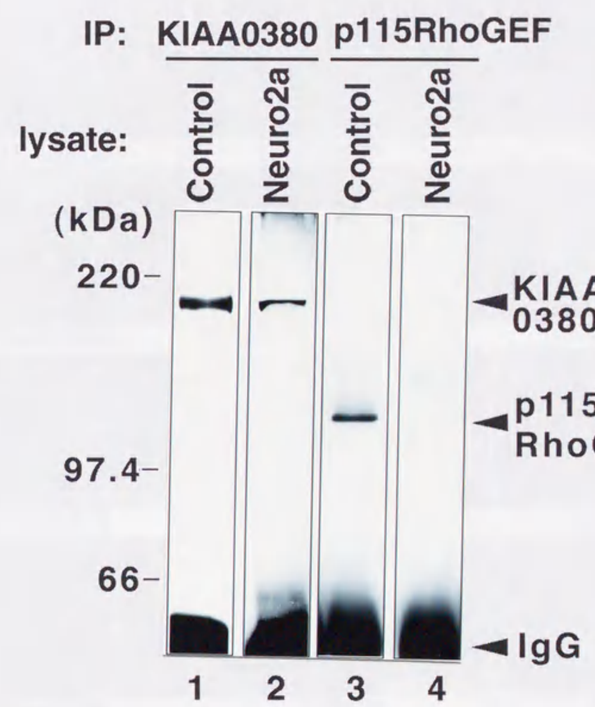

図 16　Neuro2a 細胞における内在性の KIAA0380 の発現

Neuro2a 細胞の溶解液に KIAA0380 の抗体(レーン 2)、p115RhoGEF (レーン 4)の抗体を添加し、内在性のタンパク質を免疫沈降した。KIAA0380 (レーン 1)、p115RhoGEF (レーン 3)をトランスフェクションにより COS7 細胞内で強制発現させ、それぞれに対する抗体を用いて免疫沈降したものをコントロールとした。各沈降物を SDS-PAGE して、KIAA0380 の抗体(レーン 1、2)、p115RhoGEF の抗体(レーン 3、4)でウエスタンブロットした。

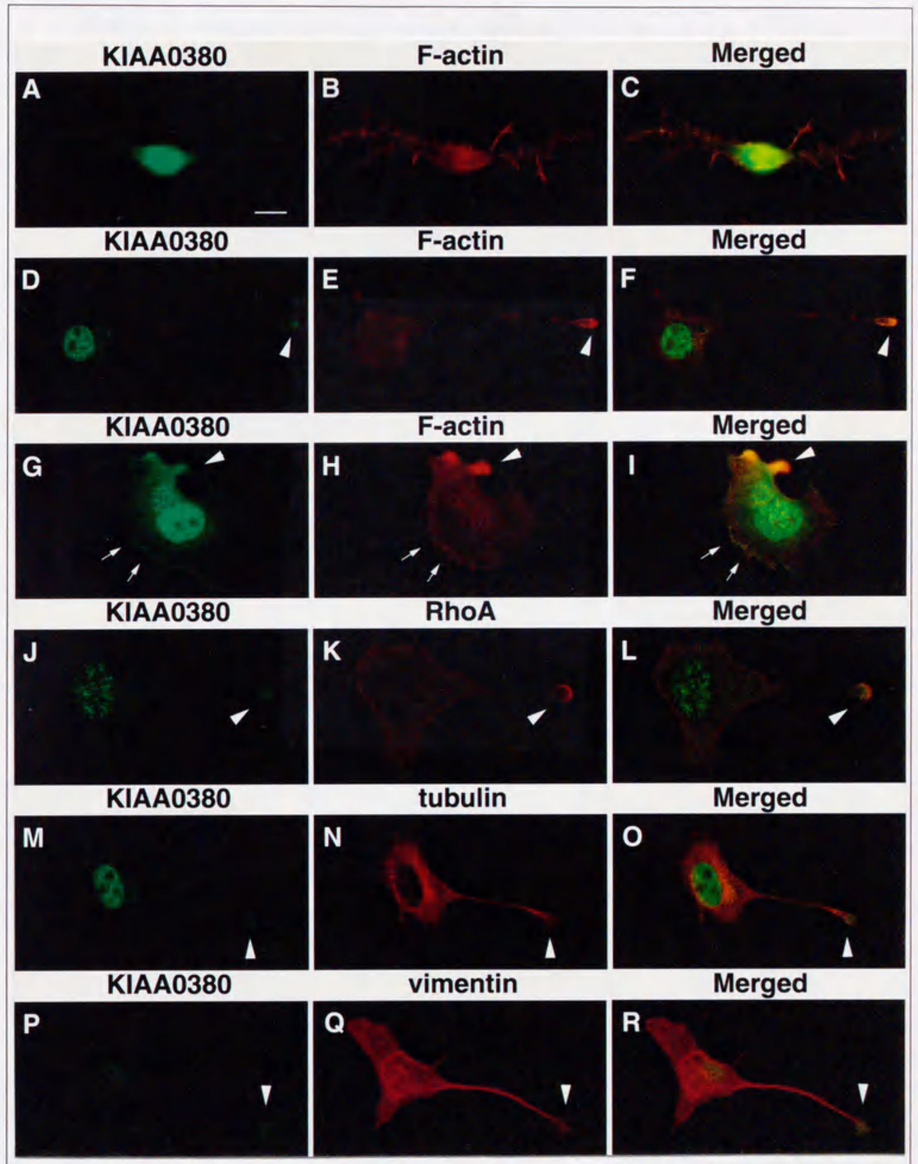

図 17　Neuro2a 細胞における KIAA0380 の細胞内局在

Neuro2a 細胞を血清非存在下で 24 時間培養し、突起を伸展した細胞を、3.7 % ホルマリンで固定した(A–C)。1 μM の LPA で刺激した後、3

分後(D, E, F)および 10 分後(G, H, I)に細胞を固定した。RhoA との二重染色をした細胞は、10 % トリクロロ酢酸で固定し、チューブリン、ビメンチンとの二重染色をした細胞は 3.7 % ホルマリンで固定した。細胞を固定後、0.2 % Triton X-100 で処理し、間接蛍光抗体染色法で染色した。1 次抗体として KIAA0380 の抗体(左側)、抗 RhoA 抗体(K)、抗チューブリン抗体(N)、抗ビメンチン抗体(Q)を用い、2 次抗体として Alexa 488 anti-rabbit IgG (左側)、Cy3 anti-mouse IgG(K, N, Q)を用いた。アクチン繊維の染色には、ローダミン-ファロイジンを用いた。突起を伸展した細胞を LPA で刺激すると、突起の退縮と細胞の球状化が誘導され、突起の先端部(D-F, G-I; 矢頭)や、細胞の周辺部に形成される actin shell と呼ばれる構造体(G-I; 矢印)に KIAA0380 が存在している様子が観察された。

た Neuro2a 細胞は、突起を伸展する。この状態で、KIAA0380 の抗体を用いて間接抗体染色法により内在性の KIAA0380 の局在を観察したところ、核が特に強く染色され、細胞質が全体的に薄く染色されたが、アクチン細胞骨格系の性状と比較した上では、際だって特徴的なパターンは観察されなかった(図 17、A-C)。しかし、1 μM のリゾフォスファチジン酸(LPA)により刺激して、突起の退縮を誘導して観察したところ、cortical アクチンが再構築を起こしている突起の先端部に、KIAA0380 が集積している様子が観察された(図 17、D-F)。LPA による細胞への刺激をさらに強くすると、伸展した突起は完全に退縮し、扁平な細胞が球状化していく。半ば突起が退縮した状態で細胞を固定し、KIAA0380 の局在を同様に観察したところ、突起が退縮したと思われる部位と(図 17、G-H; 矢頭)、細胞周辺部の cortical actin shell が形成されている場所(図 17、G-H; 矢印)に、KIAA0380 が集積していた。また、KIAA0380 が Rho 特異的な RhoGEF であることから、RhoA に対する抗体を用いて、KIAA0380 を RhoA を二重染色して観察したところ、RhoA も突起の先端部(図 17、J-L; 矢頭)に集積していた。一方、アクチン以外の細胞骨格であるチューブリン、ビメンチンについても二重染色を行ったが、一部重なり合う領域が存在する(図 17、M-R; 矢頭)ものの、KIAA0380 と全く同じ局在を示すことはなかった。すなわち、KIAA0380 と RhoA が共局在する細胞内の領域において、アクチンの再構築が誘導されている様子が観察された。神経突起の先端部におけるアクチン細胞骨格制御は、神経細胞のアクソンガイダンスに重要な成長円錐の制御を想起させる。今回得られた結果は、神経細胞のアクソンガイダンスにおける Rho シグナル伝達系の機構に KIAA0380 が関与している可能性を示すものである。

また、KIAA0380 は LPA 刺激に非依存的な核への局在も示したが、その理由はよくわからない。しかしながら、他の RhoGEF (Ect2)においても、その機能との結びつきがよくわからないものの、細胞周期の間期において核への集積がみられるような例もあり [21]、何らかの意味があるのかもしれ

ない。

8) 神経突起の退縮を制御するシグナル伝達系への関与

神経細胞において、LPA は、Rho を活性化することにより成長円錐の崩壊や神経突起の退縮を誘導する。そのシグナル伝達系は、チロシンキナーゼの活性が関与し、G_{12} あるいは G_{13} タンパク質を介していると考えられている [9, 67, 68]。G_{13} タンパク質を介した Rho シグナル伝達系に関与する RhoGEF としては、p115RhoGEF が知られおり [69]、*in vitro* の系において、G_{13} 依存的に Rho を活性化することが示されている。ところが、p115RhoGEF は主に造血性細胞に特異的に発現しており [70]、今回用いた神経芽種由来の Neuro2a 細胞には発現していない。

そこで、Neuro2a 細胞において、LPA 依存的な突起の退縮を誘導するシグナル伝達系に、KIAA0380 が関与しているかどうかを検討した。図 8 に示したように、DH ドメインを持たない KIAA0380 の変異体は、Rho に対する GEF 活性を持っていないので、DH ドメイン以下を欠いた KIAA0380 のN末端は、KIAA0380 のドミナントネガティブ変異体として作用することが期待された。そこで、この変異体を強制発現させた Neuro2a 細胞を LPA で刺激し、突起退縮に対する阻害効果がみられるかどうかを調べた。35 mm ディッシュに 40 %コンフルエントになるように播種した Neuro2a 細胞に、Myc タグを付加した KIAA0380 の N 末端をコードする発現プラスミド DNA (10 μg)をトランスフェクションした。コントロールとしては、ベクターに緑色蛍光タンパク質(GFP)を組み込んだプラスミド DNA を用いた。血清非存在下において 24 時間培養した後、1 μM の LPA で 3 分間刺激し、細胞を固定して細胞の形態を観察した。図 18 に示したように、KIAA0380 の N 末端は、LPA による突起の退縮および、細胞の球状化を有意に阻害した。KIAA0380 の N 末端には G_{12} あるいは G_{13} のαサブユニット($G\alpha_{12}$ あるいは $G\alpha_{13}$)が結合する RGS ドメインと、タンパク質-タンパク質相互作用に重要なドメインである PDZ ドメインが存在する。KIAA0380 の阻害

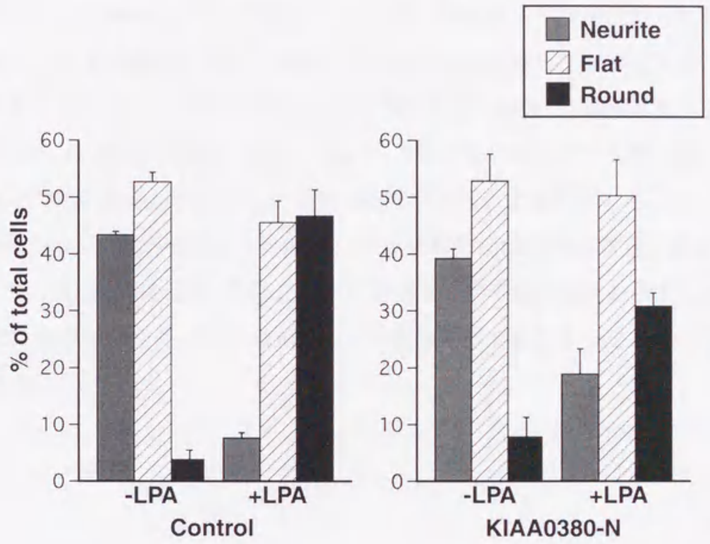

図 18　N 末端による突起の退縮に対する阻害効果

Neuro2a 細胞に、KIAA0380 の N 末端をコードする発現プラスミド DNA (10 μg)をトランスフェクションした。コントロールとしては、ベクターに緑色蛍光タンパク質(GFP)を組み込んだプラスミド DNA を用いた。血清非存在下において 24 時間培養した後、1 μM の LPA で 3 分間刺激し突起の退縮を誘導した。細胞を染色し、細胞の形態を「細胞の直径以上にその突起を伸展している(Neurite)」「突起の伸展は細胞の直径以下だが、扁平な形をしている(Flat)」「球状化している(Round)」の 3 つにわけて、その細胞数を計測した。それぞれ 100〜200 個の細胞のサンプリングを、独立して 3 回行い、その標準偏差を示した。

作用は、主に活性型の $G\alpha_{12}$ あるいは $G\alpha_{13}$ を吸収することによるものと思われるが、生体のシグナル伝達においては PDZ ドメインも協調した機能を持っている可能性もあり、それらの複合的な結果として阻害効果を示すのかもしれない。いずれにせよ、以上の結果は、LPA 受容体とカップリングした G タンパク質を介して Rho へと伝えられるシグナル伝達系に、KIAA0380 が関与していることを強く示唆するものである。

ところで、KIAA0380 の N 末端による突起退縮の阻害は完全ではない。これは、KIAA0380 の N 末端を過度に発現させると細胞毒性を示すため、完全に阻害するために十分な量の N 末端を発現できなかったためと考えられた。

考察

我々は、*in vivo* において Rho シグナル伝達系の活性化・不活性化状態を検出するシステムを確立し、そのシステムが RhoGEF の様な Rho やその下流分子の Rho キナーゼを活性化する因子を同定することが可能であることを示した。つまり、このシステムを用いて、KIAA0380 が Rho シグナル伝達系を活性化することを、*in vivo* で同定したのである。

さらに、KIAA0380 の各種変異体を細胞に発現させ、アクチン細胞骨格系の再構築と細胞の形態に及ぼす影響を、各種の細胞を用いて検討した。過去の報告によれば、神経芽種由来の N1E-115 細胞を用いた実験において、LPA により誘導されるストレスファイバーの形成と cortical アクチンの収縮は、別の現象であるとの興味深い報告がなされている [5]。報告によれば、細胞膜に移行できない活性型 Rho はストレスファイバーの形成を誘導できるが cortical アクチンの収縮は誘導できない、すなわち、LPA により誘導される cortical アクチンの収縮には Rho が細胞膜に移行することが必要であるらしい。しかしながら、Rho が LPA による刺激を受けて活性化された後、Rho が膜へ移行するのか、膜へ移行した Rho が RhoGEF によって活性化されるのかについては明らかではなかった。我々は、KIAA0380 の欠失変異体を用いた実験によって、ストレスファイバーの形成には、KIAA0380 の DH-PH ドメインで十分であるが、cortical アクチンの収縮を引き起こすためには、DH-PH ドメインに加え、その C 末端側下流にあるプロリンリッチモチーフが必要であることを明らかにした。すなわち、「ストレスファイバーの形成」と「cortical アクチンの収縮」という、アクチン細胞骨格が制御する 2 つの現象を、RhoGEF のレベルで分けることができた。

他の RhoGEF である Tiam1 においても、PH ドメインの C 末端側下流の領域が、アクチン細胞骨格の制御に重要であるとの報告がある。Tiam1 がラッフリングを引き起こすためには、DH-PH ドメインに加えて、PH ド

メインの下流に 40 アミノ酸からなる coiled-coil ドメイン様の配列と、それに続く 300 アミノ酸からなる配列が必要である[71]。今回我々が行った実験の結果は、Rho の活性化における RhoGEF の働きに関して、新たな分子機構の存在を示唆するものである。KIAA0380 の各種変異体を細胞内で強制発現させた時の細胞内局在を観察すると、DH-PH は細胞質中で斑点状に、DH-PH-Pro は細胞膜直下に、それぞれ局在することがわかる。つまり、DH-PH は、細胞質中の Rho を活性化してストレスファイバーを誘導し、DH-PH-Pro は、細胞膜直下、あるいはその近傍に存在する Rho を活性化することで cortical アクチンの収縮を引き起こすのではないかと考えられるのである。

現在までに、三量体 G タンパク質である G_{12} ファミリー(G_{12} および G_{13})が、Rho 依存的なストレスファイバーと接着斑の形成に関係していることが明らかにされている[72]。繊維芽細胞においては、構成的活性型の G_{12} や G_{13} のαサブユニット($G\alpha_{12}$ および $G\alpha_{13}$)は、ストレスファイバーの形成だけでなく、SRF 転写因子[74]の活性化やホスホリパーゼ D の活性化[74, 75]など、Rho の活性化により誘導される多くの現象を誘導する。Swiss3T3 細胞においては、$G\alpha_{12}$ と $G\alpha_{13}$ は Rho を活性化するが、$G\alpha_{i2}$ は Rho を活性化しない[72]。三量体 G タンパク質にカップリングしている受容体と、Rho の活性化との関係についても研究が進められており、そのシグナル伝達系に関わる分子が同定されつつある。例えば、LPA によって誘導される Rho の活性化は $G\alpha_{12}$ あるいは $G\alpha_{13}$ を介しており、トロンビンにより誘導される Rho の活性化は $G\alpha_{12}$ を介している[73]ことが明らかとなっている。また、神経細胞においても、神経突起の伸展、あるいは退縮を制御する生化学的なシグナルを解析することによって多くの知見が蓄積されつつある。いくつかの神経系の細胞において、LPA 受容体を始め、EP3 受容体やトロンビン受容体のようなある種の受容体とカップリングした三量体 G タンパク質が活性化すると、Rho 依存的に突起の退縮が誘導される[6,7, 77, 78]。これらの報告によると、三量体 G タンパク質の活性化により誘導される神経突

起の退縮には、Rho 依存的な cortical アクチンの収縮力が重要であるらしい。

生化学的には、p115RhoGEF が RGS ドメインを介して $G\alpha_{12}$ や $G\alpha_{13}$ と結合すること、また、$G\alpha_{13}$ により特異的に活性化されることが示されていた [69]。神経細胞において、成長円錐の崩壊、神経突起の退縮、細胞の球状化は $G\alpha_{12}$ や $G\alpha_{13}$ 依存的な現象であるから、$G\alpha_{12}$ や $G\alpha_{13}$ と結合するために必要な RGS ドメインを持つ RhoGEF が、神経突起の退縮に関与する分子であることが推測された。現在までに、RGS ドメインを持ち、$G\alpha_{12}$ や $G\alpha_{13}$ が相互作用する RhoGEF としては、p115RhoGEF と KIAA0380 が同定されている。各組織間における p115RhoGEF 遺伝子の転写量をノーザンブロットにより解析すると、p115RhoGEF は末梢血赤血球と胸腺と脾臓で多く発現しており、脳にはほとんど転写はみられない [79]。本論においても、神経芽種由来の Neuro2a 細胞での p115RhoGEF のタンパク質の発現はみられなかった。対照的に、KIAA0380 は、脳において転写産物量が特に多く、Neuro2a においてもタンパク質レベルで十分な発現がみられた。そこで、神経系の細胞においては、p115RhoGEF と似通った機構、すなわち $G\alpha_{12}$ や $G\alpha_{13}$ により直接活性化され、そのシグナルを Rho に伝える役割を、KIAA0380 が担っている可能性が考えられた。Neuro2a 細胞を用いた免疫染色の結果、KIAA0380 は、細胞体だけではなく、cortical アクチンの再構築が起こっている突起の先端部にも多く存在していた。また、COS7 細胞での強制発現系を用いた実験により、KIAA0380 が構成的活性型の $G\alpha_{12}$ や $G\alpha_{13}$ と結合することが報告されている [66]。これらの結果より、*in vivo* において、$G\alpha_{12}$ や $G\alpha_{13}$ が KIAA0380 を制御しているという可能性は十分に考えられる。我々は、KIAA0380 が $G\alpha_{12}$ や $G\alpha_{13}$ の制御下にあるのかどうかについて検討を試みたが、強制発現系では KIAA0380 が常に活性型となるために、Rho の活性化の増大を検出することはできなかった。おそらく、KIAA0380 に対する内在性の制御因子、あるいは阻害因子の量が、強制発現させた KIAA0380 に対して十分でないためであろう。

我々は、神経系の細胞における KIAA0380 の機能を解析するために、Neuro2a 細胞を用いた。Neuro2a 細胞は、LPA や血清によって誘導される Rho を介したシグナル伝達系の活性化により、速やかに突起が退縮するという特性をもつ。我々は、Neuro2a 細胞における LPA 依存的な突起退縮を制御するシグナル伝達系に KIAA0380 が関与していると考えている。この仮説は、LPA により誘導される神経突起の退縮が KIAA0380 の N 末端のタンパク質断片により阻害されるという結果に基づいている。今回の実験では、KIAA0380 の N 末端による突起退縮の阻害は完全ではない。しかしながら、KIAA0380 の N 末端の過剰な発現が細胞毒性を示すために、突起の退縮を完全に阻害するために充分な量の KIAA0380 の N 末端を発現させることができなかったためであろうと考えている。

他の研究者たちにより、完全な cortical アクチンの収縮のためには、Rho が細胞膜に局在する必要があるとの報告がなされている [5]。しかし、Rho の活性化、すなわち GTP/GDP 交換反応が細胞内のどこで起きるのかについては、まだ明らかではない。Rho が活性化されることで引き起こされる「cortical アクチンの収縮」と「ストレスファイバーの形成」という 2 つの現象が、RhoGEF のレベルで分離できるという今回の知見は、上流からのシグナルを受けた Rho が活性化される場の決定に関して、RhoGEF が重要な役割を演じていることを示唆するものである。

参考文献

1. A. J. Ridley and A. Hall. 1992. The small GTP-binding protein rho regulates the assembly of focal adhesions and actin stress fibers in response to growth factors. *Cell* **70:**389-99.

2. A. J. Ridley, H. F. Paterson, C. L. Johnston, D. Diekmann and A. Hall. 1992. The small GTP-binding protein rac regulates growth factor-induced membrane ruffling. *Cell* **70:**401-10.

3. C. D. Nobes and A. Hall. 1995. Rho, rac, and cdc42 GTPases regulate the assembly of multimolecular focal complexes associated with actin stress fibers, lamellipodia, and filopodia. *Cell* **81:**53-62.

4. R. Kozma, S. Ahmed, A. Best and L. Lim. 1995. The Ras-related protein Cdc42Hs and bradykinin promote formation of peripheral actin microspikes and filopodia in Swiss 3T3 fibroblasts. *Mol Cell Biol* **15:**1942-52.

5. O. Kranenburg, M. Poland, M. Gebbink, L. Oomen and W. H. Moolenaar. 1997. Dissociation of LPA-induced cytoskeletal contraction from stress fiber formation by differential localization of RhoA. *J Cell Sci* **110:**2417-27.

6. K. Jalink, T. Eichholtz, F. R. Postma, E. J. van Corven and W. H. Moolenaar. 1993. Lysophosphatidic acid induces neuronal shape changes via a novel, receptor-mediated signaling pathway: similarity to thrombin action. *Cell Growth Differ* **4:**247-55.

7. K. Jalink, E. J. van Corven, T. Hengeveld, N. Morii, S. Narumiya and W. H.

Moolenaar. 1994. Inhibition of lysophosphatidate- and thrombin-induced neurite retraction and neuronal cell rounding by ADP ribosylation of the small GTP-binding protein Rho. *J Cell Biol* **126:**801-10.

8. R. Kozma, S. Sarner, S. Ahmed and L. Lim. 1997. Rho family GTPases and neuronal growth cone remodelling: relationship between increased complexity induced by Cdc42Hs, Rac1, and acetylcholine and collapse induced by RhoA and lysophosphatidic acid. *Mol Cell Biol* **17:**1201-11.

9. O. Kranenburg, M. Poland, F. P. van Horck, D. Drechsel, A. Hall and W. H. Moolenaar. 1999. Activation of RhoA by lysophosphatidic acid and $G\alpha_{12/13}$ subunits in neuronal cells: induction of neurite retraction. *Mol Biol Cell* **10:**1851-7.

10. F. N. Leeuwen, H. E. Kain, R. A. Kammen, F. Michiels, O. W. Kranenburg and J. G. Collard. 1997. The guanine nucleotide exchange factor Tiam1 affects neuronal morphology; opposing roles for the small GTPases Rac and Rho. *J Cell Biol* **139:**797-807.

11. R. A. Cerione and Y. Zheng. 1996. The Dbl family of oncogenes. *Curr Opin Cell Biol* **8:**216-22.

12. N. Lamarche and A. Hall. 1994. GAPs for rho-related GTPases. *Trends Genet* **10:**436-40.

13. T. Ueda, A. Kikuchi, N. Ohga, J. Yamamoto and Y. Takai. 1990. Purification and characterization from bovine brain cytosol of a novel regulatory protein inhibiting the dissociation of GDP from and the subsequent binding of GTP to

rhoB p20, a ras p21-like GTP-binding protein. *J Biol Chem* **265:**9373-80.

14. A. Eva and S. A. Aaronson. 1985. Isolation of a new human oncogene from a diffuse B-cell lymphoma. *Nature* **316:**273-5.

15. M. J. Hart, A. Eva, T. Evans, S. A. Aaronson and R. A. Cerione. 1991. Catalysis of guanine nucleotide exchange on the CDC42Hs protein by the dbl oncogene product. *Nature* **354:**311-4.

16. D. Ron, M. Zannini, M. Lewis, R. B. Wickner, L. T. Hunt, G. Graziani, S. R. Tronick, S. A. Aaronson and A. Eva. 1991. A region of proto-dbl essential for its transforming activity shows sequence similarity to a yeast cell cycle gene, CDC24, and the human breakpoint cluster gene, bcr. *New Biol* **3:**372-9.

17. C. M. Hart and J. W. Roberts. 1994. Deletion analysis of the lambda tR1 termination region. Effect of sequences near the transcript release sites, and the minimum length of rho-dependent transcripts. *J Mol Biol* **237:**255-65.

18. Y. Zheng, D. Zangrilli, R. A. Cerione and A. Eva. 1996. The pleckstrin homology domain mediates transformation by oncogenic dbl through specific intracellular targeting. *J Biol Chem* **271:**19017-20.

19. G. G. Habets, E. H. Scholtes, D. Zuydgeest, R. A. van der Kammen, J. C. Stam, A. Berns and J. G. Collard. 1994. Identification of an invasion inducing gene, Tiam-1, that encodes a protein with homology to GDP GTP exchangers for Rho-like proteins. *Cell* **77:**537-49.

20. N. G. Pasteris, A. Cadle, L. J. Logie, M. E. Porteous, C. E. Schwartz, R. E.

Stevenson, T. W. Glover, R. S. Wilroy and J. L. Gorski. 1994. Isolation and characterization of the faciogenital dysplasia (Aarskog- Scott syndrome) gene: a putative Rho/Rac guanine nucleotide exchange factor. *Cell* **79:**669-78.

21. T. Tatsumoto, X. Xie, R. Blumenthal, I. Okamoto and T. Miki. 1999. Human ECT2 is an exchange factor for Rho GTPases, phosphorylated in G2/M phases, and involved in cytokinesis. *J Cell Biol* **147:**921-8.

22. M. F. Olson, N. G. Pasteris, J. L. Gorski and A. Hall. 1996. Faciogenital dysplasia protein (FGD1) and Vav, two related proteins required for normal embryonic development, are upstream regulators of Rho GTPases. *Curr Biol* **6:**1628-33.

23. F. Michiels, J. C. Stam, P. L. Hordijk, R. A. van der Kammen, L. Ruuls-Van Stalle, C. A. Feltkamp and J. G. Collard. 1997. Regulated membrane localization of Tiam1, mediated by the NH2-terminal pleckstrin homology domain, is required for Rac-dependent membrane ruffling and C-Jun NH2-terminal kinase activation. *J Cell Biol* **137:**387-98.

24. K. Kimura, M. Ito, M. Amano, K. Chihara, Y. Fukata, M. Nakafuku, B. Yamamori, J. Feng, T. Nakano, K. Okawa, A. Iwamatsu and K. Kaibuchi. 1996. Regulation of myosin phosphatase by Rho and Rho-associated kinase (Rho-kinase) [see comments]. *Science* **273:**245-8.

25. M. Amano, M. Ito, K. Kimura, Y. Fukata, K. Chihara, T. Nakano, Y. Matsuura and K. Kaibuchi. 1996. Phosphorylation and activation of myosin by Rho associated kinase (Rho- kinase). *J Biol Chem* **271:**20246-9.

26. K. Chihara, M. Amano, N. Nakamura, T. Yano, M. Shibata, T. Tokui, H. Ichikawa, R. Ikebe, M. Ikebe and K. Kaibuchi. 1997. Cytoskeletal rearrangements and transcriptional activation of c-fos serum response element by Rho-kinase. *J Biol Chem* **272:**25121-7.

27. T. Matsui, M. Maeda, Y. Doi, S. Yonemura, M. Amano, K. Kaibuchi and S. Tsukita. 1998. Rho-kinase phosphorylates COOH-terminal threonines of ezrin/radixin/moesin (ERM) proteins and regulates their head-to-tail association. *J Cell Biol* **140:**647-57.

28. Y. Fukata, K. Kimura, N. Oshiro, H. Saya, Y. Matsuura and K. Kaibuchi. 1998. Association of the myosin-binding subunit of myosin phosphatase and moesin: dual regulation of moesin phosphorylation by Rho associated kinase and myosin phosphatase. *J Cell Biol* **141:**409-18.

29. K. Kimura, Y. Fukata, Y. Matsuoka, V. Bennett, Y. Matsuura, K. Okawa, A. Iwamatsu and K. Kaibuchi. 1998. Regulation of the association of adducin with actin filaments by Rho- associated kinase (Rho-kinase) and myosin phosphatase. *J Biol Chem* **273:**5542-8.

30. M. Amano, K. Chihara, K. Kimura, Y. Fukata, N. Nakamura, Y. Matsuura and K. Kaibuchi. 1997. Formation of actin stress fibers and focal adhesions enhanced by Rho- kinase. *Science* **275:**1308-11.

31. T. Leung, X. Q. Chen, E. Manser and L. Lim. 1996. The p160 RhoA-binding kinase ROK alpha is a member of a kinase family and is involved in the reorganization of the cytoskeleton. *Mol Cell Biol* **16:**5313-27.

32. T. Ishizaki, M. Naito, K. Fujisawa, M. Maekawa, N. Watanabe, Y. Saito and S. Narumiya. 1997. p160ROCK, a Rho-associated coiled-coil forming protein kinase, works downstream of Rho and induces focal adhesions. *FEBS Lett* **404:**118-24.

33. Y. Kureishi, S. Kobayashi, M. Amano, K. Kimura, H. Kanaide, T. Nakano, K. Kaibuchi and M. Ito. 1997. Rho-associated kinase directly induces smooth muscle contraction through myosin light chain phosphorylation. *J Biol Chem* **272:**12257-60.

34. Y. Yasui, M. Amano, K. Nagata, N. Inagaki, H. Nakamura, H. Saya, K. Kaibuchi and M. Inagaki. 1998. Roles of Rho-associated kinase in cytokinesis; mutations in Rho- associated kinase phosphorylation sites impair cytokinetic segregation of glial filaments. *J Cell Biol* **143:**1249-58.

35. H. Goto, H. Kosako and M. Inagaki. 2000. Regulation of intermediate filament organization during cytokinesis: possible roles of Rho associated kinase. *Microsc Res Tech* **49:**173-82.

36. M. Amano, K. Chihara, N. Nakamura, Y. Fukata, T. Yano, M. Shibata, M. Ikebe and K. Kaibuchi. 1998. Myosin II activation promotes neurite retraction during the action of Rho and Rho-kinase. *Genes Cells* **3:**177 88.

37. H. Katoh, J. Aoki, Y. Yamaguchi, Y. Kitano, A. Ichikawa and M. Negishi. 1998. Constitutively active Galpha12, Galpha13, and Galphaq induce Rho-dependent neurite retraction through different signaling pathways. *J Biol Chem* **273:**28700-7.

38. E. Lazarides. 1980. Intermediate filaments as mechanical integrators of cellular space. *Nature* **283:**249-256.

39. P. M. Steinert and D. R. Roop. 1988. Molecular and cellular biology of intermediate filaments. *Annu Rev Biochem* **57:**593-625.

40. E. Fuchs and K. Weber. 1994. Intermediate filaments: structure, dynamics, function, and disease. *Annu Rev Biochem* **63:**345-82.

41. M. Inagaki, Y. Nishi, K. Nishizawa, M. Matsuyama and C. Sato. 1987. Site specific phosphorylation induces disassembly of vimentin filaments in vitro. *Nature* **328:**649-52.

42. M. Inagaki, Y. Gonda, M. Matsuyama, K. Nishizawa, Y. Nishi and C. Sato. 1988. Intermediate filament reconstitution in vitro. The role of phosphorylation on the assembly-disassembly of desmin. *J Biol Chem* **263:**5970-8.

43. R. M. Evans. 1988. Cyclic AMP-dependent protein kinase-induced vimentin filament disassembly involves modification of the N-terminal domain of intermediate filament subunits. *FEBS Lett* **234:**73-8.

44. T. Tokui, T. Yamauchi, T. Yano, Y. Nishi, M. Kusagawa, R. Yatani and M. Inagaki. 1990. Ca2(+)-calmodulin-dependent protein kinase II phosphorylates various types of non-epithelial intermediate filament proteins. *Biochem Biophys Res Commun* **169:**896-904.

45. Y. H. Chou, J. R. Bischoff, D. Beach and R. D. Goldman. 1990. Intermediate filament reorganization during mitosis is mediated by p34cdc2 phosphorylation of

vimentin. *Cell* **62:**1063-71.

46. M. Inagaki, Y. Gonda, K. Nishizawa, S. Kitamura, C. Sato, S. Ando, K. Tanabe, K. Kikuchi, S. Tsuiki and Y. Nishi. 1990. Phosphorylation sites linked to glial filament disassembly in vitro locate in a non-alpha helical head domain. *J Biol Chem* **265:**4722-9.

47. M. Kusubata, T. Tokui, Y. Matsuoka, E. Okumura, K. Tachibana, S. Hisanaga, T. Kishimoto, H. Yasuda, M. Kamijo, Y. Ohba and et al. 1992. p13suc1 suppresses the catalytic function of p34cdc2 kinase for intermediate filament proteins, in vitro. *J Biol Chem* **267:**20937-42.

48. K. Tsujimura, J. Tanaka, S. Ando, Y. Matsuoka, M. Kusubata, H. Sugiura, T. Yamauchi and M. Inagaki. 1994. Identification of phosphorylation sites on glial fibrillary acidic protein for cdc2 kinase and Ca(2+) calmodulin-dependent protein kinase II. *J Biochem (Tokyo)* **116:**426-34.

49. N. Geisler and K. Weber. 1988. Phosphorylation of desmin in vitro inhibits formation of intermediate filaments; identification of three kinase A sites in the aminoterminal head domain. *Embo J* **7:**15-20.

50. M. Kusubata, Y. Matsuoka, K. Tsujimura, H. Ito, S. Ando, M. Kamijo, H. Yasuda, Y. Ohba, E. Okumura, T. Kishimoto and et al. 1993. cdc2 kinase phosphorylation of desmin at three serine/threonine residues in the amino-terminal head domain. *Biochem Biophys Res Commun* **190:**927 34.

51. T. Yano, T. Tokui, Y. Nishi, K. Nishizawa, M. Shibata, K. Kikuchi, S. Tsuiki, T. Yamauchi and M. Inagaki. 1991. Phosphorylation of keratin intermediate

filaments by protein kinase C, by calmodulin-dependent protein kinase and by cAMP-dependent protein kinase. *Eur J Biochem* **197:**281-90.

52. J. Tanaka, M. Ogawara, S. Ando, M. Shibata, R. Yatani, M. Kusagawa and M. Inagaki. 1993. Phosphorylation of a 62 kd porcine alpha-internexin, a newly identified intermediate filament protein. *Biochem Biophys Res Commun* **196:**115-23.

53. Y. Nakamura, M. Takeda, K. J. Angelides, T. Tanaka, K. Tada and T. Nishimura. 1990. Effect of phosphorylation on 68 KDa neurofilament subunit protein assembly by the cyclic AMP dependent protein kinase in vitro. *Biochem Biophys Res Commun* **169:**744-50.

54. Y. Gonda, K. Nishizawa, S. Ando, S. Kitamura, Y. Minoura, Y. Nishi and M. Inagaki. 1990. Involvement of protein kinase C in the regulation of assembly-disassembly of neurofilaments in vitro. *Biochem Biophys Res Commun* **167:**1316-25.

55. K. Nishizawa, T. Yano, M. Shibata, S. Ando, S. Saga, T. Takahashi and M. Inagaki. 1991. Specific localization of phosphointermediate filament protein in the constricted area of dividing cells. *J Biol Chem* **266:**3074-9.

56. T. Yano, C. Taura, M. Shibata, Y. Hirono, S. Ando, M. Kusubata, T. Takahashi and M. Inagaki. 1991. A monoclonal antibody to the phosphorylated form of glial fibrillary acidic protein: application to a non-radioactive method for measuring protein kinase activities. *Biochem Biophys Res Commun* **175:**1144-51.

57. Y. Matsuoka, K. Nishizawa, T. Yano, M. Shibata, S. Ando, T. Takahashi and

M. Inagaki. 1992. Two different protein kinases act on a different time schedule as glial filament kinases during mitosis. *Embo J* **11:**2895 902.

58. K. Tsujimura, M. Ogawara, Y. Takeuchi, S. Imajoh-Ohmi, M. H. Ha and M. Inagaki. 1994. Visualization and function of vimentin phosphorylation by cdc2 kinase during mitosis. *J Biol Chem* **269:**31097-106.

59. M. Ogawara, N. Inagaki, K. Tsujimura, Y. Takai, M. Sekimata, M. H. Ha, S. Imajoh-Ohmi, S. Hirai, S. Ohno, H. Sugiura and et al. 1995. Differential targeting of protein kinase C and CaM kinase II signalings to vimentin. *J Cell Biol* **131:**1055-66.

60. M. Sekimata, K. Tsujimura, J. Tanaka, Y. Takeuchi, N. Inagaki and M. Inagaki. 1996. Detection of protein kinase activity specifically activated at metaphase-anaphase transition. *J Cell Biol* **132:**635-41.

61. Y. Takai, M. Ogawara, Y. Tomono, C. Moritoh, S. Imajoh-Ohmi, O. Tsutsumi, Y. Taketani and M. Inagaki. 1996. Mitosis-specific phosphorylation of vimentin by protein kinase C coupled with reorganization of intracellular membranes. *J Cell Biol* **133:**141-9.

62. H. Kosako, H. Goto, M. Yanagida, K. Matsuzawa, M. Fujita, Y. Tomono, T. Okigaki, H. Odai, K. Kaibuchi and M. Inagaki. 1999. Specific accumulation of Rho-associated kinase at the cleavage furrow during cytokinesis: cleavage furrow-specific phosphorylation of intermediate filaments. *Oncogene* **18:**2783-8.

63. T. Nagase, K. Ishikawa, D. Nakajima, M. Ohira, N. Seki, N. Miyajima, A. Tanaka, H. Kotani, N. Nomura and O. Ohara. 1997. Prediction of the coding

sequences of unidentified human genes. VII. The complete sequences of 100 new cDNA clones from brain which can code for large proteins in vitro. *DNA Res* **4:**141-50.

64. U. Rumenapp, A. Blomquist, G. Schworer, H. Schablowski, A. Psoma and K. H. Jakobs. 1999. Rho-specific binding and guanine nucleotide exchange catalysis by KIAA0380, a dbl family member. *FEBS Lett* **459:**313-8.

65. P. Crespo, K. E. Schuebel, A. A. Ostrom, J. S. Gutkind and X. R. Bustelo. 1997. Phosphotyrosine-dependent activation of Rac-1 GDP/GTP exchange by the vav proto-oncogene product. *Nature* **385:**169-72.

66. S. Fukuhara, C. Murga, M. Zohar, T. Igishi and J. S. Gutkind. 1999. A novel PDZ domain containing guanine nucleotide exchange factor links heterotrimeric G proteins to Rho. *J Biol Chem* **274:**5868-79.

67. C. D. Nobes, P. Hawkins, L. Stephens and A. Hall. 1995. Activation of the small GTP-binding proteins rho and rac by growth factor receptors. *J Cell Sci* **108:**225-33.

68. A. Gohla, R. Harhammer and G. Schultz. 1998. The G-protein G13 but not G12 mediates signaling from lysophosphatidic acid receptor via epidermal growth factor receptor to Rho. *J Biol Chem* **273:**4653-9.

69. M. J. Hart, X. Jiang, T. Kozasa, W. Roscoe, W. D. Singer, A. G. Gilman, P. C. Sternweis and G. Bollag. 1998. Direct stimulation of the guanine nucleotide exchange activity of p115 RhoGEF by Galpha13 [see comments]. *Science* **280:**2112-4.

70. H. C. Aasheim, F. Pedeutour and E. B. Smeland. 1997. Characterization, expression and chromosomal localization of a human gene homologous to the mouse Lsc oncogene, with strongest expression in hematopoetic tissues. *Oncogene* **14:**1747-52.

71. J. C. Stam, E. E. Sander, F. Michiels, F. N. van Leeuwen, H. E. Kain, R. A. van der Kammen and J. G. Collard. 1997. Targeting of Tiam1 to the plasma membrane requires the cooperative function of the N-terminal pleckstrin homology domain and an adjacent protein interaction domain. *J Biol Chem* **272:**28447-54.

72. A. M. Buhl, N. L. Johnson, N. Dhanasekaran and G. L. Johnson. 1995. G alpha 12 and G alpha 13 stimulate Rho-dependent stress fiber formation and focal adhesion assembly. *J Biol Chem* **270:**24631-4.

73. C. Fromm, O. A. Coso, S. Montaner, N. Xu and J. S. Gutkind. 1997. The small GTP-binding protein Rho links G protein-coupled receptors and Galpha12 to the serum response element and to cellular transformation. *Proc Natl Acad Sci U S A* **94:**10098-103.

74. M. Majumdar, T. M. Seasholtz, C. Buckmaster, D. Toksoz and J. H. Brown. 1999. A Rho Exchange Factor Mediates Thrombin and Galpha(12)-induced Cytoskeletal Responses. *J Biol Chem* **274:**26815-26821.

75. K. C. Malcolm, A. H. Ross, R. G. Qiu, M. Symons and J. H. Exton. 1994. Activation of rat liver phospholipase D by the small GTP-binding protein RhoA. *J Biol Chem* **269:**25951-4.

76. E. P. Bowman, D. J. Uhlinger and J. D. Lambeth. 1993. Neutrophil phospholipase D is activated by a membrane-associated Rho family small molecular weight GTP-binding protein. *J Biol Chem* **268:**21509 12.

77. G. Tigyi, D. J. Fischer, A. Sebok, F. Marshall, D. L. Dyer and R. Miledi. 1996. Lysophosphatidic acid-induced neurite retraction in PC12 cells: neurite- protective effects of cyclic AMP signaling. *J Neurochem* **66:**549-58.

78. F. R. Postma, K. Jalink, T. Hengeveld and W. H. Moolenaar. 1996. Sphingosine-1-phosphate rapidly induces Rho-dependent neurite retraction: action through a specific cell surface receptor. *Embo J* **15:**2388-92.

79. M. J. Hart, S. Sharma, N. elMasry, R. G. Qiu, P. McCabe, P. Polakis and G. Bollag. 1996. Identification of a novel guanine nucleotide exchange factor for the Rho GTPase. *J Biol Chem* **271:**25452-8.

80. M. F. Gebbink, O. Kranenburg, M. Poland, F. P. van Horck, B. Houssa and W. H. Moolenaar. 1997. Identification of a novel, putative Rho-specific GDP/GTP exchange factor and a RhoA-binding protein: control of neuronal morphology. *J Cell Biol* **137:**1603-13.

81. Y. Koyano, T. Kawamoto, M. Shen, W. Yan, M. Noshiro, K. Fujii and Y. Kato. 1997. Molecular cloning and characterization of CDEP, a novel human protein containing the ezrin-like domain of the band 4.1 superfamily and the Dbl homology domain of Rho guanine nucleotide exchange factors. *Biochem Biophys Res Commun* **241:**369-75.

82. D. Rubino, P. Driggers, D. Arbit, L. Kemp, B. Miller, O. Coso, K. Pagliai, K. Gray, S. Gutkind and J. Segars. 1998. Characterization of Brx, a novel Dbl family member that modulates estrogen receptor action. *Oncogene* **16:**2513-26.

83. A. S. Alberts and R. Treisman. 1998. Activation of RhoA and SAPK/JNK signalling pathways by the RhoA- specific exchange factor mNET1. *Embo J* **17:**4075-85.

84. Y. Ren, R. Li, Y. Zheng and H. Busch. 1998. Cloning and characterization of GEF-H1, a microtubule-associated guanine nucleotide exchange factor for Rac and Rho GTPases. *J Biol Chem* **273:**34954-60.

85. M. Hoshino, M. Sone, M. Fukata, S. Kuroda, K. Kaibuchi, Y. Nabeshima and C. Hama. 1999. Identification of the stef gene that encodes a novel guanine nucleotide exchange factor specific for Rac1. *J Biol Chem* **274:**17837-44.

86. T. Reid, A. Bathoorn, M. R. Ahmadian and J. G. Collard. 1999. Identification and characterization of hPEM-2, a guanine nucleotide exchange factor specific for Cdc42. *J Biol Chem* **274:**33587-93.

87. P. Penzes, R. C. Johnson, M. R. Alam, V. Kambampati, R. E. Mains and B. A. Eipper. 2000. An isoform of kalirin, a brain-specific GDP/GTP exchange factor, is enriched in the postsynaptic density fraction. *J Biol Chem* **275:**6395-403.

謝辞

本研究を遂行するにあたり、終始懇切丁寧にご指導下さいました愛知県がんセンター研究所・発がん制御研究部部長　稲垣昌樹博士に謹んで感謝の意を表します。また、研究の実施にあたり、直接ご指導下さいました同研究所・発がん制御研究部室長　永田浩一博士に深く心からお礼申し上げます。ならびに、本研究を進めるにあたり、数多くの助言、ご指導を頂きました同研究所の井澤一郎博士、伊奈田宏康博士をはじめとする発がん制御研究室の皆様に深謝いたします。

また、研究の遂行並びに論文の作成にあたり、多大なご協力と助言を頂きました名古屋大学大学院理学研究科教授　宝谷紘一博士に感謝申し上げます。

副論文

Functions of a Rho-specific Guanine Nucleotide Exchange Factor in Neurite Retraction
POSSIBLE ROLE OF A PROLINE-RICH MOTIF OF KIAA0380 IN LOCALIZATION

Hideaki Togashi, Koh-ichi Nagata , Mihoko Takagishi, Noriko Saitoh
and Masaki Inagaki

J. Biol. Chem., **275**, 29570-29578 (2000)

THE JOURNAL OF BIOLOGICAL CHEMISTRY
Vol. 275, No. 38, Issue of September 22, pp. 29570–29578, 2000
Printed in U.S.A.

Functions of a Rho-specific Guanine Nucleotide Exchange Factor in Neurite Retraction

POSSIBLE ROLE OF A PROLINE-RICH MOTIF OF KIAA0380 IN LOCALIZATION*

Received for publication, May 1, 2000, and in revised form, June 26, 2000
Published, JBC Papers in Press, July 18, 2000, DOI 10.1074/jbc.M003726200

Hideaki Togashi‡§, Koh-ichi Nagata‡¶, Mihoko Takagishi‡‖, Noriko Saitoh‡, and Masaki Inagaki‡**

From the ‡Division of Biochemistry, Aichi Cancer Center Research Institute, 1-1 Chikusa-ku, Nagoya, Aichi 464-8681, the §Division of Biological Sciences Graduate School of Science, Nagoya University, Furo-cho, Chikusa-ku, Nagoya, Aichi 464-8602, and the ‖Department of Chemical Hygiene and Nutrition, Faculty of Pharmaceutical Sciences, Nagoya City University, 3-1 Tanabe-dori, Mizuho-ku, Nagoya, Aichi 467-8603, Japan

The Rho/Rho kinase signaling pathway plays an essential role in neurite retraction and cell rounding in response to $G_{12/13}$-coupled receptor activation in neuronal cells. The Rho guanine nucleotide exchange factor involved in these processes has not been identified. To monitor the activation state of Rho kinase, we developed a vimentin head/Rho kinase chimera, which is intramolecularly phosphorylated in a Rho-dependent manner at Ser^{71} of the fused vimentin head. Using this system, we identified a clone termed KIAA0380, which contains the $G\alpha_{12/13}$-binding domain as well as a tandem of the Dbl homology/pleckstrin homology (DH/PH) domain, as an activator of Rho/Rho kinase signaling. Molecular dissection analyses revealed that a proline-rich motif C-terminally adjacent to DH/PH domain is essential for plasma membrane localization of KIAA0380 and cortical actin reorganization followed by cell rounding. In contrast, the DH/PH domain of KIAA0380 is localized in the cytoplasm, where it activates Rho/Rho kinase and induces stress fiber formation, consistent with results using p115 Rho guanine nucleotide exchange factor, which has a similar structure to KIAA0380 but lacks a proline-rich motif. These results suggest that upon stimulation, KIAA0380 translocates to the plasma membrane via the proline-rich motif and there activates Rho/Rho kinase signaling. In neuroblastoma Neuro2a cells, KIAA0380 was observed in the tips of neurites, a location where cortical actin reorganization is induced upon stimulation with lysophosphatidic acid. Ectopic expression of the N-terminal fragment inhibited lysophosphatidic acid-induced neurite retraction of Neuro2a cells. These results suggest that KIAA0380 plays an important role in neurite retraction through Rho-dependent signaling.

* This work was supported in part by grants-in-aid for scientific research and cancer research from the Ministry of Education, Science, Sports and Culture of Japan; by the Japan Society for Promotion of Science Research for the Future; by a grant-in-aid for the Second Term Comprehensive 10-Year Strategy for Cancer Control from the Ministry of Health and Welfare, Japan; by a grant from Bristol-Myers-Squibb; and by the Princess Takamatsu Cancer Research Foundation. The costs of publication of this article were defrayed in part by the payment of page charges. This article must therefore be hereby marked "*advertisement*" in accordance with 18 U.S.C. Section 1734 solely to indicate this fact.

¶ To whom correspondence may be addressed. Tel.: 81-52-762-6111 (ext. 7023); Fax: 81-52-763-5233; E-mail: knagata@aichi-cc.pref.aichi.jp.

** To whom correspondence may be addressed. Tel.: 81-52-762-6111 (ext. 7020); Fax: 81-52-763-5233; E-mail: minagaki@aichi-cc.pref.aichi.jp.

It is well established that Rho, Rac, and Cdc42, three members of the Rho family of small GTPases, control both the organization of the actin cytoskeleton and signal transduction pathways leading to gene transcription. In fibroblasts, Rho controls the assembly of actin stress fibers and associated focal adhesion complexes, while Rac and Cdc42 control the formation of lamellipodia and filopodia respectively (1–4). In addition to these effects, the three GTPases have been reported to trigger a number of additional cellular activities (1–4). For example, Rho is required for G_1 cell cycle progression, activates the serum response transcription factor, and plays a role in the cell cycle during cytokinesis.

Cytoskeletal changes mediated by Rho vary between cell types. In neuronal cell lines, Rho induces the formation of a cortical shell of F-action that mediates cytoskeletal contraction (5), which is thought to underlie growth cone collapse, neurite retraction, and rounding cell body in response to lysophosphatidic acid (LPA)[1] (5–10). However, the biochemical relationship between these varied responses remained to be clarified.

Like other small GTPases, Rho is thought to act as a molecular switch to control intracellular signal transduction pathways; it exists in either an inactive (GDP-bound) or an active (GTP-bound) conformation, and regulatory proteins that control this GDP/GTP cycle include over 15 distinct guanine nucleotide exchange factors (GEFs), around 10 GTPase-activating proteins and at least two guanine nucleotide dissociation inhibitors (11–13). Many GEFs for Rho family proteins were discovered by virtue of their ability to transform NIH3T3 cells when overexpressed or when activated by truncation. All these proteins share a 250-amino acid stretch of significant sequence similarity with Dbl, termed Dbl homology (DH) domain, adjacent to a pleckstrin homology (PH) domain (11). The DH domain was shown to be responsible for nucleotide exchange activity toward Rho family GTPases (14–16).

Several Rho targets have been identified, including Rho kinase. This kinase regulates the phosphorylation of myosin light chain (MLC) of myosin II by direct phosphorylation of MLC and by inactivation of myosin phosphatase through phosphorylation of myosin-binding subunit (17–19). In addition to MLC and

[1] The abbreviations used are: LPA, lysophosphatidic acid; DH, Dbl homology; GEF, guanine nucleotide exchange factor; PH, pleckstrin homology; RGS, regulator of G protein signaling; aa, amino acid(s); GST, glutathione *S*-transferase; PAGE, polyacrylamide gel electrophoresis; DMEM, Dulbecco's modified Eagle's medium; GTPγS, guanosine 5′-3-*O*-(thio)triphosphate; MLC, myosin light chain; VH, vimentin head; KDTT, full-length Rho kinase with mutations in the ATP- and Rho-binding sites.

myosin-binding subunit, Rho kinase phosphorylates the ERM family proteins (ezrin, radixin, moesin) and adducin both *in vitro* and *in vivo* (20–22). Rho kinase has been shown to regulate the formation of actin stress fibers and focal adhesions (23–25), smooth muscle contraction (26), myosin fiber organization and c-*fos* expression (19), efficient separation of glial filaments (27), cytokinesis (27, 28), and neurite retraction (29, 30). Despite the physiological importance of Rho kinase, direct detection of the *in vivo* activation state of Rho kinase has not been feasible.

We designed a novel *in vivo* detection system for the state of Rho kinase activation and used this system to identify the novel activator for Rho/Rho kinase signaling, KIAA0380, which was originally isolated from a human brain cDNA library in a random cloning project (31). After confirming that KIAA0380 actually functions as a Rho-specific GEF *in vitro* and *in vivo*, cell biological characterization of KIAA0380 was done. KIAA0380 induced actin reorganization followed by cell rounding in various types of cells, and induced neurite retraction and cell rounding in mouse neuroblastoma Neuro2a cells. Since KIAA0380 is composed of various functional domains that are commonly found in signaling molecules, we prepared several mutants and analyzed the physiological significance of the functional domains. Interestingly, in addition to DH/PH domain, a proline-rich motif that is C-terminally adjacent to the DH/PH domain is also essential for plasma membrane location of KIAA0380, cortical actin reorganization, and cell rounding. Our data suggest that the proline-rich motif of KIAA0380 is involved in localization to the cell membrane and to the biological activity of KIAA0380. In Neuro2a cells, the N terminus fragment of KIAA0380 inhibited LPA-mediated neurite retraction. Immunological analysis revealed that KIAA0380 is well expressed in Neuro2a cells, but another $G\alpha_{12/13}$-binding p115 RhoGEF, which is also termed Lsc (32), was not detected. Taken together, these findings suggest that, in neuronal cells, KIAA0380 functions as a RhoGEF at the cell periphery and regulates $G_{12/13}$-coupled receptor-mediated Rho activation, an event essential for neurite retraction and growth cone collapse.

EXPERIMENTAL PROCEDURES

Materials—The following constructs were kind gifts from colleagues; Dr. K. Kaibuchi (Nara Institute of Science and Technology, Nara, Japan), cDNAs of Rho kinase and the mutants; Drs. T. Nagase (Kazusa DNA Institute, Chiba, Japan) and T. Kozasa (University of Texas, Dallas, TX), KIAA0380 cDNA; Dr. A. Hall (University College London, London, United Kingdom), pRK5-Myc plasmids harboring L63RhoA, N19Rho, L61Rac, and L61Cdc42; Dr. T. Kiyono (our institute), anti-Myc antibody (9E10); Dr. G. Bollag (Onyx Pharmaceuticals, Richmond, CA), pEXV-Myc-p115 RhoGEF and anti-p115 RhoGEF antibody. Mouse Neuro2a neuroblastoma cells were kindly provided by Dr. Y. Takeda (Tokyo Metropolitan Institute of Gerontology, Tokyo, Japan). Anti-FLAG-tag antibody (M2) was purchased from Eastman Kodak Co. Other materials and chemicals were obtained from commercial sources.

Plasmid Construction—pRK5-Myc-VH-Rho kinase and pRK5-Myc-VH-Rho kinase(KDTT), which contains mutations at the ATP-binding and Rho-binding sites of the kinase and thereby functions as a kinase-negative version (29), were obtained by fusing with the intermediate filament protein vimentin head domain (aa 2–87) with respective Rho kinase cDNAs and constructed into pRK5 vector containing Myc tag.

The cDNA fragments of KIAA0380-FL (aa 1–1522), -ΔDH (Δaa 735–958), -DH/PH-C (aa 1485–1522), -DH/PH-Pro (aa 735–1119), -RGS-DH/PH(aa 301–1080), -DH/PH (aa 735–1080), -DH (aa 735–958), -N (aa 1–592), and -C (aa 1056–1522) were subcloned into pRK5-Myc vector. For site-directed mutagenesis, QuickChange site-directed mutagenesis kits (Stratagene) were used. All constructs were verified by DNA sequencing.

Expression and Purification of Recombinant Proteins—GTPases, KIAA0380-RGS-DH/PH and KIAA0380-C were expressed in *Escherichia coli* as glutathione *S*-transferase (GST) fusion proteins and purified on glutathione-Sepharose beads. The recombinant proteins were released from the beads by cleavage with human thrombin. Protein concentration was determined by the method of Bradford (33), and purity of the protein preparations was confirmed on Coomassie Blue-stained SDS-polyacrylamide gels.

Preparation and Characterization of an Anti-KIAA0380 Antibody—KIAA0380-C fragment expressed in *E. coli* was used as an antigen. A rabbit polyclonal antibody specific for KIAA0380-C fragment was produced and characterization was carried out as described elsewhere (34). Western blot analysis was done and the immunoreactive bands were visualized by making use of a horseradish peroxidase-conjugated anti-rabbit antibody (Amersham Pharmacia Biotech) and the ECL Western blotting detection system (Amersham Pharmacia Biotech).

Cell Culture, Microinjection, Transfection, and Immunofluorescence—Swiss 3T3, COS7, and Neuro2a cells were cultured in Dulbecco's modified Eagle's medium (DMEM) supplemented with 10% fetal bovine serum. MDCKII cells were maintained in DMEM containing 10% calf serum. COS7 and Neuro2a cells were transfected by the LipofectAMINE method (Life Technologies, Inc.). After 24 h, transfected COS7 cells were serum-starved for 16 h and then harvested. Transfected Neuro2a cells on poly-D-lysine-coated coverslips were maintained in a serum-starved condition for 24 h and then harvested. Swiss 3T3 and MDCKII cell nuclei were microinjected with pRK5-Myc vectors containing wild type or mutants of KIAA0380 and p115RhoGEF, as described (35). Cells were fixed in 3.7% formaldehyde in PBS for 15 min and then were subsequently permeabilized with 0.2% Triton X-100 for 5 min. Exceptionally, fixation was done using 10% trichloroacetic acid to detect RhoA. After primary antibody incubation at 37 °C for 2 h, the cells were incubated with a combination of the secondary antibody and rhodamine-conjugated phalloidin (Molecular Probes) to detect F-actin. To detect the transfected proteins, 9E10 (a mouse monoclonal anti-myc antibody) and FITC-labeled anti-mouse IgG were used. For detection of KIAA0380, affinity-purified anti-KIAA0380 antibody was used as the primary antibody, and Alexa 488 anti-rabbit IgG (Molecular Probes) as the secondary one. Anti-RhoA (Santa Cruz), anti-tubulin (Sigma), and anti-vimentin mouse monoclonal antibodies were used as primary antibodies to detect RhoA, tubulin, and vimentin, respectively. Cells were analyzed using a confocal microscope (Olympus, LSM-GB200).

In Vitro and in Vivo Analyses of GDP/GTP Exchange Activity of KIAA0380—*In vitro* GDP/GTP exchange activity of recombinant Rho, Rac, or Cdc42 (10 pmol) was measured as described (36), in the presence or absence of recombinant GST-KIAA0380-RGS-DH/PH fragment (20 pmol). Analysis of guanine nucleotides bound to Rho, Rac, and Cdc42 was made, as described (37). Briefly, COS7 cells expressing FLAG-tagged Rho, Rac or Cdc42, with or without Myc-KIAA0380, were labeled with [^{32}P]P_i at 0.1 mCi/ml for 4 h and then the cells were lysed in lysis buffer containing 20 mM Tris/HCl (pH 7.5), 150 mM NaCl, 20 mM $MgCl_2$, 1 mM Na_3VO_4, 0.5% Triton X-100, 1 mM phenylmethylsulfonyl fluoride, and 10 μg/ml aprotinin. FLAG-tagged GTPases were then immunoprecipitated with M2 anti-FLAG antibody. After denaturation of the proteins, eluted nucleotides were analyzed by polyethyleneimine thin layer chromatography. Guanine nucleotides were detected and quantitated using the BAS 2500 system (Fuji Film, Tokyo, Japan).

Immunoprecipitation—Neuro2a and COS7 cells transiently expressing KIAA0380 or p115 RhoGEF were harvested with of RIPA buffer containing 50 mM Tris/HCl (pH 8.0), 150 mM NaCl, 1.0% Nonidet P-40, 0.5% deoxycholate, and 0.1% SDS. Insoluble material was removed by centrifugation at 4 °C for 10 min at 10,000 × *g*, and 50 μl of lysate (50–90 μg of protein) was used for each assay. KIAA0380 and p115 RhoGEF were immunoprecipitated, using specific antibodies. After washing the precipitates three times with RIPA buffer, the precipitates were subjected to SDS-PAGE (7.5% gel) and proteins were transferred to nitrocellulose filters. Western blotting was done using anti-KIAA0380 and anti-p115 RhoGEF antibodies.

RESULTS

Development of a System to Detect the Activation State of Rho Kinase—The head domain of vimentin is phosphorylated specifically at Ser^{71} by Rho kinase, and the phosphorylation state of vimentin can be detected using a site- and phosphorylation state-specific antibody, TM71 (38–40). Such being the case, Ser^{71} is useful for monitoring the vimentin head phosphorylation state *in vivo* by Rho kinase. Based on this characteristic feature, we attempted to establish a chimera construct in which the vimentin head domain (aa 2–87) is fused to the N terminus of Rho kinase (Fig. 1*A*). Since Rho activates the Rho kinase pathway *in vitro* and *in vivo*, we first asked whether Rho could activate VH-Rho kinase and phosphorylate the at-

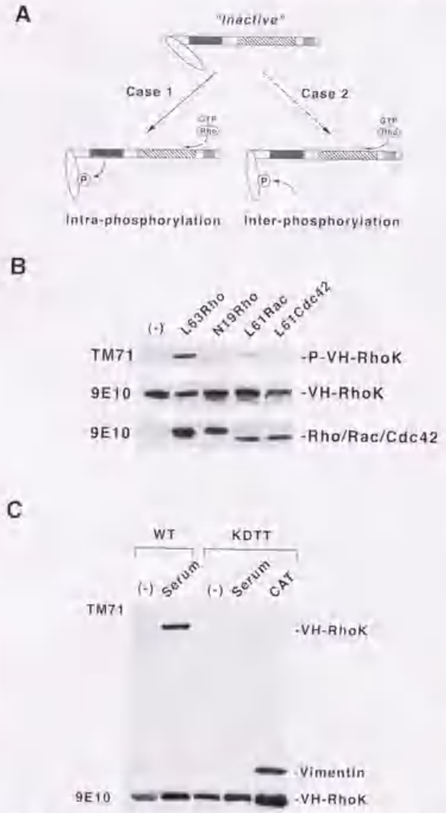

FIG. 1. **Our system for detecting the activation state of Rho kinase.** *A*, schematic representation of VH-Rho kinase. Vimentin head domain (aa 1–87) was fused to the N terminus of Rho kinase. *VH*, vimentin head domain; *Cat*, catalytic domain; *PH*, pleckstrin homology domain. Phosphorylation of Ser^{71} of VH-Rho kinase in an intramolecular (*left*) or intermolecular (*right*) manner. *B*, detection of the activation of VH-Rho kinase by Western blotting. Myc-tagged activated (Leu^{63}) RhoA, inactive (Asn^{19}) RhoA, activated (Leu^{61}) Rac, or activated (Leu^{61}) Cdc42 were transiently expressed in COS7 cells with Myc-tagged VH-Rho kinase. Cells were collected in Laemmli-SDS-PAGE sample buffer and then subjected to Western blotting using 9E10 or TM71. *C*, the phosphorylation of Ser^{71} of VH-Rho kinase is in a intramolecular manner. Myc-tagged wild-type VH-Rho kinase (*WT*) or inactive VH-Rho kinase (*KDTT*), with or without activated Rho kinase (*CAT*), was transiently expressed in COS7 cells. After culture, with or without serum for 24 h, cells were collected in Laemmli-SDS-PAGE sample buffer and then subjected to Western blotting, using 9E10 or TM71.

tached vimentin head domain at Ser^{71}. pRK5-Myc-VH-Rho kinase was co-transfected into COS7 cells using various Rho, Rac and Cdc42 constructs. Phosphorylation of VH-Rho kinase was monitored by Western blotting, using TM71. As shown in Fig. 1*B*, only the active version of Rho (L63Rho) strongly induced phosphorylation of vimentin-Ser^{71}, whereas an inactive version of Rho (N19Rho) and constitutively active Rac and Cdc42 did not do so. These results indicate that the phosphorylation at Ser^{71} of vimentin head of VH-Rho kinase is an active Rho-dependent event.

As illustrated in Fig. 1*A*, there are at least two possible molecular mechanisms for Ser^{71} phosphorylation; one is intramolecular, and the other is intermolecular. To determine which molecular mechanism underlies the observed Ser^{71} phosphorylation, we analyzed the inactive version of VH-Rho kinase, KDTT. As shown in Fig. 1*C*, fetal bovine serum induced Ser^{71} phosphorylation of wild type VH-Rho kinase but not KDTT. Even when constitutively activated Rho kinase was co-transfected with KDTT, phosphorylation of Ser^{71} did not occur (Fig. 1*C*), which strongly suggests that endogenous Rho kinase cannot interact with the vimentin head of VH-Rho kinase. In these experiments, phosphorylation of endogenous vimentin at Ser^{71} was detected, as shown in Fig. 1*C*. Taken together, we considered that the phosphorylation of Ser^{71} of VH-Rho kinase is an intramolecular event.

Since ectopically expressed constitutively active Rho kinase localizes diffusely in the cytoplasm and is no longer regulated by RhoGEF/Rho, it can phosphorylate endogenous vimentin (Fig. 1*C*). On the other hand, serum stimulation did not induce endogenous vimentin phosphorylation (Fig. 1*C*), perhaps because the intracellular localization of activated Rho kinase is restricted by RhoGEF/Rho; thus, the kinase may not interact with and phosphorylate endogenous vimentin.

Identification of KIAA0380 as an Activator for Rho-Rho Kinase Signaling—As our newly designed Rho kinase activity detection system proved useful to monitor the activation state of the kinase, this system may be able to detect novel Rho kinase activators. KIAA0380 was first isolated from a human brain cDNA library in a random cloning project (31). Since this activator contains a tandem of the DH/PH domain and functions as a RhoGEF *in vitro* (41), we asked if KIAA0380 functions as an *in vivo* activator for Rho kinase. As shown in Fig. 2*A*, KIAA0380 strongly induced phosphorylation of Ser^{71} of VH-Rho kinase, to an extent similar to that seen with p115 RhoGEF. In contrast, the deletion mutant lacking the DH domain (KIAA0380ΔDH) did not phosphorylate Ser^{71}. KIAA0380 most likely activates Rho kinase through the direct activation of Rho.

Since KIAA0380 activates VH-Rho kinase *in vivo* and consequently induces autophosphorylation of the kinase at Ser^{71}, KIAA0380 may directly activate Rho. To determine if the KIAA0380-induced Ser^{71} phosphorylation occurs through activation of Rho signaling by KIAA0380 and not through Rho-independent events, we wanted to determine if KIAA0380 would directly activate Rho both *in vitro* and *in vivo*. As for *in vitro* experiments, recombinant Rho, Rac, and Cdc42 were first complexed with nonradioactive GDP and then incubated with [^{35}S]GTPγS in the presence or absence of GST-fused KIAA0380-RGS-DH/PH. As shown in Fig. 2*B*, KIAA0380-RGS-DH/PH accelerated the binding of GTPγS to Rho but not to Rac or to Cdc42, findings consistent with reported data (41).

Since some Dbl family proteins show different substrate specificities *in vitro* and *in vivo* (42, 43), we wanted to determine if KIAA0380 would activate Rho *in vivo*. The pRK5-Flag vector harboring Rho, Rac, or Cdc42 was introduced into COS7 cells. When Rho, Rac, and Cdc42 were expressed by themselves, the bound GTP accounted for 16.4%, 5.8%, and 5.9%, respectively. We then examined the effects of KIAA0380 regarding activation of these GTPase. As shown in Fig. 2*C*, co-expression of KIAA0380 but not Rac and Cdc42, led to a increase in the GTP-bound form of Rho, up to 34.4%. These results of *in vivo* experiments indicate that KIAA0380 is a physiological Rho-specific GEF and also confirm reliability of our system for detecting Rho kinase activity.

Overexpression of KIAA0380 Induces Actin Reorganization and Marked Rounding of Swiss 3T3—RhoGEFs are important regulators of Rho-dependent actin polymerization. To confirm the involvement of KIAA0380 in actin reorganization, we microinjected pRK5-Myc-KIAA0380 into Swiss 3T3 cells and 3 h later, KIAA0380-expressing cells were identified by staining the Myc epitope. F-actin organization was examined after staining with phalloidin. Cells expressing KIAA0380 showed a marked cell rounding and actin staining was strong underneath plasma membranes of the round cell bodies (Fig. 3, *A–C*). On the other hand, p115 RhoGEF, a Rho-specific GEF structurally and highly homologous to KIAA0380, did not induce cortical actin reorganization followed by cell rounding but did induce stress fibers (Fig. 3, *D–F*).

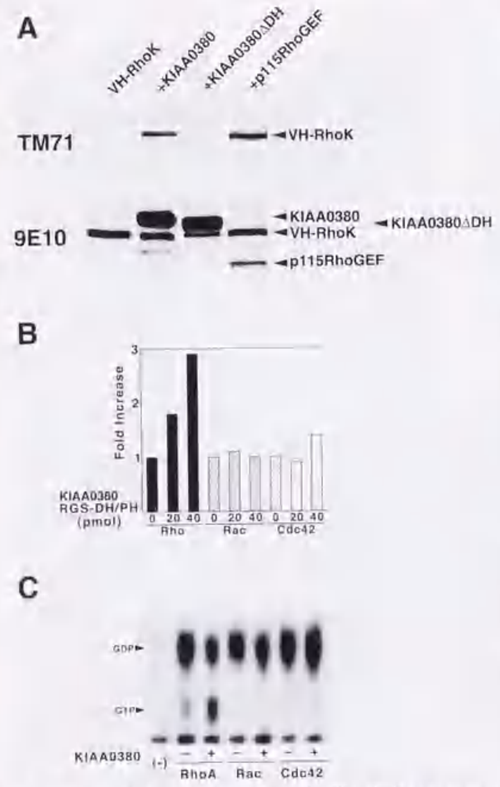

FIG. 2. **Specificity of KIAA0380 on the Rho GTP-binding protein.** *A*, the activation of VH-Rho kinase by KIAA0380. Myc-tagged KIAA0380, KIAA0380ΔDH, or p115RhoGEF was transiently expressed in COS7 cells with Myc-tagged VH-Rho kinase. Cells were collected in Laemmli-SDS-PAGE sample buffer and then subjected to Western blotting, using TM71 or 9E10. *B*, specific activation of RhoA by the fragment containing DH/PH domain of KIAA0380 *in vitro*. RhoA, Rac, Cdc42, or RGS-DH/PH proteins were expressed as GST fusion proteins in *E. coli* and affinity-purified using glutathione-Sepharose beads. Radioactivities of GTPγS binding to RhoA, Rac, or Cdc42 expressed as GST fusion protein in *E. coli* were measured. *C*, specific activation of RhoA by KIAA0380 *in vivo*. FLAG-tagged Rho or Rac or Cdc42 was transiently expressed with KIAA0380 in COS7 cells. After metabolic labeling with [^{32}P]orthophosphate, cells were lysed and FLAG-tagged GTP-binding proteins was immunoprecipitated. Radioactive nucleotides bound to GTP-binding protein were eluted and resolved by TLC. The positions of GDP and GTP standards are indicated.

Determination of Functionally Important Domains of KIAA0380—In addition to a tandem of DH and PH domains, KIAA0380 exhibits characteristic structural features such as the PDZ domain involved in protein-protein interaction and the RGS motif interacting with α subunits of G_{12} and G_{13} (31, 44). To determine the physiological significance of each structural domain, we prepared a variety of truncation and deletion mutants of KIAA0380, as shown in Fig. 4*A*, and transiently expressed them in Swiss 3T3 cells. As depicted in Fig. 4*B*, the results show that the DH domain and also the PH domain are essential for actin reorganization since the DH domain alone does not induce reorganization. Moreover, it is notable that the DH/PH domains *per se* do not induce full contraction of cells; a proline-rich motif (aa 1081–1119) adjacent to the PH domain is required for KIAA0380-induced cell rounding.

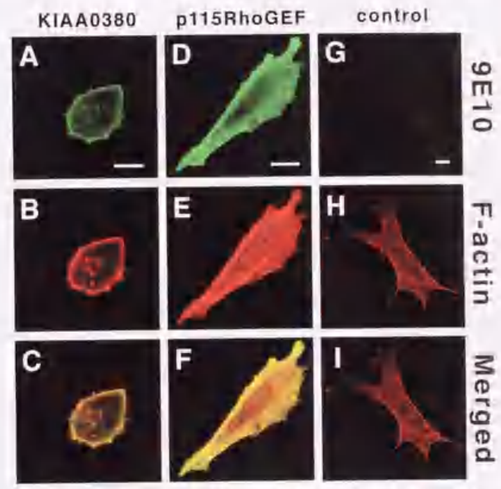

FIG. 3. **Morphological characteristics of Swiss 3T3 cells expressing KIAA0380 or p115RhoGEF.** Serum-starved Swiss 3T3 cells were microinjected with pRK5-Myc vectors containing the gene of KIAA0380 or p115RhoGEF. After 3 h, the cells were fixed and we stained F-actin using rhodamine-phalloidin (*A–C*). Cells expressing KIAA0380 (*B*, *E*, and *F*) or p115RhoGEF (*C*, *F*, and *I*) were identified by staining the Myc epitope. *A*, *D*, and *G* represent a control cell. *Bar*, 10 μm.

KIAA0380 Induces Cytoskeletal Contraction in MDCKII Cells and Inhibits Neurite Extension of Neuro2a Cells—The contraction of polymerized F-actin appeared to be strong, and the fully rounded phenotype was observed even in MDCKII cells, which have tight cell-cell attachments (Fig. 5, *A–F*). Since KIAA0380 is predominantly expressed in the brain, and cortical actin reorganization followed by cell rounding is a characteristic feature of neuronal cells in which Rho-Rho kinase signaling is activated, we next examined the effects of KIAA0380 on the morphology of Neuro2a cells. We transiently overexpressed KIAA0380 or L63Rho in Neuro2a cells and examined morphology of the cells expressing the respective proteins. After transfection, the cells were incubated in serum-free DMEM for 16 h. Transfected cells were identified by staining the Myc epitope, and F-actin organization was examined. In serum-free medium, nontransfected cells had flattened cell bodies and extended neurites (Fig. 5, *G–I*), while cells expressing KIAA0380 showed marked cell rounding and extended neurites were never apparent. In this transfectant, strong actin staining was evident in the rounded cell bodies. These results clearly indicate that activation of Rho signaling by KIAA0380 is sufficient to form cortical shells of F-actin that mediate cytoskeletal contraction and cell rounding.

Expression of KIAA0380 in Neuro2a Cells—As KIAA0380 is

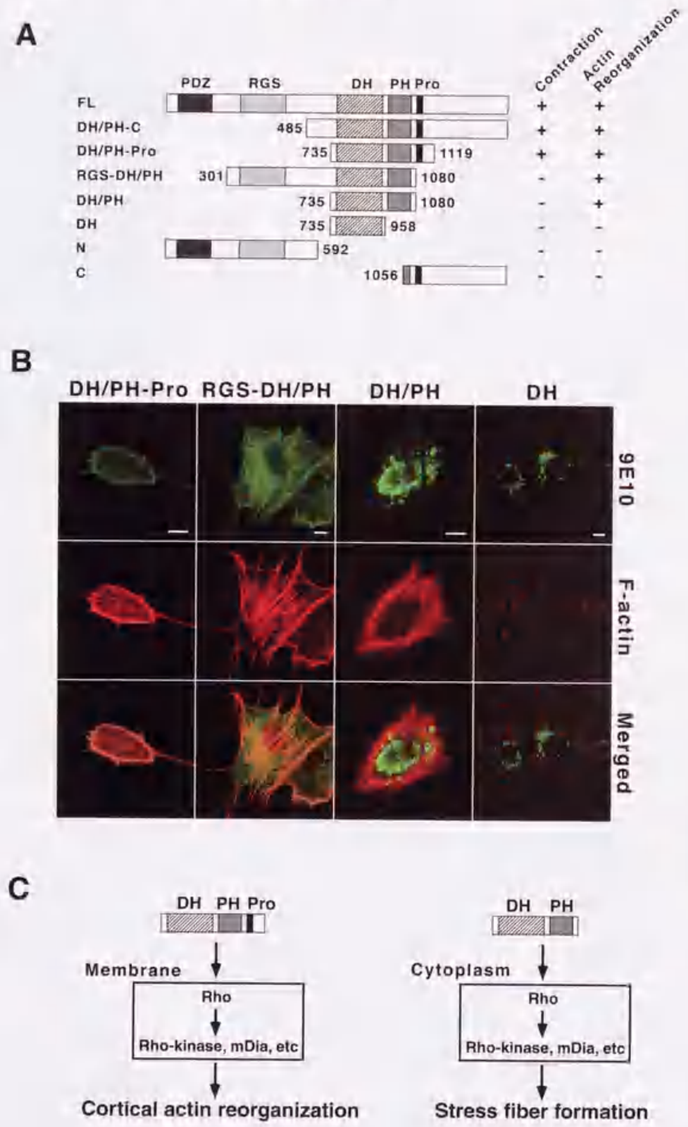

FIG. 4. **Determination of the functionally important domains of KIAA-0380.** *A*, properties of the KIAA0380 proteins with respect to cell rounding and stress fiber formation. Swiss 3T3 cells were transfected with pRK5-Myc vector containing the gene indicated: PDZ domain, RGS motif, DH, PH, and proline-rich motif (*Pro*). After transfection, the cells were cultured in serum-free DMEM for 18 h, fixed, and then stained for F-actin, using rhodamine-phalloidin. Protein-expressing cells were identified by staining the Myc epitope. "Contraction" means the protein induced fully rounded shapes, and "actin reorganization" means the protein induced stress fiber formation. Induction of the morphology in more than 80% of transfected cells was considered positive (+). *B*, morphological characteristics of Swiss 3T3 cells expressing various truncated mutants of KIAA0380. Swiss 3T3 cells were microinjected with pRK5-Myc vectors containing the gene indicated. After 3 h, the cells were fixed, stained, and identified expressing the mutant of KIAA0380, using the Myc epitope (*top*) and stained F-actin, using rhodamine-phalloidin (*middle*). *C*, possible model for Rho activation by KIAA0380 mutants inducing cortical actin reorganization or stress fiber formation.

highly expressed in the brain, it may play a role in neuronal cellular processes regulated by Rho. To elucidate related physiological functions, we developed a rabbit polyclonal antibody (α-KIAA0380-C) against the bacterially synthesized C-terminal fragment of KIAA0380 (aa 1056–1522). We first analyzed KIAA0380 protein expression in Neuro2a cells by immunoprecipitation in combination with Western blotting. As shown in Fig. 6 (*lane 2*), a relatively high level expression of KIAA0380 was observed in Neuro2a cells. In contrast, p115 RhoGEF, a KIAA0380-related RhoGEF that contains a RGS motif and can associate with $G\alpha_{12/13}$, was not detected in Neuro2a (*lane 4*). These observations are consistent with findings that KIAA0380 mRNA is highly expressed in the brain but to a lesser extent in many other tissues (31, 44). Since Neuro2a cells can be rapidly induced to produce neurites after serum withdrawal and do not express p115 RhoGEF, this cell line is pertinent to characterize KIAA0380 functions in neurite retraction.

Immunocytochemical Analyses of KIAA0380 in Neuro2a Cells—In the next set of experiments, immunocytochemical analysis was made to determine the intracellular localization of endogenous KIAA0380. Fig. 7 (*A–C*) shows that endogenous KIAA0380 is localized in the nucleus and cell body, in addition

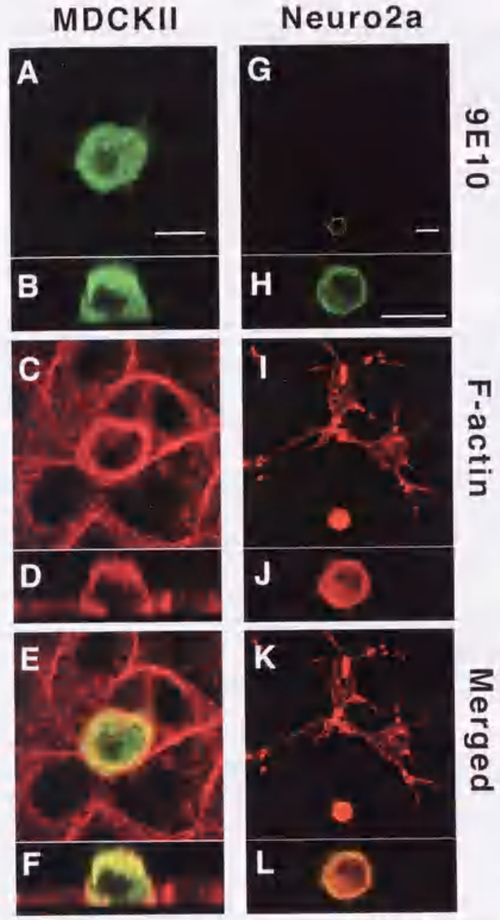

FIG. 5. **Morphological characteristics of MDCKII cells or Neuro2a cells expressing KIAA0380.** Serum-starved MDCKII cells were microinjected with pRK5-Myc vectors containing the gene of KIAA0380. After 3 h, the cells were fixed and F-actin stained using rhodamine-phalloidin (*C* and *D*). Cells expressing KIAA0380 were identified by staining the Myc epitope (*A* and *B*). The *x-z* scan (*A*, *C*, and *E*) was done along a fixed position on the *y* axis (*B*, *D*, and *F*). Neuro2a cells were transfected with pRK5-Myc vectors containing the gene of KIAA0380 and cultured in serum-free DMEM for 18 h. The cells were fixed and we stained F-actin, using rhodamine-phalloidin (*I* and *J*). Cells expressing KIAA0380 were identified by staining the Myc epitope (*G* and *H*). Staining of KIAA0380 and F-actin were merged (*K*). Cells expressing KIAA0380 were captured by short exposure (*H*, *J*, and *L*). *Bar*, 10 μM.

FIG. 6. **Characterization of affinity-purified antibody for the C termini of KIAA0380.** Detection of KIAA0380 or p115Rho-GEF by immunoprecipitation and Western blotting. COS7 cells transiently expressing KIAA0380 (*lane 1*) or Neuro2a cells (*lane 2*) were subjected to immunoprecipitation, using an affinity-purified antibody raised against the C-terminal fragment of KIAA0380 (aa 1056–1522). Samples were separated on a 7.5% polyacrylamide gel and then subjected to Western blotting, using an anti-KIAA0380 antibody. p115RhoGEF protein were precipitated, using an anti-p115RhoGEF antibody. Lysates of COS7 cells transiently expressing p115RhoGEF (*lane 3*) or Neuro2a cells (*lane 4*) were subjected to immunoprecipitation and Western blotting, using an anti-p115RhoGEF antibody.

to neurites of Neuro2a cells, and without any characteristic pattern. However, once the cells are stimulated with 1 μM LPA for 10 min, the staining pattern of KIAA0380 changes. In some cells, KIAA0380 was intensely stained in some tips of neurites where actin is reorganized (Fig. 7, *D–F*, *arrowheads*), and in other cells KIAA0380 is enriched in retracted neurites (Fig. 7, *G–I*, *arrowheads*). KIAA0380 was also enriched in cell peripheral areas where the F-actin shell is formed (Fig. 7, *G–I*, *arrows*). Since KIAA0380 is considered to be a Rho-specific GEF, we compared the intracellular KIAA0380 localization to that of endogenous Rho. As shown in Fig. 7 (*J–L*), Rho was enriched in neurite tips where KIAA0380 had accumulated, thereby suggesting direct interactions of KIAA0380 with Rho in growth cones. To determine if KIAA0380 interacts with other cytoskeletal proteins, we co-stained KIAA0380 with tubulin and vimentin. As shown in Fig. 7 (*N* and *Q*), tubulin and vimentin are distributed throughout the cytoplasm but not concentrated in neurite tips. KIAA0380 appears to co-localize with microtubules and intermediate filaments at neurite tips (Fig. 7, *M–R*). The physiological relation between KIAA0380 and these cytoskeletons remains to be clarified. KIAA0380 was also observed in the nuclei in interphase cells as is the case with Ect2 (45), although the dynamic change of distribution was not observed during cytokinesis (data not shown).

Inhibition of LPA-induced Neurite Retraction of Neuro2a by KIAA0380 Fragments—KIAA0380 mutants without a complete DH/PH domain cannot catalyze guanine nucleotide exchange of Rho (Figs. 1*B* and 2*A*). In neuronal cells, LPA activates Rho to induce growth cone collapse and neurite retraction through a $G_{12/13}$-initiated pathway that involves protein-tyrosine kinase activity (9, 46, 47). p115 RhoGEF has been shown to activate Rho in a G_{13}-dependent manner *in vitro* (48). Since p115 RhoGEF is not detectable in Neuro2a cells, KIAA0380 may have an important role in $G_{12/13}$/Rho-dependent signals, which result in neurite retraction. To investigate the role of KIAA0380 in the signaling pathway utilized by LPA, we used a KIAA0380-N fragment. Of interest, expression of KIAA0380-N (1.0 μg) in Neuro2a cells significantly inhibited cell rounding by LPA stimulation (Fig. 8). A dose-dependent inhibition by KIAA0380-N of neurite retraction was evident between 0 and 1.0 μg of the plasmid used. However, the inhibition of LPA-induced neurite retraction by KIAA0380-N was not complete, since more than 1.0 μg of the KIAA0380-N cDNA led to cytotoxicity (data not shown).

DISCUSSION

The Rho family of proteins has important roles in actin cytoskeletal reorganization and cell-matrix interactions, and all are essential determinants of neurite extension and retraction. Activation of these small GTPases in response to extracellular stimuli is regulated by their regulatory proteins such as GEF, guanine nucleotide dissociation inhibitor, and GTPase-activating protein.

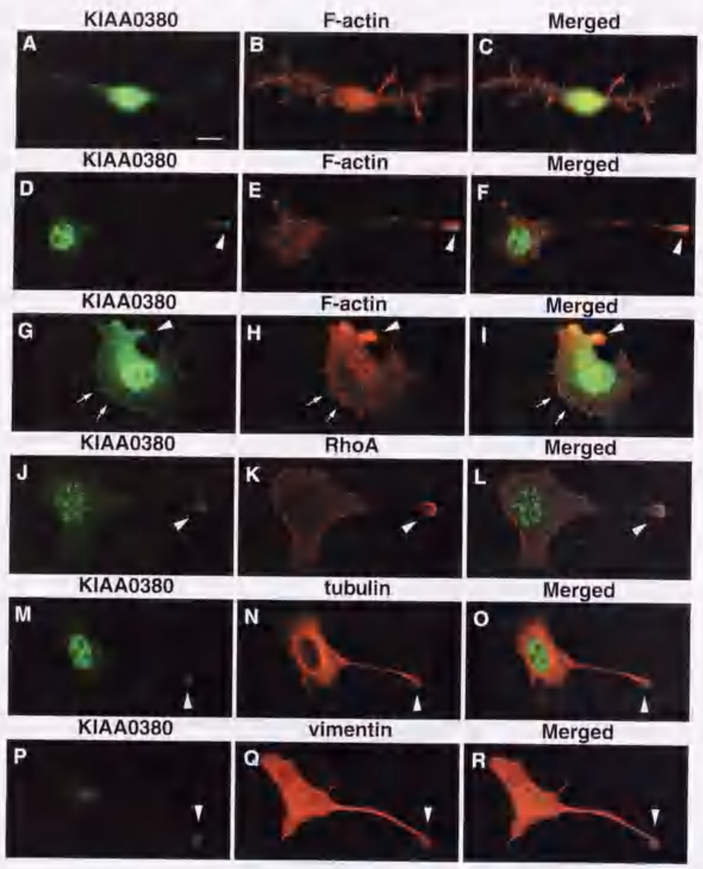

FIG. 7. **Distribution of KIAA0380 in Neuro2a cells.** Neuro2a cells were cultured on coverslips in serum-free DMEM for 24 h (*A–C*). After 1 μM LPA stimulation (*D–R*), Neuro2a cells were fixed and stained with KIAA0380, using an affinity-purified anti-KIAA0380-C antibody (*A*, *D*, *G*, *J*, *M*, and *P*) and F-actin, using rhodamine-phalloidin (*B*, *E*, and *H*) or RhoA (*K*), tubulin (*N*), or vimentin (*Q*), with respective antibodies. *Bar*, 10 μm.

Based on previous studies, it is most likely that generation of the actin-based contractile forces is required for neurite retraction (6, 7). A great deal of progress has been made in elucidating biochemical pathways governing neurite extension and retraction of neuronal cells. The activation of a certain G protein-coupled receptor, such as the LPA, thrombin, and prostaglandin EP3 receptors, was shown to induce Rho-dependent neurite retraction in several differentiated neuronal cell lines (7, 49–52). Thereafter, the G_{12} family of heterotrimeric G proteins, defined by $G\alpha_{12}$ and $G\alpha_{13}$, were found to be involved in Rho-dependent actin stress fiber formation and focal adhesion assembly, as determined by microinjection analyses (53). Using this approach, $G\alpha_{13}$ and $G\alpha_{12}$ were seen to activate Rho, but not $G\alpha_{12}$ in Swiss 3T3 cells. The constitutively activated versions of both $G\alpha_{12}$ and $G\alpha_{13}$ were found to induce a range of Rho-dependent responses, not only stress fiber formation but also serum response transcription factor (54) and phospholipase D activation (55, 56) in fibroblasts, and neurite retraction in neuronal cell lines (57). Further analyses revealed that LPA-induced Rho activation is mediated by $G\alpha_{13}$ in fibroblasts, while thrombin appears to act through $G\alpha_{12}$ (47, 58).

Although the physiological RhoGEF which links between $G\alpha_{12}/G\alpha_{13}$ and Rho is unknown, p115 RhoGEF (also termed Lsc) was found to bind to $G\alpha_{12}$ and $G\alpha_{13}$ through their RGS domain and to be selectively activated by $G\alpha_{13}$ *in vitro* (48). To date, two kinds of RhoGEF containing $G\alpha_{12}/G\alpha_{13}$-interactive RGS domains have been identified: one is p115 RhoGEF, and the other is KIAA0380. Since growth cone collapse, neurite retraction, and cell rounding in neuronal cells are $G\alpha_{12}$- and $G\alpha_{13}$-dependent processes, we assume that Rho-specific GEF containing the RGS domain, which can interact with $G\alpha_{12}$ and/or $G\alpha_{13}$, is a possible candidate as regulator of neurite retraction. KIAA0380 is structurally homologous to p115 RhoGEF and has the $G\alpha_{12}$ and $G\alpha_{13}$-interactive RGS motif. Northern analysis revealed that p115 RhoGEF is highly expressed in peripheral blood leukocytes, thymus, and spleen, but hardly detectable in the brain (32); we never detected p115 RhoGEF protein in Neuro2a cells. In contrast, KIAA0380 is dominantly expressed in the brain, at the mRNA level, and the protein is abundant in Neuro2a cells. It may be that KIAA0380 can be activated directly by $G\alpha_{12}$ and/or $G\alpha_{13}$ in a mode similar to that of p115 RhoGEF. Immunocytochemical analyses revealed that KIAA0380 is distributed not only in the cell body but also in the tips of neurites where cortical F-actin is reorganized. KIAA0380 could bind to constitutively active $G\alpha_{12}$ and $G\alpha_{13}$ mutants in the COS7 cell transfection system (44). From these observations, it is tempting to speculate that $G\alpha_{12}$ and/or $G\alpha_{13}$ regulates KIAA0380 function *in vivo*. We found no further

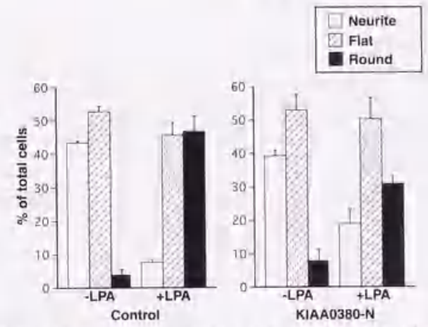

FIG. 8. **Inhibition of LPA-induced neurite retraction of Neuro2a by the N-terminal fragment of KIAA0380.** Cells were transfected with 1.0 μg of pRK5-KIAA0380-N (aa 1–592). After transfection the cells were maintained overnight in serum-free medium and were subsequently stimulated with 1 μM LPA for 3 min. Morphologies of the cell scored were as follows: round, fully contracted; flat, flattened without neurite extensions, or with extensions shorter than the soma diameter; neurite, flattened with neurite extensions longer than the soma diameter. Each value is the mean ± S.D. for 100–200 cells sampled from three independent experiments.

activation of VH-Rho kinase by $G\alpha_{12}/G\alpha_{13}$, since KIAA0380 is constitutively active in transfected cells. We assumed that endogenous KIAA0380 is regulated by an unidentified endogenous regulator(s) and the inhibitor is not sufficient when KIAA0380 is overexpressed.

We considered the possible involvement of KIAA0380 in LPA-dependent neurite contraction of neuronal Neuro2a cells. Our hypothesis that KIAA0380 functions as a RhoGEF in neurite retraction was supported by findings that the N-terminal fragment of KIAA0380 (KIAA0380-N) could block the neurite retraction induced by LPA. The inhibition of neurite retraction by KIAA0380-N was only partial. One explanation for the results is that the expression level of the KIAA0380-N fragment is inadequate to induce complete inhibition of neurite retraction while a high expression appeared to cause cytotoxicity.

We designed a detection system for the Rho kinase activation state, and this system was found to be applicable to detect RhoGEFs which activate the Rho/Rho kinase-dependent signaling pathway. Using the detection system, we found that KIAA0380 is a Rho/Rho kinase activator *in vivo*. We then assessed the effects of various KIAA0380 mutants on actin reorganization and morphological changes of various cell lines, including Swiss 3T3 and Neuro2a cells. Thereafter, we characterized KIAA0380 in neuronal cells since KIAA0380 is expressed mainly in the brain. As a model, we used Neuro2a cells, which are a convenient system for examining Rho action since these cells undergo rapid and dramatic Rho-mediated shape changes when treated with LPA or serum. Interestingly, in neuroblastoma N1E-115 cells, other authors dissociated LPA-induced cytoskeletal contraction from stress fiber formation; Rho translocation to the cell periphery is required for LPA-stimulated contractility but not for formation of stress fibers, since stress fibers can still be induced by activated Rho, which cannot bind to the cell membrane (5). However, it remained to be clarified whether Rho is activated upon LPA stimulation and then translocates to the cell periphery or whether Rho first translocates to the cell periphery and then is activated by a localizing RhoGEF. We could dissociate actin stress fiber formation from morphological change at the RhoGEF level; KIAA0380-DH/PH is sufficient for the former phenotype, whereas a proline-rich motif (aa 1081–1119) adjacent to the PH domain is required for the latter. The importance of the region extending C-terminally adjacent to the PH domain for actin reorganization has been noted for a Rac-specific GEF, Tiam1, in which the extending region contains a putative coiled coil sequence of about 40 amino acids and a following region of 300 amino acids. This extending region of about 340 amino acids is required for Tiam1-induced membrane ruffling (59). Our present results also suggest another molecular mechanism of Rho activation. The subcellular localization of KIAA0380-DH/PH is cytoplasmic with a punctate pattern, while KIAA0380-DH/PH/Pro locates underneath the plasma membrane. Thus, KIAA0380-DH/PH may activate cytoplasmic Rho and induce actin stress fibers, whereas KIAA0380-DH/PH/Pro may activate Rho located in the peripheral cell membrane or its vicinity, and consequently induce cortical actin reorganization.

In another study on full cytoskeletal contraction (but not stress fiber formation), membrane localization of Rho was required (5), although the precise intracellular location where the GTP/GDP exchange on Rho takes place was not obvious. Based on our observation that cytoskeletal contraction followed by cell rounding and stress fiber formation can be separated using different KIAA0380 mutants, we are entertaining the notion that localization of RhoGEF determines the subpopulation of activated Rho.

Acknowledgment—We are grateful to M. Ohara for critique of the manuscript.

REFERENCES

1. Ridley, A. J., and Hall, A. (1992) *Cell* **70,** 389–399
2. Ridley, A. J., Paterson, H. F., Johnston, C. L., Diekmann, D., and Hall, A. (1992) *Cell* **70,** 401–410
3. Nobes, C. D., and Hall, A. (1995) *Cell* **81,** 53–62
4. Kozma, R., Ahmed, S., Best, A., and Lim, L. (1995) *Mol. Cell. Biol.* **15,** 1942–1952
5. Kranenburg, O., Poland, M., Gebbink, M., Oomen, L., and Moolenaar, W. H. (1997) *J. Cell Sci.* **110,** 2417–2427
6. Jalink, K., Eichholtz, T., Postma, F. R., van Corven, E. J., and Moolenaar, W. H. (1993) *Cell Growth Differ.* **4,** 247–255
7. Jalink, K., van Corven, E. J., Hengeveld, T., Morii, N., Narumiya, S., and Moolenaar, W. H. (1994) *J. Cell Biol.* **126,** 801–810
8. Kozma, R., Sarner, S., Ahmed, S., and Lim, L. (1997) *Mol. Cell. Biol.* **17,** 1201–1211
9. Kranenburg, O., Poland, M., van Horck, F. P., Drechsel, D., Hall, A., and Moolenaar, W. H. (1999) *Mol. Biol. Cell* **10,** 1851–1857
10. Leeuwen, F. N., Kain, H. E., Kammen, R. A., Michiels, F., Kranenburg, O. W., and Collard, J. G. (1997) *J. Cell Biol.* **139,** 797–807
11. Certone, R. A., and Zheng, Y. (1996) *Curr. Opin. Cell Biol.* **8,** 216–222
12. Lamarche, N., and Hall, A. (1994) *Trends Genet.* **10,** 436–440
13. Ueda, T., Kikuchi, A., Ohga, N., Yamamoto, J., and Takai, Y. (1990) *J. Biol. Chem.* **265,** 9373–9380
14. Hart, M. J., Eva, A., Evans, T., Aaronson, S. A., and Cerione, R. A. (1991) *Nature* **354,** 311–314
15. Ron, D., Zannini, M., Lewis, M., Wickner, R. B., Hunt, L. T., Graziano, G., Tronick, S. R., Aaronson, S. A., and Eva, A. (1991) *Nat. New Biol.* **3,** 372–379
16. Hart, C. M., and Roberts, J. W. (1994) *J. Mol. Biol.* **237,** 255–265
17. Kimura, K., Ito, M., Amano, M., Chihara, K., Fukata, Y., Nakafuku, M., Yamamori, B., Feng, J., Nakano, T., Okawa, K., Iwamatsu, A., and Kaibuchi, K. (1996) *Science* **273,** 245–248
18. Amano, M., Ito, M., Kimura, K., Fukata, Y., Chihara, K., Nakano, T., Matsuura, Y., and Kaibuchi, K. (1996) *J. Biol. Chem.* **271,** 20246–20249
19. Chihara, K., Amano, M., Nakamura, N., Yano, T., Shibata, M., Tokui, T., Ichikawa, H., Ikebe, R., Ikebe, M., and Kaibuchi, K. (1997) *J. Biol. Chem.* **272,** 25121–25127
20. Matsui, T., Maeda, M., Doi, Y., Yonemura, S., Amano, M., Kaibuchi, K., and Tsukita, S. (1998) *J. Cell Biol.* **140,** 647–657
21. Fukata, Y., Kimura, K., Oshiro, N., Saya, H., Matsuura, Y., and Kaibuchi, K. (1998) *J. Cell Biol.* **141,** 409–418
22. Kimura, K., Fukata, Y., Matsuoka, Y., Bennett, V., Matsuura, Y., Okawa, K., Iwamatsu, A., and Kaibuchi, K. (1998) *J. Biol. Chem.* **273,** 5542–5548
23. Amano, M., Chihara, K., Kimura, K., Fukata, Y., Nakamura, N., Matsuura, Y., and Kaibuchi, K. (1997) *Science* **275,** 1308–1311
24. Leung, T., Chen, X. Q., Manser, E., and Lim, L. (1996) *Mol. Cell. Biol.* **16,** 5313–5327
25. Ishizaki, T., Naito, M., Fujisawa, K., Maekawa, M., Watanabe, N., Saito, Y., and Narumiya, S. (1997) *FEBS Lett.* **404,** 118–124
26. Kuroda, S., Kobayashi, S., Amano, M., Kimura, K., Kaibuchi, H., Nakano, T., Kaibuchi, K., and Ito, M. (1997) *J. Biol. Chem.* **272,** 12257–12260
27. Yasui, Y., Amano, M., Nagata, K., Inagaki, N., Nakamura, H., Saya, H., Kaibuchi, K., and Inagaki, M. (1998) *J. Cell Biol.* **143,** 1249–1258
28. Goto, H., Kosako, H., and Inagaki, M. (2000) *Microsc. Res. Tech.*, in press
29. Amano, M., Chihara, K., Nakamura, N., Fukata, Y., Yano, T., Shibata, M., Ikebe, M., and Kaibuchi, K. (1998) *Genes Cells* **3,** 177–188

30. Katoh, H., Aoki, J., Ichikawa, A., and Negishi, M. (1998) *J. Biol. Chem.* **273,** 2489–2492
31. Nagase, T., Ishikawa, K., Nakajima, D., Ohira, M., Seki, N., Miyajima, N., Tanaka, A., Kotani, H., Nomura, N., and Ohara, O. (1997) *DNA Res.* **4,** 141–150
32. Hart, M. J., Sharma, S., elMasry, N., Qiu, R. G., McCabe, P., Polakis, P., and Bollag, G. (1996) *J. Biol. Chem.* **271,** 25452–25458
33. Bradford, M. M. (1976) *Anal Biochem.* **72,** 248–254
34. Inada, H., Togashi, H., Nakamura, Y., Kaibuchi, K., Nagata, K., and Inagaki, M. (1999) *J. Biol. Chem.* **274,** 34932–34939
35. Nagata, K., Puls, A., Futter, C., Aspenstrom, P., Schaefer, E., Nakata, T., Hirokawa, N., and Hall, A. (1998) *EMBO J.* **17,** 149–158
36. Nagata, K., and Nozawa, Y. (1994) *Br. J. Haematol.* **88,** 706–711
37. Satoh, T., Endo, M., Nakafuku, M., Nakamura, S., and Kaziro, Y. (1990) *Proc. Natl. Acad. Sci. U. S. A.* **87,** 5993–5997
38. Goto, H., Kosako, H., Tanabe, K., Yanagida, M., Sakurai, M., Amano, M., Kaibuchi, K., and Inagaki, M. (1998) *J. Biol. Chem.* **273,** 11728–11736
39. Kosako, H., Goto, H., Yanagida, M., Matsuzawa, K., Fujita, M., Tomono, Y., Okigaki, T., Odai, H., Kaibuchi, K., and Inagaki, M. (1999) *Oncogene* **18,** 2783–2788
40. Nishizawa, K., Yano, T., Shibata, M., Ando, S., Saga, S., Takahashi, T., and Inagaki, M. (1991) *J. Biol. Chem.* **266,** 3074–3079
41. Rumenapp, U., Blomquist, A., Schworer, G., Schablowski, H., Psoma, A., and Jakobs, K. H. (1999) *FEBS Lett.* **459,** 313–318
42. Olson, M. F., Pasteris, N. G., Gorski, J. L., and Hall, A. (1996) *Curr. Biol.* **6,** 1628–1633
43. Crespo, P., Schuebel, K. E., Ostrom, A. A., Gutkind, J. S., and Bustelo, X. R. (1997) *Nature* **385,** 169–172
44. Fukuhara, S., Murga, C., Zohar, M., Igishi, T., and Gutkind, J. S. (1999) *J. Biol. Chem.* **274,** 5868–5879
45. Tatsumoto, T., Xie, X., Blumenthal, R., Okamoto, I., and Miki, T. (1999) *J. Cell Biol.* **147,** 921–928
46. Nobes, C. D., Hawkins, P., Stephens, L., and Hall, A. (1995) *J. Cell Sci.* **108,** 225–233
47. Gohla, A., Harhammer, R., and Schultz, G. (1998) *J. Biol. Chem.* **273,** 4653–4659
48. Hart, M. J., Jiang, X., Kozasa, T., Roscoe, W., Singer, W. D., Gilman, A. G., Sternweis, P. C., and Bollag, G. (1998) *Science* **280,** 2112–2114
49. Jalink, K., and Moolenaar, W. H. (1992) *J. Cell Biol.* **118,** 411–419
50. Tigyi, G., Fischer, D. J., Sebok, A., Marshall, F., Dyer, D. L., and Miledi, R. (1996) *J. Neurochem.* **66,** 549–558
51. Postma, F. R., Jalink, K., Hengeveld, T., and Moolenaar, W. H. (1996) *EMBO J.* **15,** 2388–2392
52. Katoh, H., Negishi, M., and Ichikawa, A. (1996) *J. Biol. Chem.* **271,** 29780–29784
53. Buhl, A. M., Johnson, N. L., Dhanasekaran, N., and Johnson, G. L. (1995) *J. Biol. Chem.* **270,** 24631–24634
54. Fromm, C., Coso, O. A., Montaner, S., Xu, N., and Gutkind, J. S. (1997) *Proc. Natl. Acad. Sci. U. S. A.* **94,** 10098–10103
55. Malcolm, K. C., Ross, A. H., Qiu, R. G., Symons, M., and Exton, J. H. (1994) *J. Biol. Chem.* **269,** 25951–25954
56. Bowman, E. P., Uhlinger, D. J., and Lambeth, J. D. (1993) *J. Biol. Chem.* **268,** 21509–21512
57. Katoh, H., Aoki, J., Yamaguchi, Y., Kitano, Y., Ichikawa, A., and Negishi, M. (1998) *J. Biol. Chem.* **273,** 28700–28707
58. Gohla, A., Offermanns, S., Wilkie, T. M., and Schultz, G. (1999) *J. Biol. Chem.* **274,** 17901–17907
59. Stam, J. C., Sander, E. E., Michiels, F., van Leeuwen, F. N., Kain, H. E., van der Kammen, R. A., and Collard, J. G. (1997) *J. Biol. Chem.* **272,** 28447–28454

参考論文

1. Balance between Activities of Rho Kinase and Type 1 Protein Phosphatase Modulates Turnover of Phosphorylation and Dynamics of Desmin/Vimentin Filaments

   Hiroyasu Inada, Hideaki Togashi, Yu Nakamura, Kozo Kaibuchi, Koh-ichi Nagata and Masaki Inagaki

   J. Biol. Chem., **274**, 34932-34939 (1999)

2. 4-Hydroxy-17-methylincisterol, an Inhibitor of DNA Polymerase-α Activity and the Growth of Human Cancer Cells *in vitro*

   Hideaki Togashi, Yoshiyuki Mizushina, Masaharu Takemura, Fumio Sugawara, Hiroyuki Koshino, Yoshiaki Esumi, Jun Uzawa, Hiroyuki Kumagai, Akio Matsukage, Syonen Yoshida and Kengo Sakaguchi

   Biochem. Pharmacol., **56**, 583-90 (1998)

3. An Ergosterol Peroxide, a Natural Product That Selectively Enhances the Inhibitory Effect of Linoleic Acid on DNA Polymerase β

   Yoshiyuki Mizushina, Ichiro Watanabe, Hideaki Togashi, Linda Hanashima, Masaharu Takemura, Keisuke Ohta, , Hiroyuki Koshino, Yoshiaki Esumi, Jun Uzawa, Akio Matsukage, Syonen Yoshida and Kengo Sakaguchi

   Biol Pharm Bull., **21**, 444-8, (1998)

THE JOURNAL OF BIOLOGICAL CHEMISTRY
Vol. 274, No. 49, Issue of December 3, pp. 34932–34939, 1999
Printed in U.S.A.

Balance between Activities of Rho Kinase and Type 1 Protein Phosphatase Modulates Turnover of Phosphorylation and Dynamics of Desmin/Vimentin Filaments*

(Received for publication, July 12, 1999, and in revised form, September 16, 1999)

Hiroyasu Inada‡, Hideaki Togashi‡§, Yu Nakamura¶, Kozo Kaibuchi‖, Koh-ichi Nagata, and Masaki Inagaki**

From the Division of Biochemistry, Aichi Cancer Center Research Institute, 1-1 Chikusa-ku, Nagoya, Aichi 464-8681, the §Division of Biological Sciences Graduate School of Science, Nagoya University, Furo-cho, Chikusa-ku, Nagoya, Aichi 464-8602, the ¶Department of Neuropsychiatry, Osaka University Medical School, 2-2 Yamadaoka, Suita-shi, Osaka 565-0871, and the ‖Division of Signal Transduction, Nara Institute of Science and Technology, 8916-5 Takayama, Ikoma 630-0101, Japan

To analyze the cell cycle-dependent desmin phosphorylation by Rho kinase, we developed antibodies specifically recognizing the kinase-dependent phosphorylation of desmin at Thr-16, Thr-75, and Thr-76. With these antibodies, phosphorylation of desmin was observed specifically at the cleavage furrow in late mitotic Saos-2 cells. We then found that treatment of the interphase cells with calyculin A revealed phosphorylation at all the three sites of desmin. We also found that an antibody, which specifically recognizes vimentin phosphorylated at Ser-71 by Rho kinase, became immunoreactive after calyculin A treatment. This calyculin A-induced interphase phosphorylation of vimentin at Ser-71 was blocked by Rho kinase inhibitor or by expression of the dominant-negative Rho kinase. Taken together, our results indicate that Rho kinase is activated not only in mitotic cells but also interphase ones, and phosphorylates intermediate filament proteins, although the apparent phosphorylation level is diminished to an undetectable level due to the constitutive action of type 1 protein phosphatase. The balance between intermediate filament protein phosphorylation by Rho kinase and dephosphorylation by type 1 protein phosphatase may affect the continuous exchange of intermediate filament subunits between a soluble pool and polymerized intermediate filaments.

Like other of the Ras superfamily of small GTPases, Rho acts as a molecular switch to control a variety of cellular processes: it regulates signal transduction pathways linking extracellular stimuli to the assembly of actin stress fibers and focal adhesion complexes; it is required for G_1 progression and activates serum response factor transcription factor when quiescent fibroblasts are stimulated to grow; and it plays a role in cell cycle during cytokinesis (for reviews, see Refs. 1–3). Much effort has been directed toward identifying target proteins for Rho that mediate the various biological activities of the protein. Several target proteins that interact only with active, GTP-bound Rho have been identified, including protein kinase N (4, 5), Rho kinase/ROKα/ROCKII (6–8), citron kinase (9), rhophilin (5), rhotekin (10), and mDia (11). Among them, Rho kinase has been reported to be involved in several of the cellular processes mentioned above: regulation of myosin phosphorylation (12–14), formation of stress fibers and focal adhesions (15–17), neurite retraction (18–21), and cytokinesis (22–24).

Intermediate filaments (IFs)[1] constitute major components of the cytoskeleton and the nuclear envelope in most cell types (for a review, see Ref. 25). Although IFs were thought to be relatively stable as compared with other cytoskeletons such as actin filaments and microtubules, intensive *in vitro* investigations revealed that site-specific phosphorylation by several kinases, such as protein kinase A, protein kinase C (PKC), Ca^{2+}/calmodulin kinase II (CaMKII), and cdc2 kinase, dynamically alters their filament structure (26) (for reviews, see Refs. 27–29). Thereafter, some of the above kinases were found to be *in vivo* IF kinases, using site- and phosphorylation state-specific antibodies that recognize a phosphorylated Ser/Thr residue and its flanking sequence; cdc2 kinase is activated in early mitotic cells, PKC is activated from metaphase to anaphase, and CaMKII is activated in response to receptor-mediated phosphoinositide hydrolysis (30–32). Rho kinase also has been identified as an *in vivo* IF protein kinase, which site-specifically phosphorylates glial fibrillary acidic protein and vimentin at a cleavage furrow during cytokinesis (22–23). We have shown that Rho kinase plays an essential role in efficient segregation of glial filaments during cytokinesis because mutations in Rho kinase phosphorylation sites impaired segregation of glial filaments into daughter cells and consequently formed an unusually long bridge-like cytoplasmic structure between the daughter cells (24). We clarified that desmin, another type III IF protein, restrictedly expressed in smooth, cardiac, and skeletal muscles, also serves as a substrate for Rho kinase and identified Thr-16, Thr-75, and Thr-76 as the major phosphorylation sites *in vitro* (33). The intracellular localization of Rho kinase remains to be determined. In nonmuscle cells, this kinase, once activated, was found to translocate from the cytosol to plasma membrane (7). It was also reported that Rho kinase is colocalized with the vimentin filament in serum-starved fibroblasts, and when activated, it translocates to cell

* This work was supported in part by grants-in-aid for scientific research and cancer research from the Ministry of Education, Science, Sports and Culture of Japan; by the Japan Society of the Promotion of Science Research for the Future; and by a grant from Bristol-Myers-Squibb. The costs of publication of this article were defrayed in part by the payment of page charges. This article must therefore be hereby marked "*advertisement*" in accordance with 18 U.S.C. Section 1734 solely to indicate this fact.

‡ The first two authors contributed equally to this work.
** To whom correspondence should be addressed. Tel.: 81-52-6111, ext. 8824; Fax: 81-52-763-5233; E-mail: minagaki@aichi-cc.pref.aichi.jp.

[1] The abbreviations used are: IF, intermediate filament; PKC, protein kinase C; CaMKII, Ca^{2+}/calmodulin kinase II; CA, calyculin A; OA, okadaic acid; PP1, type 1 protein phosphatase; PP2A, type 2A protein phosphatase; GST, glutathione *S*-transferase; CAT, catalytic domain; MDCK, Madin-Darby canine kidney.

peripheral regions (34). Therefore, Rho kinase may be active at cell-cell and cell-substrate contact regions in interphase cells. This hypothesis is supported by several lines of experiments showing the Rho kinase-mediated regulation of ezrin, radixin, and moesin proteins (35, 36), adducin (37), and focal complexes (15–17).

In the present work, we newly developed site- and phosphorylation state-specific antibodies for the three Rho kinase phosphorylation sites of desmin in order to analyze the physiological significance of desmin phosphorylation by Rho kinase. Using these antibodies, we found that all the three sites were phosphorylated specifically at the cleavage furrow during cytokinesis. This evidence strongly supports our proposal that Rho kinase acts as a cleavage furrow kinase for IF proteins.

Although various kinases are activated spatiotemporally during the cell cycle and phosphorylate IF proteins, it has been suggested that protein phosphatase is also important for maintenance of the filament structure and plasticity because the IF structure is immediately altered when the cells are treated with protein phosphatase inhibitors (38–41).

We also investigated novel functional aspects of Rho kinase on desmin and vimentin in interphase cells, using the phosphatase inhibitors calyculin A (CA) and ocadaic acid (OA). Rho kinase is active to some extent in interphase cells, as well as mitotic cells, although the phosphorylation is apparently masked due to effects of type 1 protein phosphatase (PP1). Our data allow for a new proposal regarding dynamic exchange of type III IF subunits between a soluble pool and the polymerized IFs: Rho kinase- and PP1-mediataed IF protein phosphorylation and deposphorylation, respectively, may influence steady state equilibrium.

EXPERIMENTAL PROCEDURES

Materials and Chemicals—Recombinant desmin was prepared and purified from *Escherichia coli*, as described (33). GST-CAT (the catalytic domain of Rho kinase, amino acids 6–553) was prepared and purified, as described (13). Desmin was phosphorylated by GST-CAT, as described (33). pEF-BOS-Myc-CAT, pEF-BOS-Myc-RB/PH(TT) (the mutated Rho-binding domain with PH-domain of Rho kinase and acts as a dominant-negative form of Rho kinase, amino acids 941–1388 (20)), and pEF-BOS-Myc-COIL (the coil domain of Rho kinase, amino acids 421–701) were constructed, as described (15, 20). Anti-Rho kinase and GK71 antibodies were generated, as described (42, 23). The antibodies 4A4, YT33, and MO82, which recognize vimentin phosphorylation at specific sites by cdc2 kinase (Ser-55), PKC (Ser-33), and CaMKII (Ser-82) respectively, were developed, as described (29, 43). CA and OA were purchased from Wako Pure Chemical Industries, Ltd. (Osaka, Japan) and Sigma, respectively. HA1077 was purchased from Asahi Chemical Industry (Shizuoka, Japan), and Y-27632 was kindly provided by Yoshitomi Pharmaceuticals Ltd. (Saitama, Japan).

Preparation and Characterization of Antibodies—Desmin peptides PD16 (Cys-Ser-Ser-Tyr-Arg-Arg-phosphoThr^{16}-Phe-Gly-Gly-Ala-Pro), D16 (Cys-Ser-Ser-Tyr-Arg-Arg-Thr-Phe-Gly-Gly-Ala-Pro), PD75 (Cys-Ala-Ser-Arg-Leu-Gly-phosphoThr^{75}-Thr-Arg-Thr-Pro-Ser), D75 (Cys-Ala-Ser-Arg-Leu-Gly-Thr-Thr-Arg-Thr-Pro-Ser), PD76 (Cys-Ser-Arg-Leu-Gly-Thr-phosphoThr^{76}-Arg-Thr-Pro-Ser-Ser), D76 (Cys-Ser-Arg-Leu-Gly-Thr-Thr-Arg-Thr-Pro-Ser-Ser), PD75–76 (Cys-Ala-Ser-Arg-Leu-Gly-phosphoThr^{75}-phosphoThr^{76}-Arg-Thr-Pro-Ser-Ser) were chemically synthesized by Peptide Institute Inc. (Osaka, Japan). PD16, PD75, and PD76 were also synthesized as antigens conjugated keyhole limpet hemocyanin at the NH_2-terminal cysteine residue. Polyclonal antibodies against PD16 (α-PD16), PD75 (α-PD75), and PD76 (α-PD76) were described previously (23, 44). Characterization of the antibodies were carried out as described elsewhere in detail (23).

Cell Culture and Transfection—Human osteosarcoma Saos2 cells (a gift from Dr. H. Saya, Kumamoto University, Kumamoto, Japan), MDCK cells and NIH3T3 cells were cultured in Dulbecco's modified Eagle's medium containing 10% fetal bovine serum, penicillin, and streptomycin in an atmosphere of 5% CO_2. Saos2 cells were seeded on coverslips in six-well plates at 1×10^5 cells/well, and the next day, cells were transfected with pEF-BOS-Myc-RhoK-CAT, using LipofectAMINE Plus™ (Life Technologies, Inc.). Forty-eight h after transfection, the cells were fixed for immunocytochemistry. In some experiments, Saos-2, MDCK, and NIH3T3 cells were seeded on 100-mm plates at 1×10^6 cells/plate or 24-well plates at 1×10^4 cells/well; the next day, the cells were treated with various concentrations of CA or OA, and then cells were harvested for immunoblot analysis or were fixed for immunocytochemistry.

Immunocytochemistry and Immunoblotting—Cells fixed with 3.7% formaldehyde/phosphate-buffered saline for 10 min, followed by treatment with methanol for 10 min at −20 °C, were stained with rabbit polyclonal antibodies (α-PD16, α-PD75, α-PD76, α-desmin, α-Rho kinase, and GK71) and mouse monoclonal antibodies (9E10 and α-vimentin) for 2 h at 37 °C. The immunoreactivities were visualized by incubation with Alexa™ 488 goat anti-rabbit antibody (Molecular Probes) and with FluoroLink™ Cy™2 labeled goat anti-mouse antibody (Amersham Pharmacia Biotech) for 1 h at 37 °C, and then the samples were examined under a confocal microscope (Olympus, LSM-GB200). For immunoblotting, lysate of 1×10^5 CA- or OA-treated cells were subjected to SDS-polyacrylamide gel electrophoresis and transferred onto polyvinylide difluoride membranes (Immobilon-P, Millipore). The membranes were then incubated with polyclonal and monoclonal antibodies, as described above, for 2 h at room temperature, and visualized by making use of horseradish peroxidase-conjugated anti-rabbit or anti-mouse antibodies (Amersham Pharmacia Biotech) and the ECL immunoblotting detection system (Amersham Pharmacia Biotech). In some experiments, quantification of the phosphorylation level was done using laser densitometry, and the level was expressed in arbitrary optical density units. In cell suspension experiments, NIH3T3 cells were detached from culture dishes by trypsin treatment. Cells were then once washed by centrifugation, resuspended in the medium, and treated with various concentrations of CA or OA followed by immunoblot and immunocytochemical analyses.

Treatment with Rho Kinase Inhibitors and Microinjection of a Dominant Negative Rho Kinase Expression Vector—NIH3T3 cells were seeded on 100-mm plates at 1×10^6 cells/plate or 24 well plates at 1×10^4 cells/well; next day, the cells were preincubated with various concentrations of HA1077 or Y-27632 for 30 min, and then CA was added (final concentration, 20 nM). After treatment with CA for for 15 min, the cells were harvested for immunoblot analysis or were fixed for immunocytochemistry. For microinjection, NIH3T3 cell were seeded on 13-mm glass coverslips at 1×10^4 cells/slip. The next day, pEF-BOS-Myc-RB/PH(TT) (0.1 mg/ml) or pEF-BOS-Myc-COIL (0.1 mg/ml) was microinjected into the nuclei of the cells. Twenty-four h after injection, the cells were treated with 20 nM CA for 15 min and were fixed for immunocytochemical analysis.

RESULTS

Production and Characterization of Antibodies for Rho Kinase Phosphorylation Sites of Desmin—We reported that desmin is phosphorylated by Rho kinase at Thr-16, Thr-75, and Thr-76 *in vitro* (33). To investigate the phosphorylation of desmin by Rho kinase during the cell cycle, we developed three rabbit polyclonal antibodies (α-PD16, α-PD75, and α-PD76) against the synthetic phosphopeptides PD16, PD75, and PD76, respectively (Fig. 1*A*). The reactivity of α-PD16, α-PD75, and α-PD76 to desmin phosphorylated at Thr-16, Thr-75, and Thr-76 was investigated by immunoblotting. In Fig. 1*B*, α-PD16, α-PD75, and α-PD76 reacted with the phosphorylated desmin by Rho kinase but not unphosphorylated desmin. As shown in Fig. 1*C*, inhibition assays were carried out using synthetic peptides to analyze the epitope specificity of these antibodies. The immunoreactivity of α-PD16 was prevented by preincubation of phosphopeptide PD16 but not nonphosphopeptide D16 or other phosphopeptides/nonphosphopeptides, such as PD75, D75, PD76, D76, and PD75–76. Likewise, the reaction of α-PD75 was blocked by preincubation with phosphopeptide PD75. The immunoreactivity of α-PD76 was blocked by preincubation with PD76 and partly blocked with PD75–76. Thus, α-PD16 and α-PD75 specifically recognized the phosphorylation of desmin at Thr-16 and Thr-75, respectively. On the other hand, α-PD76 was found to recognize double phosphorylation at Thr-75 and Thr-76 as well as the monophosphorylation of desmin at Thr-76.

Phosphorylation of Desmin-Thr-16, Thr-75 and Thr-76 by Active Rho Kinase in Saos-2 Cells—To investigate the phospho-

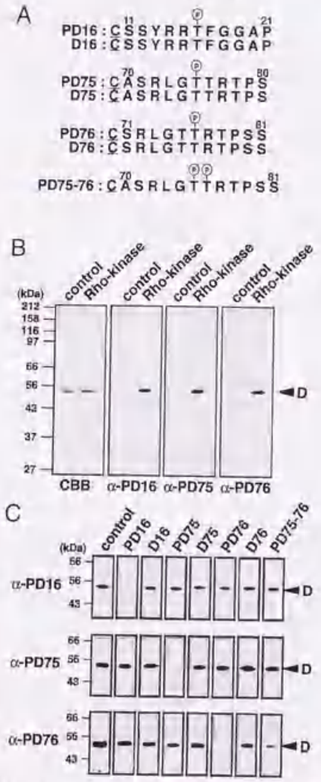

FIG. 1. **Characterization of antibodies α-PD16, α-PD75, and α-PD76, analyzed by immunoblotting.** *A*, amino acid sequences of the synthetic peptides PD16/D16, PD75/D75, PD76/D76, and PD75–76 used in this study. *B*, desmin was unphosphorylated (*control*) or phosphorylated at about 0.9 mol of phosphate/mol of protein by GST-Rho kinase. 80 ng of the protein was subjected to SDS-polyacrylamide gel electrophoresis. The membranes were then immunoblotted with α-PD16, α-PD75, or α-PD76 or stained with Coomassie Brilliant Blue (*CBB*). Deamin is indicated by an *arrowhead*. *C*, specificity of α-PD16, α-PD75, and α-PD76, using an inhibition assay. 80 ng of desmin phosphorylated by GST-Rho kinase was immunoblotted with α-PD16, α-PD75, or α-PD76 after absorption with synthetic peptides (60 mg/ml each of PD16, D16, PD75, D75, PD76, D76, or PD75–76). Control shows the reactivity of α-PD16, α-PD75, or α-PD76 after preincubation with Tris-buffered saline containing 0.1% Tween-20.

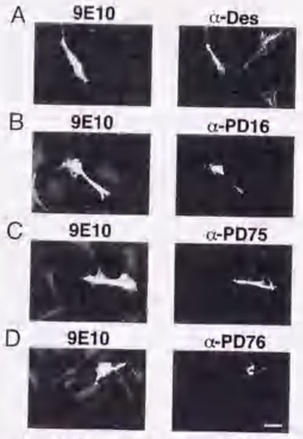

FIG. 2. **Phosphorylation at Thr-16, Thr-75, and Thr-76 of desmin in Saos-2 cells expressing constitutive active Rho kinase.** Saos-2 cells were transfected with pEF-BOS-Myc-CAT and double-stained, as described under "Experimental Procedures" with 9E10 for Myc epitope-tagged RhoK-CAT (*left panels*) and α-Des (*A, right panel*), α-PD16 (*B, right panel*), α-PD75 (*C, right panel*), or α-PD76 (*D, right panel*). *Scale bar*, 20 μm.

rylation of desmin by Rho kinase in cells, we asked whether Rho kinase could phosphorylate Thr-16, Thr-75, and Thr-76 of desmin in Saos-2 human osteoblast cells ectopically expressing the constitutively active version of Rho kinase (Fig. 2). Cells were transiently transfected with pEF-BOS-Myc mammalian expression vector encoding the constitutively activated catalytic domain of bovine Rho kinase (RhoK-CAT). The cells were double-stained with monoclonal antibody 9E10 for the Myc epitope-tagged RhoK-CAT and α-Des (Fig. 2*A*), α-PD16 (Fig. 2*B*), α-PD75 (Fig. 2*C*), or α-PD76 (Fig. 2*D*). Immunocytochemical analyses revealed that phosphorylation of Thr-16, Thr-75, and Thr-76 of desmin occurred in cells expressing RhoK-CAT (Fig. 2, *B–D*). As is the case with vimentin (23), phosphorylation of desmin by Rho kinase induces collapse, a dynamic change of desmin-IF organization (Fig. 2, *A–D*). This phosphorylation was not detected in the cells expressing the catalytic domain mutated at the ATP-binding site (CAT-KD; K121G) (data not shown), indicating that the kinase domain is essential for the desmin phosphorylation we observed. These results show that the constitutive active form of Rho-kinse phosphorylates all three *in vitro* Rho kinase phosphorylation sites of desmin in cells.

Specific Phosphorylation of Desmin-Thr-16, Thr-75, and Thr-76 at Cleavage Furrow during the Cell Cycle—In the next set of experiments, based on the foregoing biochemical and immunocytochemical observation that Thr-16, Thr-75, and Thr-76 of desmin are *in vivo* phosphorylation sites by Rho kinase, the spatial and temporal distribution of the three phosphorylated sites in Saos-2 cells was analyzed using α-PD16, α-PD75, and α-PD76. Under the conditions used, all the immunoreactivity of α-PD16, α-PD75, and α-PD76 was detected only in late mitotic cells and specifically at the cleavage furrow (Fig. 3) but not in interphase cells (Fig. 4*A*) or in early mitotic cells, such as prometaphase or metaphase (data not shown). When desmin was stained with α-Des, which reacts with phosphorylated and unphosphorylated desmin, the filamentous structures were observed in mitotic daughter cells (Fig. 3) and in interphase cells (Fig. 4*A*). In late mitotic Saos-2 cells, Rho kinase also accumulates specifically at the cleavage furrow, as illustrated in Fig. 3, findings that strongly suggest a direct interaction of the kinase with desmin. From these results, we conclude that Rho kinase acts as desmin kinase at the cleavage furrow during cytokinesis. On the basis of the *in vitro* observation that phosphorylation of desmin by Rho kinase inhibits filament formation (33), we propose that desmin filaments are phosphorylated by Rho kinase and depolymerized at the cleavage furrow during cytokinesis, and hence the segregation of desmin into daughter cells is efficient.

Phosphorylation of Thr-16, Thr-75, and Thr-76 of Desmin in Interphase Cells Treated with Calyculin A—Phosphorylation of IF proteins may play a role in IF structural organization. Rho kinase was found to be co-localized with IF filament in interphase cells (34). To assess the possible function(s) of Rho kinase in IF reorganization, we next analyzed the activation state of Rho kinase on desmin in interphase cells. Intact interphase

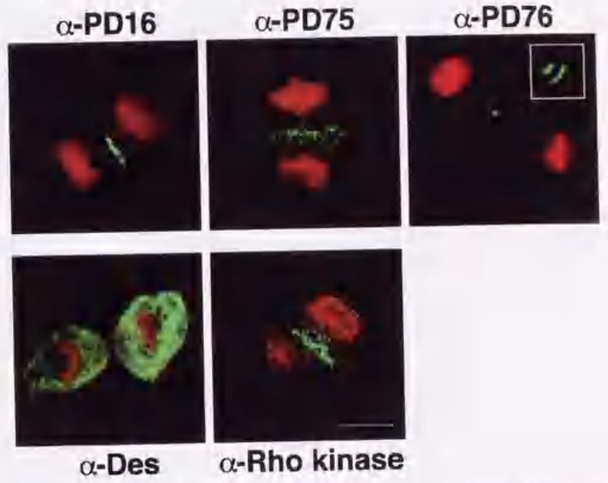

FIG. 3. **Immunofluorescence staining of Saos-2 cells with α-PD16, α-PD75, and α-PD76.** Confocal micrographic images of Saos-2 cells stained with α-PD16, α-PD75, α-PD76, α-desmin, or α-Rho kinase (*green*). DNAs were stained with propidium iodide (*red*). Images represent projections of Z series scans. *Inset* depicts magnified view at the cleavage furrow area. *Scale bar*, 10 μm.

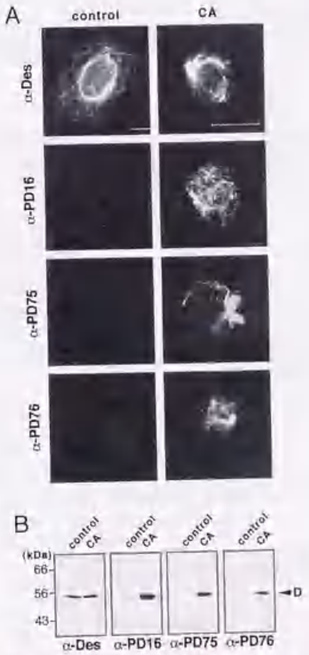

FIG. 4. **Phosphorylation of desmin by Rho kinase in response to CA in Saos-2 cells.** *A*, Saos-2 cells were treated with 20 nM CA for 20 min (*right panels*). Control cells (*left panels*) were untreated. Cells were fixed and stained with α-desmin, α-PD16, α-PD75, or α-PD76. *Scale bars*, 10 μm. *B*, cells were untreated (*control*) or treated with 20 nM CA for 20 min (*CA*) and analyzed by immunoblotting. Desmin (*D*) is indicated by the *arrowhead*.

cells showed a characteristic network of desmin filaments spanning the cytoplasm, determined using an anti-desmin antibody (Fig. 4*A*, *α-Des, left panel*). After treatment with the phosphatase inhibitor CA (20 nM) for 20 min, cells began to round up, the organization of desmin filament was altered, and the IF network collapsed to form a desmin-containing arc near the perinuclear region (Fig. 4*A*, *α-Des, right panel*). All the immunoreactivity of α-PD16, α-PD75, and α-PD76 appeared in interphase cells treated with CA (Fig. 4*A*, *right panels*). Although the staining patterns varied, the filamentous structure was clearly disrupted and the desmin filaments had collapsed. To confirm that Thr-16, Thr-75, and Thr-76 of desmin were phosphorylated in response to CA, immunoblot analysis was performed. As shown in Fig. 4*B*, α-PD16, α-PD75, or α-PD76-immunoreactive band was observed when interphase cells were treated with CA. Taken together, it is most likely that Rho kinase is to some extent activated even in interphase cells, and an unidentified CA-sensitive phosphatase causes the rapid phosphate turnover on IFs.

Phosphorylation of Vimentin by Rho Kinase in Response to Calyculin A—Because we determined that Ser-71 of vimentin is a specific site for Rho-kinse, and Ser-33, Ser-55, and Ser-82 residues of vimentin are sites specific for PKC, cdc2 kinase, and CaMKII, respectively (29), vimentin is a suitable substrate to verify that Rho kinase, rather than other kinases, phosphorylates IF proteins and regulates their structure and plasticity in interphase cells. We next examined phosphorylation states of vimentin, widely expressed in culture cells, in response to CA, using several types of site- and phosphorylation state-specific antibodies for vimentin. We found that the phosphorylation of Ser-71 appeared in the vimentin filament (Fig. 5) determined using an antibody, GK71, that recognizes the phosphorylation of vimentin-Ser-71 (23). On the other hand, the phosphorylation of Ser-33, Ser-55, and Ser-82 was not observed, and it did not increase in interphase cells treated with CA, respectively (Fig. 5), indicating that PKC and cdc2 kinase are not involved in vimentin phosphorylation in interphase Saos-2 cells. CaMKII activity was to some extent detectable but the level was less altered by CA treatment. Moreover, we found an increase in the phosphorylation level of other Rho kinase substrates, such as the myosin binding subunit of myosin phosphatase and myosin light chain (data not shown). Collectively, we concluded that Rho kinase is mainly responsible for IF protein phosphorylation in interphase Saos-2 cells.

To determine whether CA-induced vimentin phosphorylation by Rho kinase could be observed in other cells, MDCK cells and NIH3T3 cells were used (Fig. 6, *B* and *C*). When MDCK

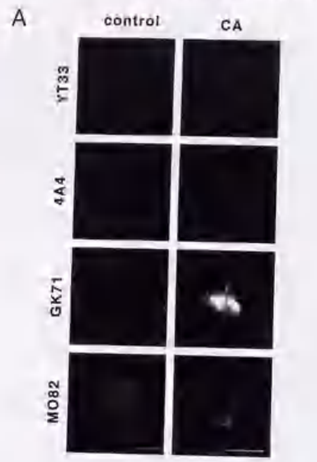

FIG. 5. **Phosphorylation of vimentin by PKC, Cdc2 kinase, and CaMKII in response to CA in Saos-2 cells.** *A*, Saos-2 cells were treated with (*CA*) or without (*control*) 20 nM CA for 20 min. Cells were fixed and stained with YT33, 4A4, GK71, or MO82. *Scale bars*, 10 μm. *B*, cells were untreated (*control*) or treated with 20 nM CA for 20 min (*CA*) and analyzed by immunoblotting. Vimentin is indicated by the *arrowhead*.

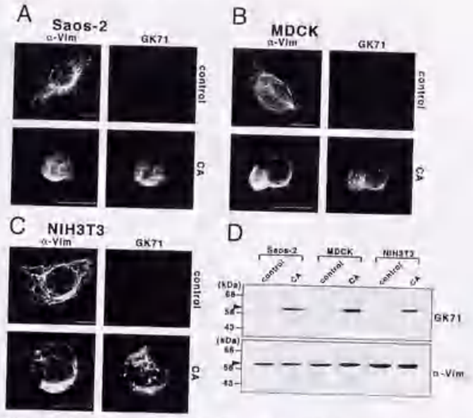

FIG. 6. **Phosphorylation of vimentin by Rho kinase in response to CA in MDCK and NIH3T3 cells.** *A–C*, Saos-2, MDCK, and NIH3T3 cells were treated with 20 nM CA for 20 min (*A, bottom panels*), with 25 nM CA for 20 min (*B, bottom panels*), and with 20 nM CA for 15 min (*C, bottom panels*), respectively. Control cells were left untreated with CA (*A–C, top panels*). In each experiment, cells were double-stained with α-vimentin (*α-Vim*) (*left panels*) and GK71 (*right panels*). *Scale bars*, 10 μm. *D*, cells were untreated (*control*) or treated with CA as described above and analyzed by immunoblotting.

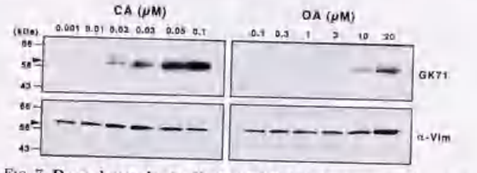

FIG. 7. **Dose-dependent effects of CA and OA on the phosphorylation at Ser-71 of vimentin in NIH3T3 cells.** NIH3T3 cells were treated with the indicated concentrations of CA or OA for 15 min. Cells were harvested and subjected to immunoblotting analysis, as described under "Experimental Procedures." GK71-immunoreactivity is depicted in *top panels*. The same immunoblot membranes were reprobed with α-vimentin antibody (*α-Vim*) (*bottom panels*).

and NIH3T3 cells were treated with 25 nM CA for 20 min and 20 nM CA for 15 min, respectively, the morphology of the vimentin filament network and phosphorylation state of vimentin-Ser-71 were analyzed. Fig. 6, *B* and *C*, shows that these cells also began to round up, and the vimentin organization was altered. GK71 reacted with vimentin in these interphase cells (Fig. 6, *B* and *C*). In Fig. 6*D*, the CA-induced vimentin-Ser-71 phosphorylation was also confirmed by immunoblot analysis. As in Saos-2 cells, the phosphorylation of Ser-33 and Ser-55 was not observed in MDCK and NIH3T3 cells treated with CA (data not shown). The weak phosphorylation of Ser-82 was less altered (data not shown). These results suggest that Rho kinase-mediated phosphorylation of vimentin in response to CA is a general feature in vimentin-expressing cells.

Different Dose Response Effects of Calyculin A and Okadaic Acid on the Immunoreactivity of GK71—We then used immunoblots to examine the appearance of vimentin phosphorylation by Rho kinase in NIH3T3 cells using OA, another potent inhibitor of PP1 and type 2A protein phosphatase (PP2A). There were obvious differences between the dose-response effects of CA and OA (Fig. 7). The immunoreactivity of GK71 appeared first at a dose range of 10–20 nM in CA-treated cells, but at 3–10 μM in OA-treated cells. An approximately 100-fold difference in inhibitory sensitivity would mean that OA has a 50–100-fold weaker effect than CA on PP1. OA and CA are reported to inhibit PP2A with a similar potency (45, 46). In the course of this experiment, we found that CA-treated cells became round and readily detached from culture dishes, as compared with findings in case of OA treatment. Thus, the GK71 immunoreactivity detected in the above experiments may reflect morphological change of the cells rather than phosphatase inhibition. To rule out this possibility, we did the same experiments using suspended and round NIH3T3 cells instead of those attached to culture dishes. Consequently, CA and OA showed comparable effects on GK71 reactivity of suspended and round NIH3T3 cells to findings in the cells attached to culture dishes (data not shown). From these data, taken together, we conclude that PP1 dephosphorylates Ser-71 of vimentin in intact interphase cells.

Effects of Rho Kinase Inhibitors and Expression of the Dominant Negative Form of Rho Kinase on Vimentin Phosphorylation in Response to Calculin A—Recently, it has been reported that chemical compounds such as HA1077 and Y-27632 selectively inhibit the activity of Rho kinase (47–49). To confirm that Ser-71 of vimentin is phosphorylated by Rho kinase and not other kinases in interphase cells treated with CA, we investigated the effects of the two Rho kinase inhibitors. NIH3T3 cells were preincubated with these inhibitors (10 μM) for 30 min and then treated with CA and double-stained with α-vimentin and GK71. When cells were preincubated with the inhibitors, CA-induced immunoreactivity of GK71 was completely blocked

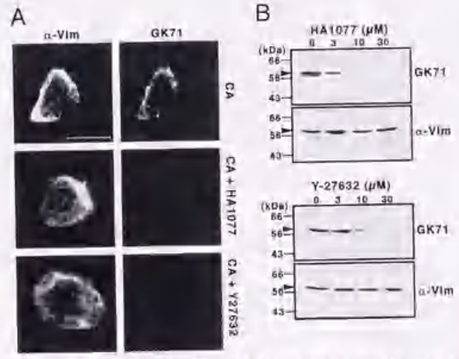

FIG. 8. **Effects of Rho kinase inhibitors on vimentin phosphorylation in response to calyculin A.** *A*, after preincubation of NIH3T3 cells with buffer (*top panel*) or 10 μM each of HA1077 and Y-27632 for 30 min (*middle* and *bottom panels*), cells were treated with 20 nM CA for 15 min and double-stained with α-vimentin (*α-Vim*) and GK71, as described under "Experimental Procedures." *Scale bars*, 10 μm. *B*, dose-dependent effects of HA1077 and Y-27632 on the immunoreactivity of GK71. NIH3T3 cells were preincubated with indicated doses of HA1077 or Y-27632 for 30 min and then treated with 20 nM CA for 15 min. The cells were then collected and analyzed by immunoblotting.

(Fig. 8*A*). Immunoblot analyses also revealed that GK71-immunoreactivity was inhibited by both of HA1077 and Y-27632 (Fig. 8*B*). Furthermore, a dominant-negative form of Rho kinase, RB/PH(TT), was used to confirm that the Ser-71 was phsophorylated by Rho kinase. Twenty-four hours after the microinjection of RB/PH(TT) expression plasmid into nuclei of NIH3T3 cells, the cells were treated with 20 nM CA for 15 min and analyzed using 9E10 for the Myc epitope-tagged RB/PH(TT) and GK71. When cells were microinjected with pEF-BOS-COIL, which contains the coil domain of Rho kinase, as a control, GK71-immunoreactivity was observed both in COIL-expressing cells (Fig. 9*A*, *arrow*) and nonexpressing cells (Fig. 9*A*, *arrowhead*). On the other hand, in cells expressing RB/PH(TT) the GK71 immunoreactivity was not observed after CA treatment (Fig. 9*B*, *arrow*). Under these conditions, Ser-71 phosphorylation was detected in cells not expressing of RB/PH(TT) (Fig. 9*B*, *arrowhead*). We conclude that Rho kinase phosphorylates vimentin at Ser-71, in response to CA in interphase cells. Our results strongly suggest that the constitutive phosphorylation of IF proteins by Rho kinase occurs significantly, whereas a more extensive phosphate turnover occurs on IFs by PP1 in interphase cells.

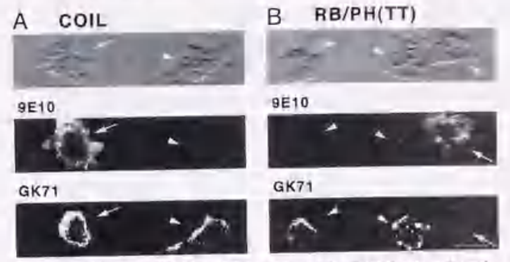

FIG. 9. **Effects of RB/PH(TT) on vimentin Ser-71 phosphorylation in response to CA.** COIL (*A*) (as a control) or RB/PH(TT) (*B*) was microinjected into the nuclei of cells. After a 24-h culture, cells were treated with 20 nM CA for 15 min, as described under "Experimental Procedures," and double-immunostained with 9E10 for Myc epitope-tagged RB/PH(TT) and COIL (*middle panels*) and GK71 (*bottom panels*). *Top panels* are transmittance images of the same frame as the *middle* and *bottom panels*. *Arrows* indicate cells expressing RB/PH(TT) or COIL, whereas *arrowheads* indicate neighboring, unmicroinjected cells. *Scale bars*, 10 μm.

DISCUSSION

We earlier clarified that desmin can serve as a good substrate for Rho kinase *in vitro* (33). In the present study, using newly developed site- and phosphorylation state-specific antibodies for Rho kinase phosphorylation sites of desmin, Rho kinase is found to phosphorylate desmin specifically at the cleavage furrow during cytokinesis, as is the case with other type III IF proteins, glial fibrillary acidic protein, and vimentin (22, 23). We have found that Rho kinase itself accumulates at the cleavage furrow in Saos-2 human osteoblast cells, as was noted in U251 human glioma cells (42). Thus, it is a common phenomenon for all type III IF proteins that Rho kinase acts as a cleavage furrow kinase, and it is most likely that Rho kinase regulates the organization of these IFs during cytokinesis via a common molecular mechanism, which ensures effective segregation of IFs into daughter cells. Citron kinase, another Rho target protein with a kinase domain homologous to that of Rho kinase, was also found to localize to the cleavage furrow and the midbody of Hela cells (50). Citron kinase is thought to work in the contractile process rather than actin reorganization (50). The different and redundant functions of Rho kinase and citron kinase in cytokinetic process remain to be elucidated. These two kinases may participate in different steps during cytokinesis because citron kinase does not phosphorylate any type III IF proteins in the conditions under which Rho kinase does.[2]

To date, little is known of precise molecular mechanisms of spatiotemporal Rho kinase activation in cytokinesis. It is possible that Rho kinase is recruited to the cleavage furrow and is activated during cytokinesis. Another possibility is that accumulation of Rho kinase with basal activity at the cleavage furrow in late mitotic cells, but not local activation of the kinase at the cleavage furrow, is sufficient for exerting its role in cytokinesis. Regardless, in both cases, when net Rho kinase activity becomes dominant over phosphatase activity due to accumulation and/or activation at the cleavage furrow, Rho kinase phosphorylates various substrates (such as IF proteins, myosin light chain, and ezrin, radixin, and moesin) and facilitates cytokinesis.

It has been reported that phosphatases play an essential role for the maintenance and structural integrity of IFs in interphase cells, determined using the protein phosphatase inhibitors CA and OA. CA and OA are potent inhibitors for PP1 and PP2A and are often used to demonstrate the involvement of PP1 and PP2A in a biological cellular processes. CA and OA inhibit PP2A with a similar potency, whereas OA is 50–100-fold weaker than CA as a PP1 inhibitor. CA and OA are weakly sensitive and completely insensitive to other phosphatases, protein phosphatases 2B and 2C, respectively. In the course of experiments on desmin/vimentin phosphorylation with site- and phosphorylation state-specific antibodies, we investigated the effects of CA and OA and determined that PP1 functions as a desmin/vimentin phosphatase. PP1 is known to play a pivotal role in the cell cycle and is regulated by the interaction of the catalytic subunit with a variety of regulatory proteins that have as an important role to localize the enzyme and to determine substrate specificity. The involvement of PP1 in IF integrity was suggested for vimentin when CA and OA were used (38). In neuronal cells, PP2A was identified to be a neurofilament-associated phosphatase that may preserve the filamen-

[2] H. Inada, H. Togashi, Y. Nakamura, K. Kaibuchi, K.-i. Nagata, and M. Inagaki, unpublished observation.

tous structure of neurofilament (51). As for keratin 8/18, PP1 and/or PP2A is suggested to function in disassembly and reorganization (39, 40). Although protein phosphatases responsible for IF organization have been noted in some cell systems, as mentioned above, the kinase(s) that phosphorylates IFs in interphase cells is unknown. Only CaMK may be a candidate for a major role in keratin 8/18 phosphorylation in interphase cells (39). Utilizing a series of site- and phosphorylation state-specific antibodies, we have shown here that Rho kinase phosphorylates desmin and/or vimentin in interphase Saos-2, NIH3T3, and MDCK cells, but the phosphorylation was evident only after CA treatment. In comparison, vimentin phosphorylation by PKC and cdc2 kinase did not appear in NIH3T3 cells even after CA treatment, and the phosphorylation level by CaMKII was not altered by CA treatment. Furthermore, we confirmed that Rho kinase induces phosphorylation of vimentin in CA-treated interphase NIH3T3 cells, using Rho kinase inhibitors (47) and expression of the dominant-negative form of Rho kinase, RB/PH(TT) (20); the phosphorylation of the Rho-kianse specific site, Ser-71, on vimentin was completely blocked by pretreatment with Y-27632, HA1077 or the ectopic expression of RB/PH(TT). Thus, Rho kinase functions as an interphase IF kinase (although dephosphorylation activity of PP1 on desmin and vimentin is thought to be higher than the phosphorylation activity by Rho kinase in interphase cells).

The present study sheds light on the tightly balanced activity of Rho kinase and PP1 in interphase cells. As for the biological significance of IF protein phosphorylation by Rho kinase observed here, one can speculate the modulation of IF protein dynamics. Ectopically expressed or microinjected IF proteins were found to be incorporated into preexisting IFs along their entire surface (52, 53). Consistent with these observations, transient expression of assembly-deficient mutant keratin in epithelial cells (54) and microinjection of peptides derived from IF sequence motifs essential for IF assembly (55) disrupted the endogenous IF system. These results clearly indicate that IFs are highly dynamic, and a continuous exchange of subunit proteins occurs on the entire filament surface between a soluble pool and the polymerized IFs, reaching a steady state equilibrium (56). Mechanisms regulating the equilibrium state are unknown. Based on the results observed in this study, we consider that Rho kinase is one candidate that, together with PP1, modulates the equilibrium between a soluble IF protein pool and a polymerized protein pool. The balance of Rho kinase and PP1 activities seems essential not only for modulating IF structure and plasticity but also for cell-substrate adhesion, cell motility, and actin reorganization in interphase cells. Further analyses are required to clarify the molecular mechanism of the concerted action of Rho kinase and PP1 in individual cellular processes, including IF protein dynamics in interphase.

As for the effects of CA and OA observed on Rho kinase activity, it must be noted that CA and OA act as strong tumor promoters. It is possible that CA, and maybe OA, causes tumor promotion by disturbing the balance between Rho kinase and PP1 activities. If such is indeed the case, increments in Rho kinase activity by diminishing PP1 may explain some characteristic features of cancer cells, including abnormal growth, invasion, and metastasis.

Acknowledgments—We thank Yoshitomi Pharmaceutical Industries, Ltd. for kindly providing Y-27632, Drs. H. Tsuiki and H. Saya (Kumamoto University) for providing Saos-2 cells, and Dr. H. Kosako (our laboratory) for preparing the anti-Rho kinase antibody. We are grateful to K. Kuromiya for secretarial services, K. Hara for technical assistance, and M. Ohara for a critique of the manuscript.

REFERENCES

1. Van Aelst, L., and D'Souza-Schorey, C. (1997) *Genes Dev.* **11,** 2295–2322
2. Hall, A. (1998) *Science* **279,** 509–514
3. Kaibuchi, K., Kuroda, S., and Amano, M. (1999) *Annu. Rev. Biochem.* **68,** 459–486
4. Amano, M., Mukai, H., Ono, Y., Chihara, K., Matsui, T., Hamajima, Y., Okawa, K., Iwamatsu, A., and Kaibuchi, K. (1996) *Science* **271,** 648–650
5. Watanabe, G., Saito, Y., Madaule, P., Ishizaki, T., Fujisawa, K., Morii, N., Mukai, H., Ono, Y., Kakizuka, A., and Narumiya, S. (1996) *Science* **271,** 645–648
6. Matsui, T., Amano, M., Yamamoto, T., Chihara, K., Nakafuku, M., Ito, M., Nakano, T., Okawa, K., Iwamatsu, A., and Kaibuchi, K. (1996) *EMBO J.* **15,** 2208–2216
7. Leung, T., Manser, E., Tan, L., and Lim, L. (1995) *J. Biol. Chem.* **270,** 29051–29054
8. Ishizaki, T., Maekawa, M., Fujisawa, K., Okawa, K., Iwamatsu, A., Fujita, A., Watanabe, N., Saito, y., Kakizuka, A., Morii, N., and Narumiya, S. (1996) *EMBO J.* **15,** 1885–1893
9. Madaule, P., Furuyashiki, T., Reid, T., Ishizaki, T., Watanabe, G., Morii, N., and Narumiya, S. (1995) *FEBS Lett.* **377,** 243–248
10. Reid, T., Furuyashiki, T., Ishizaki, T., Watanabe, G., Watanabe, N., Fujisawa, K., Morii, N., Madaule, P., and Narumiya, S. (1996) *J. Biol. Chem.* **271,** 13556–13560
11. Watanabe, N., Madaule, P., Reid, T., Ishizaki, T., Watanabe, G., Kakizuka, A., Saito, Y., Nakano, K., Jockusch, B. M., and Narumiya, S. (1997) *EMBO J.* **16,** 3044–3056
12. Kimura, K., Ito, M., Amano, M., Chihara, K., Fukata, Y., Nakafuku, M., Yamamori, B., Feng, J., Nakano, T., Okawa, K., Iwamatsu, A., and Kaibuchi, K. (1996) *Science* **273,** 245–248
13. Amano, M., Ito, M., Kimura, K., Fukata, Y., Chihara, K., Nakano, T., Matsuura, Y., and Kaibuchi, K. (1996) *J. Biol. Chem.* **271,** 20246–20249
14. Chihara, K., Amano, M., Nakafuku, N., Yano, T., Shibata, M., Tokui, T., Ichikawa, H., Ikebe, R., Ikebe, M., and Kaibuchi, K. (1997) *J. Biol. Chem.* **272,** 25121–25127
15. Amano, M., Chihara, K., Kimura, K., Fukata, Y., Nakafuku, N., Matsuura, Y., and Kaibuchi, K. (1997) *Science* **275,** 1308–1311
16. Leung, T., Chen, X.-Q., Manser, E., and Lim, L. (1996) *Mol. Cell. Biol.* **16,** 5313–5327
17. Ishizaki, Y., Naito, M., Fujisawa, K., Maekawa, M., Watanabe, N., Saito, Y., and Narumiya, S. (1997) *FEBS Lett.* **404,** 118–124
18. Kozma, R., Sarner, S., and Lim, L. (1997) *Mol. Cell. Biol.* **17,** 1201–1211
19. Katoh, H., Aoki, J., Ichikawa, A., and Negishi, M. (1998) *J. Biol. Chem.* **273,** 2489–2492
20. Amano, M., Chihara, K., Nakamura, N., Fukata, Y., Yano, T., Shibata, M., Ikebe, M., and Kaibuchi, K. (1998) *Genes to Cells* **3,** 177–188
21. Hirose, M., Ishizaki, T., Watanabe, N., Uehata, M., Kranenburg, O., Moolenaar, W. H., Matsumura, F., Maekawa, M., Bito, H., and Narumiya, S. (1998) *J. Cell Biol.* **141,** 1625–1636
22. Kosako, H., Amano, M., Yanagida, M., Tanabe, K., Nishi, Y., Kaibuchi, K., and Inagaki, M. (1997) *J. Biol. Chem.* **272,** 10333–10336
23. Goto, H., Kosako, H., Tanabe, K., Yanagida, M., Sakurai, M., Amano, M., Kaibuchi, K., and Inagaki, M. (1998) *J. Biol. Chem.* **273,** 11728–11736
24. Yasui, Y., Amano, M., Nagata, K., Inagaki, N., Nakamura, H., Saya, H., Kaibuchi, K., and Inagaki, M. (1998) *J. Cell Biol.* **143,** 1249–1258
25. Fuchs, E., and Weber, K. (1994) *Annu. Rev. Biochem.* **63,** 345–382
26. Inagaki, M., Nishi, Y., Nishizawa, K., Matsuyama, M., and Sato, C. (1987) *Nature* **328,** 649–652
27. Eriksson, J. E., Opel, P., and Goldman, R. D. (1992) *Curr. Opin. Cell Biol.* **4,** 99–104
28. Fuchs, E., and Cleveland, D. W. (1998) *Science* **279,** 514–519
29. Inagaki, M., Matsuoka, Y., Tsujimura, K., Ando, S., Tokui, T., Takahashi, T., and Inagaki, N. (1996) *BioEssays* **18,** 481–487
30. Ogawara, M., Inagaki, N., Tsujimura, K., Takai, Y., Sekimata, M., Ha, M. H., Imajoh-Ohmi, S., Hirai, S., Ohno, S., Sugiura, H., Yamauchi, T., and Inagaki, M. (1995) *J. Cell Biol.* **131,** 1055–1066
31. Takai, Y., Ogawara, M., Tomono, Y., Moritoh, C., Imajoh-Ohmi, S., Tsutsumi, O., Taketani, Y., and Inagaki, M. (1996) *J. Cell Biol.* **133,** 141–149
32. Inagaki, N., Goto, H., Ogawara, M., Nishi, Y., Ando, S., and Inagaki, M. (1997) *J. Biol. Chem.* **272,** 25195–25199
33. Inada, H., Goto, H., Tanabe, K., Nishi, Y., Kaibuchi, K., Inagaki, M. (1998) *Biochem. Biophys. Res. Commun.* **253,** 21–25
34. Sin, W.-C., Chen, X.-Q., Leung, T., and Lim, L. (1998) *Mol. Cell. Biol.* **18,** 6325–6339
35. Matsui, T., Maeda, M., Doi, Y., Yonemura, S., Amano, M., Kaibuchi, K., Tsukita, S., and Tsukita, S. (1998) *J. Cell Biol.* **140,** 647–657
36. Fukata, Y., Kimura, K., Oshiro, N., Saya, H., Matsuura, Y., and Kaibuchi, K. (1998) *J. Cell Biol.* **141,** 409–418
37. Kimura, K., Fukata, Y., Matsuoka, Y., Bennett, V., Matsuura, Y., Okawa, K., Iwamatsu, A., and Kaibuchi, K. (1998) *J. Biol. Chem.* **273,** 5542–5548
38. Eriksson, J. E., Brautigan, D. L., Vallee, R., Olmsted, J., Fujiki, H., and Goldman, R. D. (1992) *Proc. Natl. Acad. Sci. U. S. A.* **89,** 11093–11097
39. Toivola, D. M., Goldman, R. D., Garrod, D. R., and Eriksson, J. E. (1997) *J. Cell Sci.* **110,** 23–33
40. Toivola, D. M., Omary, M. B., Ku, N.-O., Peltola, O., Baribault, H., and Eriksson, J. E. (1998) *Hepatology* **28,** 116–128
41. Eriksson, J. E., and Goldman, R. D. (1993) *Adv. Protein Phosphatase* **7,** 335–357
42. Kosako, H., Goto, H., Yanagida, M., Matsuzawa, K., Fujita, M., Tomono, Y., Okigaki, T., Odai, H., Kaibuchi, K., and Inagaki, M. (1999) *Oncogene* **18,** 2783–2788
43. Tsujimura, K., Ogawara, M., Takeuchi, Y., Imajoh-Ohmi, S., Ha, M. H., and Inagaki, M. (1994) *J. Biol. Chem.* **269,** 31097–31106

44. Nishizawa, K., Yano, T., Shibata, M., Ando, S., Saga, S., Takahashi, T., and Inagaki, M. (1991) *J. Biol. Chem.* **266,** 3074–3079
45. Ishihara, H., Martin, B. L., Brautigan, D. L., Karaki, H., Ozaki, H., Kato, Y., Fusetani, N., Watabe, S., Hashimoto, K., Uemura, D., and Hartshorne, D. J. (1989) *Biochem. Biophys. Res. Commun.* **159,** 871–877
46. Takai, A., Sasaki, K., Nagai, H., Mieskes, G., Isobe, M., Isono, K., and Yasumoto, T. (1995) *Biochem. J.* **306,** 657–665
47. Uehata, M., Ishizaki, T., Satoh, H., Ono, T., Kawahara, T., Morishita, T., Tamakawa, H., Yamagami, K., Inui, J., Maekawa, M., and Narumiya, S. (1997) *Nature* **389,** 990–994
48. Itoh, K., Yoshioka, K., Akedo, H., Uehata, M., Ishizaki, Y., and Narumiya, S. (1999) *Nat. Medicine* **5,** 221–225
49. Sahai, E., Ishizaki, T., Narumiya, S., and Treisman, R. (1999) *Curr. Biol.* **9,** 136–145
50. Madaule, P., Eda, M., Watanabe, N., Fujisawa, K., Matsuoka, T., Bito, H., Ishizaki, T., and Narumiya, S. (1998) *Nature* **394,** 491–494
51. Saito, T., Shima, H., Osawa, Y., Nagao, M., Hemmings, B. A., Kishimoto, T., and Hisanaga, S. (1995) *Biochemistry* **34,** 7376–7384
52. Ngai, J., Coleman, T. R., and Lazarides, E. (1990) *Cell* **60,** 415–427
53. Sarria, A. J., Nordeen, S. K., and Evans, R. M. (1990) *J. Cell Biol.* **111,** 553–565
54. Albers, K., and Fuchs, E. (1987) *J. Cell Biol.* **105,** 791–806
55. Goldman, R. D., Khuon, S., Chou, Y. H., Opal, P., and Steinert, P. M. (1996) *J. Cell Biol.* **134,** 971–983
56. Foisner, R. (1997) *BioEssays* **19,** 297–305

Biochemical Pharmacology, Vol. 56, pp. 583–590, 1998.

ISSN 0006-2952/98/$19.00 + 0.00
PII S0006-2952(98)00197-X

4-Hydroxy-17-methylincisterol, an Inhibitor of DNA Polymerase-α Activity and the Growth of Human Cancer Cells *In Vitro*

Hideaki Togashi, Yoshiyuki Mizushina,* Masaharu Takemura,† Fumio Sugawara,* Hiroyuki Koshino,‡ Yasuaki Esumi,‡ Jun Uzawa,‡ Hiroyuki Kumagai,§ Akio Matsukage,‖ Shonen Yoshida† and Kengo Sakaguchi*¶*

*Department of Applied Biological Science, Science University of Tokyo, Noda, Chiba 278-8510; †Laboratory of Cancer Cell Biology, Research Institute for Disease Mechanism and Control, Nagoya University School of Medicine, Nagoya, Aichi 466-8550; ‡The Institute of Physical and Chemical Research (Riken), Wako, Saitama 351-0198; §Central Research Laboratory, Mercian Corp., Fujisawa 251-0052; and ‖Laboratory of Cell Biology, Aichi Cancer Center Research Institute, Nagoya, Aichi 464-0021, Japan

ABSTRACT. An ergosterol derivative, 4-hydroxy-17-methylincisterol (HMI), was found to be an inhibitor of mammalian DNA polymerases *in vitro*. HMI inhibited the activity of calf thymus DNA polymerase α (pol. α). Among the polymerases tested, pol. α was the most sensitive to inhibition by HMI, and the inhibition was concentration dependent. The inhibitory effect of HMI on pol. α was almost the same as that shown by aphidicolin, a well-known potent pol. α inhibitor. HMI had relatively less effect on rat DNA pol. β, human immunodeficiency virus type 1 reverse transcriptase (HIV-RT), and calf thymus terminal deoxynucleotidyl transferase (TdT) *in vitro*, and did not influence the activities of prokaryotic DNA polymerases such as Klenow Fragment of DNA polymerase I, or the DNA-metabolic enzyme DNase I. HMI was found to be able to prevent the growth of human cancer cell lines originating from patients with leukemia or various solid tumors; its IC_{50} values ranged from 7.5 to 12 μM. We also synthesized other ergosterol derivatives and tested them, and found that two compounds, 17-methylincisterol and 4-acetyl-17-methylincisterol, have similar inhibitory effects. BIOCHEM PHARMACOL **56**;5:583–590, 1998. © 1998 Elsevier Science Inc.

KEY WORDS. DNA polymerase α; enzyme inhibitor; ergosterol derivative; 4-hydroxy-17-methylincisterol

We have been studying eukaryotic DNA polymerases [1–8]. In the process of our investigations, the need for an inhibitor of each of the DNA polymerases has arisen. Given that the roles of the DNA polymerases *in vivo* are still obscure, the elucidation of the precise role of each DNA polymerase and the use of appropriate inhibitors would be quite useful. We therefore established an assay method to detect DNA polymerase inhibitors, and have used it to screen the extracts of many organisms for the inhibitors. In addition to the use mentioned above, such inhibitors could also be employed as anticancer chemotherapy agents, because they inhibit cell proliferation.

In the extract screening, an important aspect was the type of natural product we examined as a source of inhibitors. Not only were several fungi, mushrooms, and higher plants found to produce such inhibitors [9–12], but some algae were also indicated to produce them (our unpublished data). Some of the inhibitors were a restricted group of highly degraded steroids called incisterols, which are reportedly produced by marine organisms such as sponges and mollusks [13]. A member of the incisterol family has also been synthesized from vitamin D_2 [14]. Another synthesized incisterol, γ-hydroxy-α,β-unsaturated lactone, which is a true natural product [13], was reported to be a potent fish toxic agent. Thus, the principal role of an incisterol in sponges is probably a defensive role against predators [14]. Interestingly, some of the incisterol family members easily synthesized from ergosterol were mammalian DNA polymerase-specific inhibitors. Our primary concern in the present study was to synthesize some members of the incisterol family, and to identify their biochemical properties as DNA polymerase inhibitors. These incisterols were HMI**, MI, and AcMI, which are moderately similar to γ-hydroxy-α,β-unsaturated lactone. They were also found to be able to kill human cancer cells *in vitro*. Our

¶ Corresponding author: Kengo Sakaguchi, Department of Applied Biological Science, Science University of Tokyo, Noda, Chiba 278-8510, Japan. Tel. 81-471-24-1501 (Ext. 3409); FAX 81-471-23-9767; E-mail: kengo@rs.noda.sut.ac.jp.

Received 9 February 1998; accepted 11 May 1998.

** *Abbreviations:* AcMI, 4-acetyl-17-methylincisterol; DNase I, deoxyribonuclease I; HIV-RT, human immunodeficiency virus type 1 reverse transcriptase; HMI, 4-hydroxy-17-methylincisterol; MI, 17-methylincisterol; MTT, 3-(4,5-dimethylthiazol-2-yl)-2,5-diphenyl tetrazolium bromide; pol., DNA polymerase; TdT, terminal deoxynucleotidyl transferase; and T_m, melting temperature.

TABLE 1. Assignments of NMR spectra of HMI

Position	^{13}C	^{1}H	HMBC*
1	171.83		H-2
2	111.97	5.61 (d, J = 2.0 Hz)	H-8
3	171.19		H-2, 8
4	105.39		H-2, 5
5	35.23	2.30 (ddd, J = 2.4, 3.9, 13.7 Hz, α)	H-6
		1.84 (ddd, J = 4.9, 13.0, 13.7 Hz, β)	H-5, 12
6	35.10	1.96 (ddd, J = 2.4, 3.9, 13.7 Hz, β)	H-5, 12
		1.63 (ddd, J = 3.9, 13.0, 13.2 Hz, α)	
7	48.89		H-5, 6, 8, 12
8	50.40	2.66 (ddd, J = 2.0, 5.9, 11.2 Hz)	H-2, 12
9	21.37	1.72 (m, α), 1.48 (m, β)	H-8
10	28.88	1.90 (m, α), 1.47 (m, β)	†
11	55.35	1.50 (m)	H-12, 13, 14, 15
12	11.76	0.60 (s)	H-6, 8
13	40.15	2.05 (m)	H-14, 15, 16
14	21.03	1.04 (d, J = 6.8 Hz)	H-15
15	134.71	5.17 (dd, J = 8.3, 15.2 Hz)	H-13, 14, 16
16	132.84	5.26 (dd, J = 7.3, 15.1 Hz)	H-13, 15, 21
17	42.85	1.86 (m)	H-15, 16, 19, 20, 21
18	33.07	1.49 (m)	H-19, 20
19	19.66	0.83 (d, J = 6.8 Hz)	H-20
20	19.98	0.84 (d, J = 6.8 Hz)	H-19
21	17.62	0.92 (d, J = 6.8 Hz)	H-16

*Heter-nuclear multiple bond connectivity.
†No cross-peak was observed in an HMBC experiment.

present study is the first investigation of the mode of the molecular action of the incisterol family agents as eukaryotic DNA polymerase-specific antitumor agents.

MATERIALS AND METHODS

Synthesis of Compounds

The methods used to synthesize HMI, MI, and AcMI were as follows. For HMI, a chloroform solution (300 mL) containing 3 g of ergosterol was irradiated for 9 hr with UV light (wavelength, 312 nm) with constant air-bubbling of the solution. The oily residue after evaporation was dissolved in 5 mL of chloroform, applied to a silica gel column (100–200 mesh, 5.0 × 50.0 cm), and eluted with chloroform. The fractions with the inhibitory activity of DNA polymerase were collected and evaporated *in vacuo*. The residue was dissolved in 1.5 mL of ethyl acetate:hexane (5:4), loaded onto a silica gel column (300 mesh, 2.0 × 15.0 cm), and then eluted with the same solvent. Similarly, the fractions with the inhibitory activity were collected and evaporated *in vacuo*. The residue, after being redissolved in methanol, was further purified by HPLC on a C18 silica gel column (YMC A-323, eluent, 90% acetonitrile; flow rate, 6 mL/min; detection, UV absorbance at 210 nm; retention time, 5.2 min). Finally, 3.6 mg of HMI was obtained. HMI was identified by ^{1}H and ^{13}C NMR data. Analysis of positive FAB mass and FAB high resolution mass were performed on a glycerol matrix, and were recorded on a mass spectrometer (JEOL JMS HX110). $[M + H]^+$:obsd. *m/z* 333.2425; calcd. *m/z* 333.2430 for $C_{21}H_{33}O_3$. NMR measurements were performed on a JEOL JNM Alpha 600 spectrometer. The ^{1}H and ^{13}C spectra were recorded in $CDCl_3$ solution at 600 and 100 MHz, the chemical shifts given relative to tetramethylsilane, and the $CDCl_3$ solvent peaks were δ 0.00 and 77.0 ppm, respectively. The data obtained are summarized in Table 1. MI was obtained from HMI by treating HMI with methanolic HCl [14]. The yield of MI from HMI was 25%. AcMI was also synthesized from HMI. HMI in pyridine and acetic anhydride (1:1) was exposed for 12 hr and then purified using a C18 silica gel column (HPLC, YMC A-323, eluent, 90% acetonitrile; flow rate, 6 mL/min; detection, UV absorbance at 210 nm; retention time, 7.2 min). The yield of AcMI from HMI was 86%. MI and AcMI were confirmed by a comparison of the ^{1}H NMR data of HMI.

Enzymes and DNA Polymerase Assays

The DNA polymerases and the DNA metabolic enzymes used are the same as those described in previous reports [9, 15, 16]. HMI, MI, and AcMI were dissolved in DMSO. Three microliters of the dissolved sample was mixed with 12 μL of each enzyme in 50 mM Tris–HCl (pH 7.5) containing 0.1 mM EDTA, 1 mM dithiothreitol, and 50% glycerol, and then kept at 4° for 10 min. Five microliters of each of the preincubated solutions was added to 20 μL of each of the enzyme standard reaction mixtures, and then each of the enzyme activities was measured under the conditions described in previous reports [9, 15, 16].

Effects of HMI on Various Human Cancer Cells In Vitro

For the investigation of the *in vitro* effects of HMI, K562 (leukemia), MKN28 (stomach cancer), PC6 (lung cancer), MCF7 (breast cancer), HT29 (colon cancer), and HT1080 (fibrosarcoma) cells were used. The cells were cultured using RPMI 1640 medium without phenol red, supplemented with 10% fetal bovine serum as a standard medium. The cells were cultured at 37° in the standard medium in humidified 5% CO_2–95% air. The cytotoxicity of HMI was investigated as follows. A high concentration of HMI dissolved in DMSO was stocked. Approximately 2×10^3 cells/well were inoculated in a 96-well micro-plate, and the HMI stock solution, diluted with standard medium to various concentrations, was applied to each well. After incubation for 72 h, the survival rate was measured by an MTT assay [17].

Thermal Transition of DNA

Thermal transition profiles of double-stranded DNA to single-stranded DNA with or without HMI were obtained with a spectrophotometer (U3210) equipped with a thermoelectric cell holder. Calf thymus DNA (6 mg/mL) was dissolved in 0.1 M sodium phosphate buffer (pH 7.0) containing 1% DMSO. The solution temperature was equilibrated at 78° for 10 min, and then increased by 1° at 2-min intervals for each measurement point. Any change in the absorbance of HMI itself at each temperature point was automatically subtracted from that of DNA plus HMI in the spectrophotometer.

RESULTS

Chemical Structures of the Incisterols as DNA Polymerase Inhibitors

As noted earlier in the paper, some incisterols are produced by marine organisms such as sponges and mollusks [13], and others are easily synthesized from ergosterol. One of the synthesized incisterols, γ-hydroxy-α,β-unsaturated lactone, has been found to be a potent fish toxic agent [14]. We found here that some of the incisterols are mammalian DNA polymerase-specific inhibitors: HMI, MI, and AcMI.

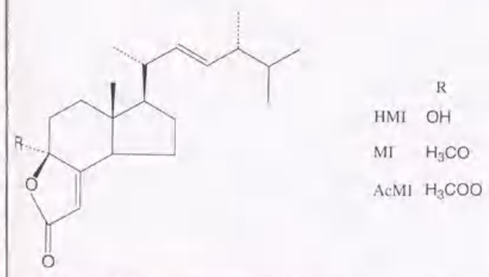

FIG. 1. Chemical structures of HMI, MI, and AcMI.

TABLE 2. Abilities of three ergosterol derivatives to inhibit cell proliferation of various cancer cells (IC_{50})

	IC_{50} (μg/mL)					
	K562	MKN28	PC6	MCF7	HT29	HT1080
HMI	2.5	2.7	2.9	4	2.9	2.5
MI	4.3	12.5	16.5	12.5	13.5	7
AcMI	12	5.6	17	13.5	6.6	5.4

Concentration–response studies were performed twice, the results were plotted on graphs, and the effective concentration of each analog that inhibited 50% growth was calculated. Cell lines: K562 (leukemia), MKN28 (stomach cancer), PC6 (lung cancer), MCF7 (breast cancer), HT29 (colon cancer), and HT1080 (fibrosarcoma).

Their chemical structures, as shown in Fig. 1, are moderately similar to that of γ-hydroxy-α,β-unsaturated lactone. As described below, they were found not only to be a DNA polymerase inhibitor, but were also shown to efficiently prevent the growth of human cancer cells *in vitro* as follows.

Effects of the Incisterols on Various Human Cancer Cells In Vitro

At first, we investigated *in vitro* the cytotoxic effect of HMI on K562, MKN28, PC6, MCF7, HT29, and HT1080 cells originating from patients with cancer. The incisterols prevented the proliferation of each of these cell lines, as shown in Table 2. All of the cell lines were influenced by the addition of HMI at similar concentrations and in a concentration-response fashion (10^{-5} to 10^{-4} mol/mL). The concentrations of HMI required for 50% growth inhibition (IC_{50}) were 2.5 to 4 μg/mL (7.5 to 12 μM). MI and AcMI also inhibited the proliferation of all of the cell

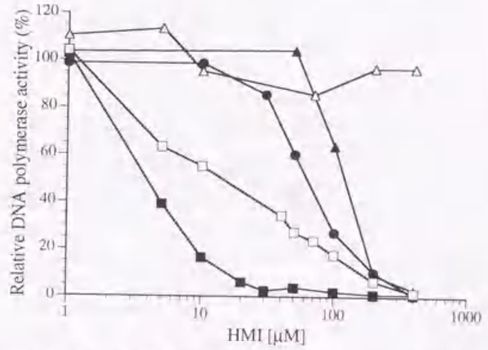

FIG. 2. Effect of HMI on various DNA polymerases. Reactions were carried out for 1 hr under the conditions described in Materials and Methods with the indicated concentrations of HMI. This experiment was performed three times. The enzymes tested and the symbols used are as follows: calf thymus pol. α (■); rat pol. β (●); HIV-RT (▲); calf thymus TdT (□); and the Klenow Fragment of pol. I (△). The specific radioactivity of [^{3}H]dTTP was 1660 cpm/pmol. The 100% values were 57 pmol (■); 138 pmol (●); 72 pmol (▲); 38 pmol (□); and 80 pmol (△).

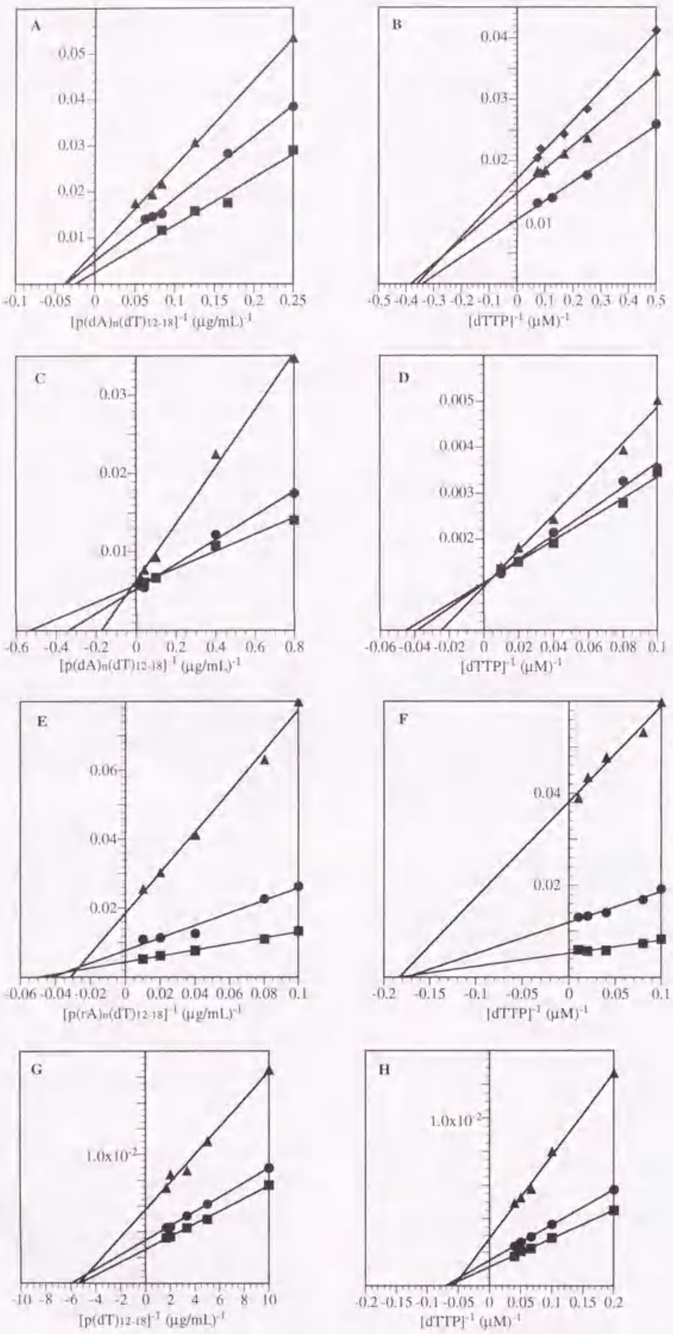

lines at concentrations similar to those of HMI (Table 2). The incisterols as DNA polymerase inhibitors were cytotoxic to the human cancer cells *in vitro*.

Inhibition by HMI of DNA Polymerases and Other DNA Metabolic Enzymes

Next we investigated the effect of one of the cytotoxic incisterols, HMI, on DNA polymerases and other DNA metabolic enzymes. As shown in Fig. 2, HMI at 10 μM was found to strongly inhibit the activities of calf thymus pol. α and to moderately inhibit the activities of calf thymus TdT, but this concentration did not influence the activities of rat pol. β, HIV-RT, or the Klenow Fragment of pol. I. The inhibition of HMI was concentration dependent, with 50% inhibition for pol. α and TdT observed at 4 and 10 μM, respectively, and almost complete inhibition (more than 80%) at 10 and 100 μM, respectively. A difference of inhibition was not observed with the use of calf thymus activated DNA as the template-primer instead of poly(dA)/oligo$(dT)_{12-18}$. Actually, neither pol. I, the other prokaryotic DNA polymerase, *Taq* polymerase, nor the DNA metabolic enzyme bovine DNase I was inhibited by 10 μM HMI (data not shown). HMI at less than 10 μM hardly inhibited the activities of pol. β and HIV-RT (Fig. 2). HMI appeared to be an inhibitor specifically for the mammalian DNA polymerases, especially the α-type, *in vitro*.

The effect of HMI on pol. α was almost the same as that of aphidicolin, the well-known pol. α inhibitor [18]. The finding that a derivative of ergosterol or vitamin D_2 is a potent pol. α inhibitor has never been described, to our knowledge.

Mode of Inhibition of Pol. α, Pol. β, HIV-RT, and TdT by HMI

To elucidate the mechanism of inhibition by HMI of pol. α, pol. β, HIV-RT, and TdT, the extent of inhibition as a function of the DNA template-primer or nucleotide substrate concentration was studied (Fig. 3). In the kinetic analysis, poly(dA)/oligo$(dT)_{12-18}$ and dTTP were used as the DNA template-primer and substrate, respectively.

Double-reciprocal plots of the results show that the inhibition of pol. α, HIV-RT, and TdT by HMI was non-competitive with the DNA template (Fig. 3, A, E, and G), since there was no change in the apparent K_m value (21 μg/mL for pol. α, 20 μg/mL for HIV-RT, and 0.19 μg/mL for TdT), while the V_{max} value decreased to 35% in the presence of 10 μM HMI for pol. α (Fig. 3A), to 56% in the presence of 70 μM HMI for HIV-RT (Fig. 3E), and to 46% in the presence of 10 μM HMI for TdT (Fig. 3G). Similarly, the apparent K_m for the substrate dTTP was unchanged, and the V_{max} was decreased to 61% in the presence of 15 μM HMI for pol. α (Fig. 3B), to 43% in the presence of 70 μM HMI for HIV-RT (Fig. 3F), and to 40% in the presence of 5 μM HMI for TdT (Fig. 3H). The inhibition, therefore, was also clearly noncompetitive with respect to the substrate dTTP (Fig. 3). In contrast, HMI inhibition of pol. β activity was competitive with the DNA template and the substrate (Fig. 3, C and D). In the case of the DNA template, the apparent V_{max} was unchanged at 17 pmol/hr, whereas a three-fold increase in K_m was observed in the presence of 50 μM HMI (Fig. 3C). The V_{max} for the substrate (dTTP) was 1 nmol/hr, and the K_m for the substrate increased from 22 to 26 and 40 pmol/mL in the presence of 0, 30, and 50 μM HMI, respectively (Fig. 3D). HMI may interact with or affect both of the binding sites on pol. β, thereby decreasing its affinity with the DNA template and substrate, whereas HMI may bind or interact with a domain distinct from the template or substrate binding sites on pol. α, HIV-RT, and TdT. The results indicate that the HMI-binding sites on the enzymes are structurally different from each other, especially between pol. β and the others, and that HMI binds directly to the DNA template-binding or the substrate-binding site on pol. β, since the incisterols bear no structural resemblance to either the DNA template or the substrate. Competitive and non-competitive inhibitors bind within and outside the active sites of the enzymes, respectively.

Interaction of HMI and Double-Stranded DNA

To determine whether the effect of HMI resulted in binding to DNA or enzyme, the interaction of HMI with double-stranded DNA (dsDNA) was investigated by means

FIG. 3. Kinetic analysis of the inhibition of DNA polymerases by HMI. The effects of HMI on the K_m and V_{max} values of the DNA template-primer and dTTP substrate were determined, and the results are displayed as Lineweaver–Burk plots. These experiments were performed twice. (A) Pol. α activity was assayed with the concentrations of template-primer (poly$(dA)_n$/oligo$(dT)_{12-18}$) indicated, after preincubation of the enzyme with 5 μM (■), 10 μM (●), or 15 μM (▲) HMI. (B) Pol. α activity was assayed with the concentrations of substrate (dTTP) indicated, after preincubation of the enzyme with 1 μM (●), 5 μM (▲) or 10 μM (◆) HMI. (C) DNA polymerase β activity was assayed with the concentrations of template-primer (poly$(dA)_n$/oligo$(dT)_{12-18}$) indicated, after preincubation of the enzyme without (■) or with 30 μM (●) or 50 μM (▲) HMI. (D) Pol. β activity was assayed with the concentrations of substrate (dTTP) indicated, after preincubation of the enzyme without (■) or with 30 μM (●) or 50 μM (▲) HMI. (E) HIV-RT activity was assayed with the concentrations of template-primer (poly$(rA)_n$/oligo$(dT)_{12-18}$) indicated, after preincubation of the enzyme without (■) or with 70 μM (●) or 120 μM (▲) HMI. (F) HIV-RT activity was assayed with the concentrations of substrate (dTTP) indicated, after preincubation of the enzyme without (■) or with 70 μM (●) or 120 μM (▲) HMI. (G) TdT activity was assayed with the concentrations of substrate (oligo$(dT)_{12-18}$) indicated, after preincubation of the enzyme without (■) or with 5 μM (●) or 10 μM (▲) HMI. (H) TdT activity was assayed with the concentrations of substrate (dTTP) indicated, after preincubation of the enzyme without (■) or with 5 μM (●) or 10 μM (▲) HMI.

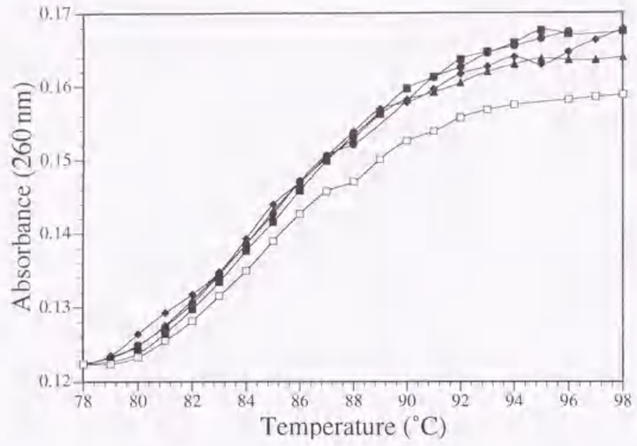

FIG. 4. Effect of HMI on the thermal transition of calf thymus double-stranded DNA in 0.1 M sodium-phosphate buffer (pH 7.0). This experiment was performed three times. The concentrations (μM) of HMI used were 0 (■); 12.5 (●); 25 (▲); and 50 μM (◆), and that of ethidium bromide was 5 μg/mL (□).

of thermal transition of dsDNA with or without HMI. The T_m of dsDNA, with increasing concentrations of HMI (from 0 to 50 μM), was measured precisely by a spectrophotometer equipped with a thermoelectric cell holder. As described in Materials and Methods, calf thymus dsDNA at 6 mg/mL was dissolved in 0.1 M sodium phosphate buffer (pH 7.0) containing 1% DMSO. HMI at more than 50 μM could not be dissolved under these conditions. In the concentration range used, the thermal transition of T_m was not observed (Fig. 4), whereas the ethidium bromide used as the positive control, a typical intercalating compound, produced a clear thermal transition (Fig. 4). These results indicated that HMI did not bind to DNA.

Effects of MI and AcMI on DNA Polymerases

We studied the changes in polymerase inhibition when the hydroxyl group at position 4 in HMI was replaced with a methyl or acetyl group. These alterations produced MI and AcMI, respectively (Fig. 1). As shown in Fig. 5, substitution of the hydroxyl group with the methyl group or the acetyl group in HMI decreased the inhibitory effects on pol. β, HIV-RT, and TdT. Interestingly, the inhibition by MI or AcMI of pol. α remained strong (Fig. 5). These data suggest that the hydroxyl group at position 4 of an incisterol may be required for inhibition.

DISCUSSION

Our original interest was to study the *in vivo* roles of eukaryotic DNA polymerases. Another interest was to find a cytotoxic agent useful as an anticancer chemotherapy agent. As described earlier, we have established an assay method to detect DNA polymerase inhibitors, and have used it to screen extracts of many organisms to find DNA polymerase inhibitors [9, 15]. Some of the inhibitors found were a restricted group of highly degraded steroids called incisterols. The incisterols have been synthesized from vitamin D_2. They were HMI, MI, and AcMI, which are moderately similar to γ-hydroxy-α,β-unsaturated lactone, and which are easily synthesized from ergosterol.

To elucidate the inhibition mechanism of HMI, the extent of inhibition as a function of DNA template-primer or dTTP substrate concentrations was studied (Fig. 3). The addition of an excess of protein (100 μg/mL of BSA) did not affect the binding in either case (data not shown), suggesting that the effect of HMI did not result from the nonspecific adhesion of HMI to the enzymes, but rather that it bound selectively to special sites. The K_i values for pol. α, pol. β, HIV-RT, and TdT, obtained from Dixon plots calculated from the kinetic values in Fig. 3, were found to be 4.8, 16.0, 14.0, and 7.2 μM for template (-primer), and 13.6, 46.5, 6.0, and 4.4 μM for substrate dTTP, respectively. The data suggest that the lower the K_i value, the stronger the inhibition. The K_i value of pol. α for the DNA template was higher than those of the other enzymes, suggesting that the affinity of HMI to pol. α is higher at the DNA template-binding site than to the others. HMI was thought to have little or no effect on the T_m of dsDNA (Fig. 4), and could be expected to interact with each of the enzymes themselves directly.

Because the incisterols found here are broadly effective (although relatively specific for pol. α) on mammalian polymerases, the compounds examined are not inhibitors applicable to our original interest. The incisterols, therefore, should be tested to determine whether they are capable of preventing mammalian cell proliferation, since they can inhibit the activity of the replicative polymerase. They were found to be able to kill human cancer cells *in vitro* (Table 2). The concentration range of IC_{50} values for these cells was quite similar to that of the 50% inhibition for pol. α *in vitro*, suggesting that the prevention of the cell proliferation resulted from the inhibition of the replicative polymerase; these compounds may be clinically useful as cytotoxic agents.

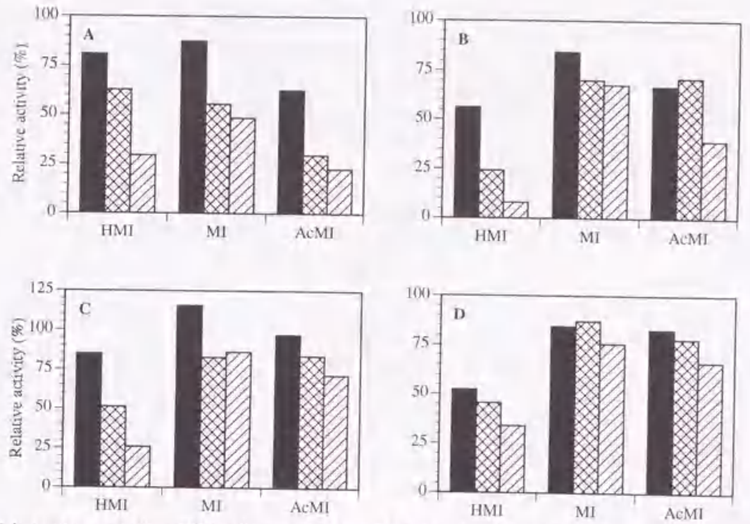

FIG. 5. Effects of derivatives on various DNA polymerases. Three derivatives dissolved in DMSO were preincubated with pol. α (A), pol. β (B), TdT (C), and HIV-RT (D) on ice for 20 min. After preincubation, the DNA polymerase activity was measured as described in Materials and Methods. These experiments were performed twice. [^{3}H]-dTMP incorporation in the absence of compounds was taken as 100%, corresponding to 4.2 pmol/hr (A); 2.8 pmol/hr (B); 13 pmol/hr (C); and 10 pmol/hr (D). The solid bars, cross-hatched bars, and lined bars indicate 3.75, 7.5, and 15 μM of derivatives (A); 80, 100, and 120 μM (B); 7.5, 15, and 30 μM (C); and 30, 60, and 120 μM (D), respectively.

We are grateful to Dr. H. Taguchi of our department for helpful discussions. This work was supported by Grant-in-Aid 362-0157-09266218 from the Ministry of Education, Science, Sports, and Culture of Japan.

References

1. Aoyagi N, Matsuoka S, Furunobu A, Matsukage A and Sakaguchi K, *Drosophila* DNA polymerase δ: Purification and characterization. *J Biol Chem* **269:** 6045–6050, 1994.
2. Aoyagi N, Oshige M, Hirose F, Kuroda K, Matsukage A and Sakaguchi K, DNA polymerase ε from *Drosophila melanogaster*. *Biochem Biophys Res Commun* **230:** 297–301, 1997.
3. Boyd JB, Mason JM, Yamamoto AH, Brodberg RK, Banga SS and Sakaguchi K, A genetic and molecular analysis of DNA repair in *Drosophila*. *J Cell Sci Suppl* **6:** 39–40, 1987.
4. Boyd JB, Sakaguchi K and Harris PV, DNA metabolizing enzymes of *Drosophila*. In: *The Eukaryotic Nucleus: Molecular Biochemistry and Macromolecular Assemblies* (Eds. Strauss PR and Wilson SH), Vol. 1, pp. 293–314, The Telford Press, New York, 1989.
5. Matsuda S, Takami K, Sono A and Sakaguchi K, A meiotic DNA polymerase from *Coprinus cinereus*? Further purification and characterization. *Chromosoma* **102:** 631–636, 1993.
6. Sakaguchi K, Hotta Y and Stern H, Chromatin-associated DNA polymerase activity in meiotic cells of lily and mouse. *Cell Struct Funct* **5:** 323–334, 1980.
7. Sakaguchi K and Lu BC, Meiosis in *Coprinus*: Characterization and activities of two forms of DNA polymerase during meiotic stages. *Mol Cell Biol* **2:** 752–757, 1981.
8. Sakaguchi K and Boyd JB, Purification and characterization of a DNA polymerase β from *Drosophila*. *J Biol Chem* **260:** 10406–10411, 1985.
9. Mizushina Y, Tanaka N, Yagi H, Kurosawa T, Onoue M, Seto H, Horie T, Aoyagi N, Yamaoka M, Matsukage A, Yoshida S and Sakaguchi K, Fatty acids selectively inhibit eukaryotic DNA polymerase activities *in vitro*. *Biochim Biophys Acta* **1308:** 256–262, 1996.
10. Mizushina Y, Tanaka N, Kitamura A, Tamai K, Ikeda M, Takemura M, Sugawara F, Arai T, Matsukage A, Yoshida S and Sakaguchi K, The inhibitory effect of novel triterpenoid compounds, fomitellic acids, on DNA polymerase β. *Biochem J* **330:** 1325–1332, 1998.
11. Tanaka N, Kitamura A, Mizushina Y, Sugawara F and Sakaguchi K, Fomitellic acids, triterpenoid inhibitors of eukaryotic DNA polymerases from a basidiomycete, *Fomitella fraxinea*. *J Nat Prod* **61:** 193–197, 1998.
12. Mizushina Y, Watanabe I, Ohta K, Takemura M, Sahara H, Takahashi N, Gasa S, Sugawara F, Matsukage A, Yoshida S and Sakaguchi K, Studies on inhibitors of mammalian DNA polymerase α and β. Sulfolipids from a pteridophyte,

Athyrium iuponicum. *Biochem Pharmacol* **55:** 537–541, 1998.
13. Ciminiello P, Fattorusso E, Magno S, Mangoni A and Pansini M, Incisterols, a new class of highly degraded sterols from the marine sponge *Dictyonella incisa*. *J Am Chem Soc* **112:** 3505–3509, 1990.
14. Francesco R, Aldo S, Irene I, Assunta G and Guido S, Synthesis of (17*R*)-17-methylincisterol, a highly degraded marine steroid. *Tetrahedron Lett* **36:** 4303–4306, 1995.
15. Mizushina Y, Yagi H, Tanaka N, Kurosawa T, Seto H, Katsumi K, Onoue M, Ishida H, Iseki A, Nara T, Morohashi K, Horie T, Onomura Y, Narusawa M, Aoyagi N, Takami K, Yamaoka M, Inoue Y, Matsukage A, Yoshida S and Sakaguchi K, Screening of inhibitor of eukaryotic DNA polymerases produced by microorganisms. *J Antibiot* (*Tokyo*) **49:** 491–492, 1996.
16. Mizushina Y, Yoshida S, Matsukage A and Sakaguchi K, The inhibitory action of fatty acids on DNA polymerase β. *Biochim Biophys Acta* **1336:** 509–521, 1997.
17. Mosmann T, Rapid colorimetric assay for cellular growth and survival: Application to proliferation and cytotoxicity assays. *J Immunol Methods* **65:** 55–63, 1983.
18. Ikegami S, Taguchi T and Ohashi M, Aphidicolin prevents mitotic cell division by interfering with the activity of DNA polymerase-α. *Nature* **275:** 458–460, 1978.

An Ergosterol Peroxide, a Natural Product That Selectively Enhances the Inhibitory Effect of Linoleic Acid on DNA Polymerase β

Yoshiyuki MIZUSHINA,[a] Itiro WATANABE,[a] Hideaki TOGASHI,[a] Linda HANASHIMA,[a] Masaharu TAKEMURA,[b] Keisuke OHTA,[a,c] Fumio SUGAWARA,[a] Hiroyuki KOSHINO,[d] Yasuaki ESUMI,[d] Jun UZAWA,[d] Akio MATSUKAGE,[e] Shonen YOSHIDA,[b] and Kengo SAKAGUCHI*,[a]

Department of Applied Biological Science, Science University of Tokyo,[a] Noda, Chiba 278-8510, Japan, Laboratory of Cancer Cell Biology, Research Institute for Disease Mechanism and Control, Nagoya University School of Medicine,[b] Nagoya 466-8550, Japan, Third Section of Research and Development, Toyo Suisan Kaisha, Ltd.,[c] Minato, Tokyo 108-0075, Japan, The Institute of Physical and Chemical Research (Riken),[d] Wako, Saitama 351-0198, Japan and Laboratory of Cell Biology, Aichi Cancer Center Research Institute,[e] Nagoya 464–0021, Japan.
Received December 8, 1997; accepted January 19, 1998

As described previously (Mizushina Y., Tanaka N., Yagi H., Kurosawa T., Onoue M., Seto H., Horie T., Aoyagi N., Yamaoka M., Matsukage A., Yoshida S., and Sakaguchi K., *Biochim. Biophys. Acta*, 1308, 256—262, 1996), linoleic acid (LA) inhibits the activities of mammalian DNA polymerases. We found a natural product from a basidiomycete, *Ganoderma lucidum*, that enhances this effect of LA in a special manner. The structure was identified to be an ergosterol peroxide, 5,8-epidioxy-5α,8α-ergosta-6,22*E*-dien-3β-ol by spectroscopic analyses. The ergosterol peroxide (EPO) itself scarcely inhibited the activities of calf thymus DNA polymerase α (pol. α) or rat DNA polymerase β (pol. β). However, when EPO at 0.25 mM was present, 10 μM or less of LA almost completely inhibited the pol. β activity, while almost complete inhibition by LA itself was achieved at 80 μM or higher. Interestingly, under the same conditions, EPO did not affect the LA-effect on pol. α. The action mode of the EPO was discussed.

Key words DNA polymerase; enzyme inhibitor; ergosterol peroxide; linoleic acid; basidiomycete; *Ganoderma lucidum*

Eukaryotic DNA polymerases are designated as α, β, γ, δ and ε, each responsible for different DNA syntheses.[1] The current intense interest in understanding the precise *in vivo* role of the polymerases and of the factors controlling their activity has prompted us to undertake a major search for wide inhibitors of these enzymes.[2—10] The search for DNA polymerase β (pol. β) inhibitors is especially urgent, because the role of pol. β *in vivo* is still obscure. Although several pol. β inhibitors have been reported, including nucleotide analogs,[11,12] flavonoids,[3] sulfate- or sialic acid-containing glycolipids,[14,15] phospholipids[16,17] triterpenoids[18,19] and fatty acids,[20—22] more potent agents are still needed.

We have previously reported the establishment of an assay[20,21] to detect DNA polymerase inhibitors and have used it to screen microbial secondary metabolites.[21] In the present study, colonies of actinomycetes, fungi and mycelia of basidiomycetes were collected from field soil near our laboratory. All the mycelia from the actinomycetes (*ca.* 1500 strains), fungi (200 strains) and basidiomycetes (200 strains) were homogenized in a Waring blender, and their acetone-soluble extracts were evaluated in a DNA polymerase assay system. We found that strong inhibitory activity for the polymerases was present in the homogenate of the fruiting caps of a basidiomycete, *Ganoderma lucidum*, and the major component was identified as linoleic acid (LA). However, the greatest activity disappeared in the final step of the purification by high-performance liquid chromatography (HPLC). We therefore investigated other compounds separated in the final step of the HPLC which could enhance the inhibitory effect of the fatty acid, and found that 5,8-epidioxy-5α,8α-ergosta-6,22*E*-dien-3β-ol (EPO), one of the sterol peroxides which were isolated from marine invertebrates such as tunicate, coral, sponge and sea hare by Gunatilaka *et al.*, filled that role.[23] The biological activities of EPO have not been reported yet. The addition of EPO to a polymerase reaction mixture led to a decrease in the minimum inhibitory concentration (MIC) of LA against pol. β activity, but did not affect the inhibitory effect on DNA polymerase α (pol. α). We report here the isolation and spectroscopic analyses of EPO, as well as its biochemical action with and without LA.

* To whom correspondence should be addressed.

MATERIALS AND METHODS

Materials Nucleotides and chemically synthesized template-primers such as poly(dA) and oligo(dT)$_{12-18}$ were purchased from Pharmacia (Uppsala, Sweden). [^{3}H]-deoxythymidine 5′-triphosphate (dTTP) (43 Ci/mmol) was purchased from New England Nuclear Corp. (Boston, MA). All other reagents, including LA, were of analytical grade and were purchased from Wako Chemical Industries (Osaka, Japan).

Enzymes and DNA Polymerase Assays The DNA polymerases and DNA metabolic enzymes used and the enzyme assay methods are the same as those described in previous reports.[20—22] EPO was dissolved in dimethyl sulfoxide (DMSO), and 4 μl of the dissolved sample was mixed with 16 μl of each enzyme (final 0.05 units) in 50 mM Tris–HCl (pH 7.5) containing 0.1 mM EDTA, 1 mM dithiothreitol and 50% glycerol, then kept at 0 °C for 10 min. Eight ml of each of the preincubated solutions was added to 16 μl of each of the enzyme standard reaction mixtures, then each of the enzyme activities was measured.

Extraction and Purification of EPO from the Fruiting Caps of the Basidiomycete, *Ganoderma lucidum* The fruiting caps of the mushroom *Ganoderma lucidum* were purchased from Japan Microbe Chemical Co. (Tokyo, Japan). After homogenization in a Waring blender, the fruiting caps were extracted with acetone for 3 d. The evaporated extract

Table 1. Fatty Acids in the Fruiting Caps of the Basidiomycete, *Ganoderma lucidum*

Fatty acid	Symbol	Composition rate (%)
cis-9 Tetradecenoic acid	14:1Δ9*cis*	0.5
Hexadecanoic acid (Palmitic acid)	16:0	2.8
cis-9 Hexadecenoic acid (Palmitoleic acid)	16:1Δ9*cis*	0.8
Octadecanoic acid (Stearic acid)	18:0	1.1
cis-9 Octadecenoic acid (Oleic acid)	18:1Δ9*cis*	1.8
cis-9, *cis*-12 Octadecadienoic acid (LA)	18:2Δ9-12*cis*	93.0

was partitioned between EtOAc and H_2O and adjusted to pH 7. The evaporated organic layer was subjected to silica gel column chromatography and then eluted with *n*-hexane/2-propanol (v/v 16 : 1). The active fractions were collected and then purified by preparative HPLC (on a YMC A-323 column (C_{18}-ODS) 10 i.d. ×250 mm in CH_3CN with the flow rate of 6.0 ml/min, detected with UV at 210 nm) to give a white powder.

Positive FAB-MS and high resolution (HR)-FAB-MS were run on a glycerol matrix, and were recorded on a JEOL JMS HX110 mass spectrometer. $[M+H]^+$ obsd. *m/z* 429.3289; calcd. *m/z* 429.3368 for $C_{28}H_{45}O_3$. NMR measurements were performed on a Bruker AC-300 Plus spectrometer. ^1H and ^{13}C spectra were recorded in $CDCl_3$ solution at 300 and 75 MHz, and the chemical shifts are given relative to tetramethylsilane (TMS); $CDCl_3$ solvent peaks are δ 0.00 and 77.0 ppm, respectively. ^{13}C; δ (ppm) 135.4, 135.2, 132.3, 130.7, 82.1, 79.4, 6.5, 56.2, 51.6, 51.0, 44.5, 42.8, 39.7, 39.3, 36.9 (overlapped), 34.7, 33.1, 30.1, 28.6, 23.4, 20.9, 20.6, 19.6, 18.2, 17.1, 14.1, 12.9: ^1H; δ (ppm) 6.50 (1H, d, J=8.5 Hz), 6.25 (1H, d, J=8.5 Hz), 5.22 (1H, dd, J=7.1, 15.2 Hz), 5.14 (1H, dd, J=7.8, 15.2 Hz), 3.96 (1H, m), 3.49 (1H, s), 2.2—1.2 (20H, m), 1.01 (3H, d, J=6.6 Hz), 0.90 (3H, d, J=6.8 Hz), 0.88 (3H, s), 0.83 (3H, s), 0.83 (3H, d, J=6.9 Hz), 0.82 (3H, s), 0.81 (3H, d, J=6.7 Hz).

Figure 1 shows the chemical structure of the ergosterol peroxide, EPO (A) and the deoxidized form, ergosterol (B).

Fatty Acid Analysis of the Basidiomycete, *Ganoderma lucidum* The fatty acid fraction of fruiting caps of the basidiomycete *Ganoderma lucidum* was isolated by silica gel column chromatography using *n*-hexane/2-propanol (v/v 16 : 1). Gas chromatography analysis was performed with a Hewlett Packard 5890 Series II system equipped with a hydrogen flame ionization detector (FID) with flow rate of 1 ml/min on a Spelco Wax (df 0.2 μm) at 200—220 °C (2 °C/min).

RESULTS AND DISCUSSION

Presence of a New Compound That Facilitates the Inhibitory Effect of LA on Pol. β The basidiomycete *Ganoderma lucidum* is a medicinal mushroom used in traditional Chinese medicine, and has been called *reishi* or *mannentake*. The powder of the dried *reishi* has been used as a cancer chemotherapy agent in ancient China, and was used in the Imperial Court. We found potent activity in the fruiting caps of this mushroom in that it inhibits rat pol. β activity. We then tried to extract the effective fraction. The inhibitory agent was found in the final step of the purification to be fatty acids, as elucidated by gas chromatography analysis, which were mostly composed of LA (Table 1). Since we reported previously that longer-chain fatty acids than C_{18} could be potent inhibitors of eukaryotic DNA polymerases,[20] we speculated that LA could itself be the inhibitor. However, the active fractions of *reishi* extract in each of the purification steps before the HPLC originally seemed to be a much stronger inhibitor for pol. β than the fatty acid (Table 2), so we further attempted to purify the inhibitor. The elution pattern of the final HPLC step of the purification showed an inhibitory–activity peak (peak I in Table 2), and it was LA. However, in the presence of 25 μM LA, another new inhibitor peak (peak II in Table 2) occurred in the elution pattern. The LA level used (25 μM) was one-third of its MIC. We therefore suspected that the *reishi* powder must contain something to help or to strengthen the inhibitory effect of LA. The remainder of this report describes the purification and characterization of the newly identified compound.

Table 2. IC_{50} Values for the Inhibition of DNA Polymerase Activities of EPO in Each of the Purification Steps

Purification step	IC_{50} value (μg/ml)	
	Calf pol. α	Rat pol. β
Acetone extract	25	30
EtOAc/H_2O partition	20	20
Silica gel column chromatography	10	0.7
HPLC peak I (LA)	8	12
HPLC peak II (EPO)	210	450

The standard reaction mixture for calf thymus pol. α (24 μl final volume) contained 50 mM Tris·HCl (pH 7.5), 1 mM dithiothreitol, 1 mM $MgCl_2$, 10 μM poly(dA), 5 μM $(dT)_{12-18}$, 10 μM [^{3}H]-dTTP (100 cpm/pmol), 15% (v/v) glycerol and 8 μl inhibitor–enzyme mixture solution. The standard reaction mixture for rat pol. β was the same reaction mixture as used above, but also contained 150 mM KCl. The purification samples were dissolved in DMSO and sonicated for 30 s. Four μl of the sonicated sample was mixed with 16 μl of each enzyme (final 0.05 units). These inhibitor–enzyme mixtures (8 μl) were added to 16 μl of each of the enzyme's standard reaction mixtures. After incubation at 37 °C for 60 min, the radioactive DNA products were collected on DEAE-cellulose paper (DE81) discs as described by Lindahl *et al.*,[24] and radioactivity was measured in a scintillation counter. One unit of enzyme activity was defined as the amount of enzyme that catalyzes the incorporation of 1 nmol of deoxyribonucleoside triphosphates into synthetic template-primers (*i.e.* poly(dA)/oligo$(dT)_{12-18}$, A/T=2/1) in 60 min at 37 °C under the normal reaction conditions for each enzyme. Enzyme activity in the absence of an inhibitor was taken as 100%.

Purification of the *Reishi* Compound from the Fruiting Caps, and Its Chemical Structure The active compound from the fruiting caps of the mushroom was extracted and purified as described in Materials and Methods. The molecular formula $C_{28}H_{44}O_3$ was determined by positive HR-FAB-MS. In the ^{13}C-NMR, two of four olefinic carbon signals at δ 135.4, 135.2, 132.3 and 130.7 ppm showed the presence of two olefins in its structure. The simple doublet olefin protons at δ 6.50 (J=8.5 Hz) and 6.25 (J=8.5 Hz) showed further *cis* olefin couplings by protons. The relative down-field shifted carbon signals at δ 82.1 and 79.4 ppm suggested the peroxide residue was related to the above olefin. The doublets of dou-

blets olefin protons at δ 5.22 (J=7.1, 15.2 Hz) and 5.14 (J= 7.8, 15.2 Hz) implied *trans* olefin coupled with a methin proton, respectively. In accordance with the presence of six methyls and the molecular formula, the structure of the active compound was identified as ergosterol peroxide, EPO (Fig. 1A). EPO is a derivative of ergosterol (Fig. 1B). EPO is one of the nine rare sterols which were previously isolated from marine invertebrates such as tunicate, common pillar coral, sponge and sea hare by Gunatilaka *et al.*.[23]

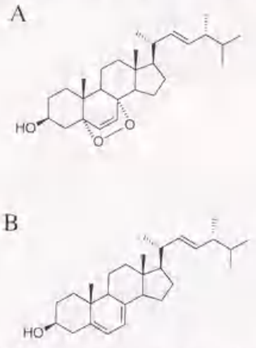

Fig. 1. Chemical Structures of EPO from the Fruiting Caps of Basidiomycete, *Ganoderma lucidum* (A) and the Deoxidized Form, Ergosterol (B)

Inhibition by EPO of the Activities of DNA Polymerases with or without LA As shown in Fig. 2, the inhibition by EPO itself was too weak to consider EPO as an inhibitor of calf pol. α (Fig. 2B) or rat pol. β (Fig. 2D).

However, when LA was present in the polymerase reaction mixture, the EPO inhibitory patterns were greatly changed (Fig. 2). As described previously,[20] LA at 80 μM or more nearly completely inhibited the activities of pol. α and pol. β, and at less than 25 μM, LA lost such activity (Fig. 2A and C). Figure 2C shows the dose-curves of the effect of LA with 250 μM of EPO on pol. β activity. The inhibition was dose-dependent, with 50% inhibition of pol. β observed at a dose of 3 μM; almost complete inhibition (more than 80—90%) was achieved at 10 to 15 μM. However, the weak pol. α-inhibitory activity by EPO at 250 μM was revised with 5 μM LA (Fig. 2A). To compare the effect of EPO with other similar compounds, we tested the enhancing effect of an ergosterol which is the deoxidized form of EPO (Fig. 1B). The ergosterol, despite structural similarity, did not have any effect on the activities of pol. α or pol. β (Fig. 2A and C). When dodecanoic acid (C_{12}-fatty acid) was used instead of LA (C_{18}-fatty acid), EPO had no such effect (Fig. 2B and D). However, LA and longer chain fatty acids did have the effect (data not shown).

EPO did not influence the activities of cauliflower DNA

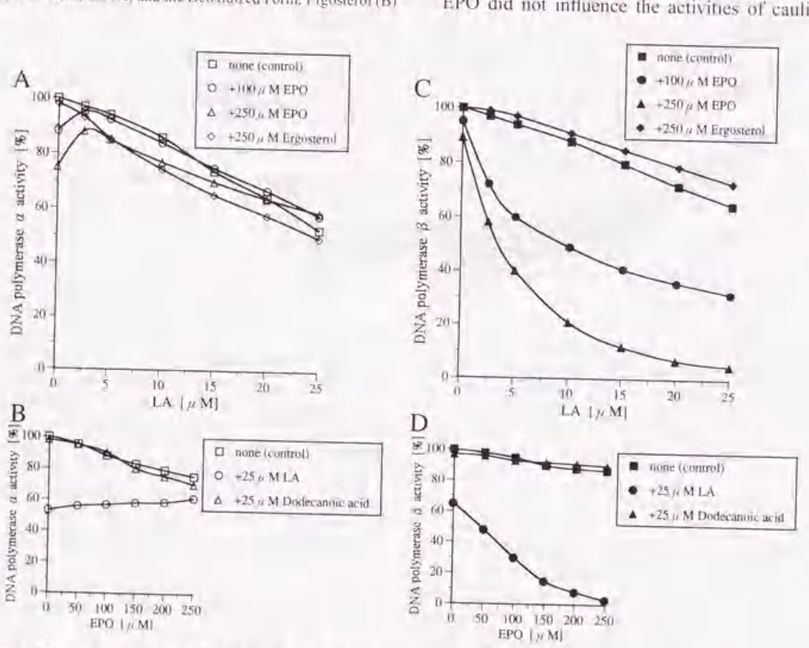

Fig. 2. Inhibition of pol. α (A, B) and β (C, D) Activities by EPO, LA and the Mixture of Both

Ergosterol and dodecanoic acid were used as the control agents of EPO and LA, respectively. The standard reaction mixture for calf pol. α (24 μl final volume) contained 50 mM Tris–HCl (pH 7.5), 1 mM dithiothreitol, 1 mM $MgCl_2$, 10 μM poly(dA), 5 μM $(dT)_{12-18}$, 10 μM [^{3}H]-dTTP (100 cpm/pmol), 15% (v/v) glycerol and 8 μl inhibitor-enzyme mixture solution. The standard reaction mixture for rat pol. β was the same reaction mixture as used above, but also contained 150 mM KCl. EPO and LA were dissolved in DMSO and sonicated for 30 s. Four μl of the sonicated sample was mixed with 16 μl of each enzyme (final 0.05 units). These inhibitor–enzyme mixtures (8 μl) were added to 16 μl of each of the enzyme's standard reaction mixtures. After incubation at 37 °C for 60 min, the radioactive DNA products were collected on DEAE-cellulose paper (DE81) discs, as described by Lindahl *et al.*,[21] and radioactivity was measured in a scintillation counter. One unit of enzyme activity was defined as the amount of enzyme that catalyzes the incorporation of 1 nmol of deoxyribonucleoside triphosphates into synthetic template-primers (*i.e.* poly(dA)·oligo(dT)$_{12-18}$, A/T=2/1) in 60 min at 37 °C under the normal reaction conditions for each enzyme. Enzyme activity in the absence of an inhibitor was taken as 100%.

Table 3. The effect of EPO, LA and the Mixture of Both on the Activities of Various DNA Polymerases and Other DNA-Metabolic Enzymes

Enzyme	EPO (250 μM)	LA (25 μM)	EPO (250 μM) + LA (25 μM)	EPO/(EPO+LA)
Calf pol. α	74	53	59	1.25
Rat pol. β	90	65	5	18
Plant pol. II (β-like)	103	100	101	1.02
HIV-RT	160	101	175	0.91
E. coli pol. I (Klenow fragment)	111	98	101	1.10
Taq pol.	108	98	105	1.03
T4 pol.	110	104	106	1.04
Calf TdT	118	96	108	1.09
Bovine DNase I	104	100	106	0.98

% of relative activity. The standard reaction mixture for calf pol. α, *E. coli* pol. I (Klenow fragment), Taq pol., T4 pol., and calf thymus TdT (24 μl final volume) contained 50 mM Tris–HCl (pH 7.5), 1 mM dithiothreitol, 1 mM $MgCl_2$, 10 μM poly(dA), 5 μM $(dT)_{12-18}$, 10 μM [^{3}H]-dTTP (100 cpm/pmol), 15% (v/v) glycerol and 8 μl of an inhibitor–enzyme mixture solution. The standard reaction mixture for rat pol. β and plant pol. II (β-like) was the same reaction mixture as used above, but also contained 150 mM KCl. The standard reaction mixture for HIV-RT contained 50 mM Tris–HCl (pH 7.5), 1 mM dithiothreitol, 1 mM $MgCl_2$, 10 μM poly(rA), 5 μM $(dT)_{12-18}$, 10 μM [^{3}H]-dTTP (100 cpm/pmol), 15% (v/v) glycerol, 80 mM KCl and 8 μl of an inhibitor–enzyme mixture solution. EPO and LA were dissolved in DMSO and sonicated for 30 s. Four μl of the sonicated sample was mixed with 16 μl of each enzyme (0.05 units). These inhibitor–enzyme mixtures (8 μl) were added to 16 μl of each of the enzyme's standard reaction mixtures. After incubation at 37 °C for 60 min, except Taq pol., which was incubated at 74 °C for 60 min, the radioactive DNA products were collected on DEAE-cellulose paper (DE81) discs as described by Lindahl *et al.*,[21] and radioactivity was measured in a scintillation counter. One unit of enzyme activity was defined as the amount of enzyme that catalyzes the incorporation of 1 nmol of deoxyribonucleoside triphosphates into synthetic template-primers (*i.e.* poly(dA)·oligo(dT)$_{12-18}$, A/T=2/1) in 60 min at 37 °C under the normal reaction conditions for each enzyme. Bovine DNase I activity was measured as described previously.[25] Enzyme activity in the absence of an inhibitor was taken as 100%.

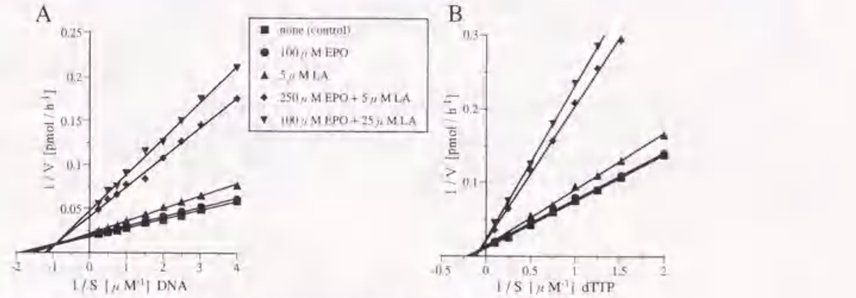

Fig. 3. Kinetic Analysis of the Inhibition of pol. β (0.05 units) by EPO, LA and the Mixture of Both

The effects of the mixture of EPO and LA on the K_m and V_{max} values of the DNA template-primer and nucleotide substrate were determined, and the results are displayed as Lineweaver-Burk plots. (A) Pre-incubation with pol. β in the presence of 100 μM EPO (●), 5 μM LA (▲), 250 μM EPO and 5 μM LA (◆) and 100 μM EPO and 25 μM LA (▼). The pol. β activity was then assayed using the concentrations of poly(dA)/oligo(dT) (2/1) indicated as the template/primer. The pol. β activity in the absence of the inhibitors (■). (B) The pol. β activity was assayed with the concentrations of substrate (dTTP) indicated, after the pre-incubation of pol. β without (■) or with 100 μM EPO (●), 5 μM LA (▲), 250 μM EPO and 5 μM LA (◆) and 100 μM EPO and 25 μM LA (▼).

polymerase II (plant pol. II), the prokaryotic DNA polymerases, *i.e.*, the Klenow fragment of DNA polymerase I (pol. I), T4 DNA polymerase (T4 pol.) and Taq polymerase (Taq pol.), the DNA metabolic enzyme bovine deoxyribonuclease I (DNase I), calf thymus terminal deoxynucleotidyl transferase (TdT) or the human immunodeficiency virus type 1 reverse transcriptase (HIV-RT) at all (Table 3). LA with EPO also did not influence the activities of pol. α, plant pol. II, the prokaryotic DNA polymerases , DNase I, TdT or HIV-RT (Table 3), suggesting that LA in coexistence with EPO changes to a potent inhibitor specific to the mammalian pol. β *in vitro*. An excess amount of LA did not affect these non-pol. β type EPO-effects (data not shown). EPO appears to contribute only to the pol. β inhibition by LA, but does not affect the inhibition by LA of other enzymes.

Mode of DNA Polymerase β Inhibition by EPO To elucidate the mechanism of the EPO effect on the pol. β inhibition, the extent of inhibition as a function of DNA template-primer or nucleotide substrate concentration was studied (Fig. 3). In the kinetic analysis, poly(dA)/oligo(dT)$_{12-18}$ A/T=2/1 and nucleotide dTTP were used as the DNA template-primer and substrate, respectively. Double reciprocal plots of the results show that the inhibition of pol. β by the mixture of EPO and LA was intermediate, between competitive and non-competitive reactions with either the DNA template (Fig. 3A) or substrate (Fig. 3B). The K_m (Michaelis constant) for the DNA template increased from 0.53 to 0.83 μM in the presence of EPO and LA (Fig. 3A), while its V_{max} (maximum velocity) decreased from 50 to 22 pmol/h in the presence of EPO and LA (Fig. 3A). Similarly, the apparent K_m for the substrate dTTP was increased by 2.5-fold in the presence of EPO and LA (Fig. 3B), whereas a 48% decrease in the V_{max} was observed in the presence of EPO and LA (Fig. 3B). Since LA competitively inhibited pol. β, as described previously,[20] and since EPO itself weakly and non-competitively inhibited the pol. β activity (data not shown), these two reaction modes may be mixed. As described previously,[20—22] LA may interact with or affect both of the binding sites on pol. β, thereby decreasing its affinity for the DNA template and substrate. EPO may therefore enhance the

inhibitory effect of LA by interacting with an other domain distinct from the template-binding and catalytic sites on pol. *β*.

Acknowledgments We are grateful to Drs. H. Taguchi and M. Ikekita of our department for helpful discussion. We thank Mr. J. Nishikawa and Dr. Y. Minegishi for providing the fruiting caps of basidiomycete, *Ganoderma lucidum*. This work was supported by a Grant-in-Aid (No. 362–0157–09266218) from the Ministry of Education, Science, Sports, and Culture of Japan.

REFERENCES AND NOTES

1) Kornberg A., Baker T., "DNA Replication", W. H. Freeman and Co., New York, 1992, Chapter 6, pp. 197—225.
2) Sakaguchi K., Hotta Y., Stern H., *Cell Struct. Funct.*, **5**, 323—334 (1980).
3) Sakaguchi K., Lu B. C., *Mol. Cell. Biol.*, **2**, 752—757 (1981).
4) Sakaguchi K., Boyd J. B., *J. Biol. Chem.*, **260**, 10406—10411 (1985).
5) Boyd J. B., Mason J. M., Yamamoto A. H., Brodberg R. K., Banga S. S., Sakaguchi K., *J. Cell Sci. Suppl.*, **6**, 39—40 (1987).
6) Boyd J. B., Sakaguchi K., Harris P. V., "The Eukaryotic Nucleus; Molecular Biochemistry and Macromolecular Assemblies", Vol. 1, ed. by Strauss P. R., Wilson S. H., The Telford Press, New York, 1989, pp. 293—314.
7) Matsuda S., Takami K., Sono A., Sakaguchi K., *Chromosoma*, **102**, 631—636 (1993).
8) Aoyagi N., Matsuoka S., Furunobu A., Matsukage A., Sakaguchi K., *J. Biol. Chem.*, **269**, 6045—6050 (1994).
9) Aoyagi N., Oshige M., Hirose F., Kuroda K., Matsukage A., Sakaguchi K., *Biochem. Biophys. Res. Commun.*, **230**, 297—301 (1997).
10) Sawado T., Sakaguchi K., *Biochem. Biophys. Res. Commun.*, **232**, 454—460 (1997).
11) Izuta S., Saneyoshi M., Sakurai T., Suzuki M., Kojima K., Yoshida S., *Biochem. Biophys. Res. Commun.*, **179**, 776—783 (1991).
12) Horie T., Mizushina Y., Takemura M., Sugawara F., Matsukage A., Yoshida S., Sakaguchi K., *Int. J. Mol. Med.*, **1**, 83—90 (1998).
13) Ono K., Nakane H., Fukushima M., *Eur. J. Biochem.*, **172**, 349—353 (1988).
14) Simbulan C. M. G., Taki T., Koizumi K. T., Suzuki M., Savoysky E., Shoji M., Yoshida S., *Biochim. Biophys. Acta*, **1205**, 68—74 (1994).
15) Mizushina Y., Watanabe I., Ohta K., Takemura M., Sahara H., Takahashi N., Gasa S., Sugawara F., Matsukage A., Yoshida S., Sakaguchi K., *Biochem. Pharmacol.*, **55**, 537—541 (1998).
16) Murofushi K. M., Shiota M., Kaji K., Yoshida S., Murofushi H., *J. Biol. Chem.*, **267**, 21512—21517 (1992).
17) Murofushi K. M., Kobayashi S., Onumura K., Matsumoto M., Shiota M., Shoji M., Murofushi H., *Biochim. Biophys. Acta*, **1258**, 57—60 (1995).
18) Tanaka N., Kitamura A., Mizushina Y., Sugawara F., Sakaguchi K., *J. Nat. Prod.*, **61**, 193—197 (1998).
19) Mizushina Y., Tanaka N., Kitamura A., Tamai K., Ikeda M., Takemura M., Sugawara F., Arai T., Matsukage A., Yoshida S., Sakaguchi K., *Biochem. J.*, **330**, 1325—1332 (1998).
20) Mizushina Y., Tanaka N., Yagi H., Kurosawa T., Onoue M., Seto H., Horie T., Aoyagi N., Yamaoka M., Matsukage A., Yoshida S., Sakaguchi K., *Biochim. Biophys. Acta*, **1308**, 256—262 (1996).
21) Mizushina Y., Yagi H., Tanaka N., Kurosawa T., Seto H., Katsumi K., Onoue M., Ishida H., Iseki A., Nara T., Morohashi K., Horie T., Onomura Y., Narusawa M., Aoyagi N., Takami K., Yamaoka M., Inoue Y., Matsukage A., Yoshida S., Sakaguchi K., *J. Antibiot.*, **49**, 491—492 (1996).
22) Mizushina Y., Yoshida S., Matsukage A., Sakaguchi K., *Biochim. Biophys. Acta*, **1336**, 509—521 (1997).
23) Gunatilaka A. A. L., Gopichand Y., Schmitz F. J., Djerassi C., *J. Org. Chem.*, **46**, 3860—3866 (1981).
24) Lindahl T. J., Weinberg F., Morris P. W., Roeder R. A., Rutter W. J., *Science*, **170**, 447—449 (1970).
25) Lu B. C., Sakaguchi K., *J. Biol. Chem.*, **266**, 21060—21066 (1991).